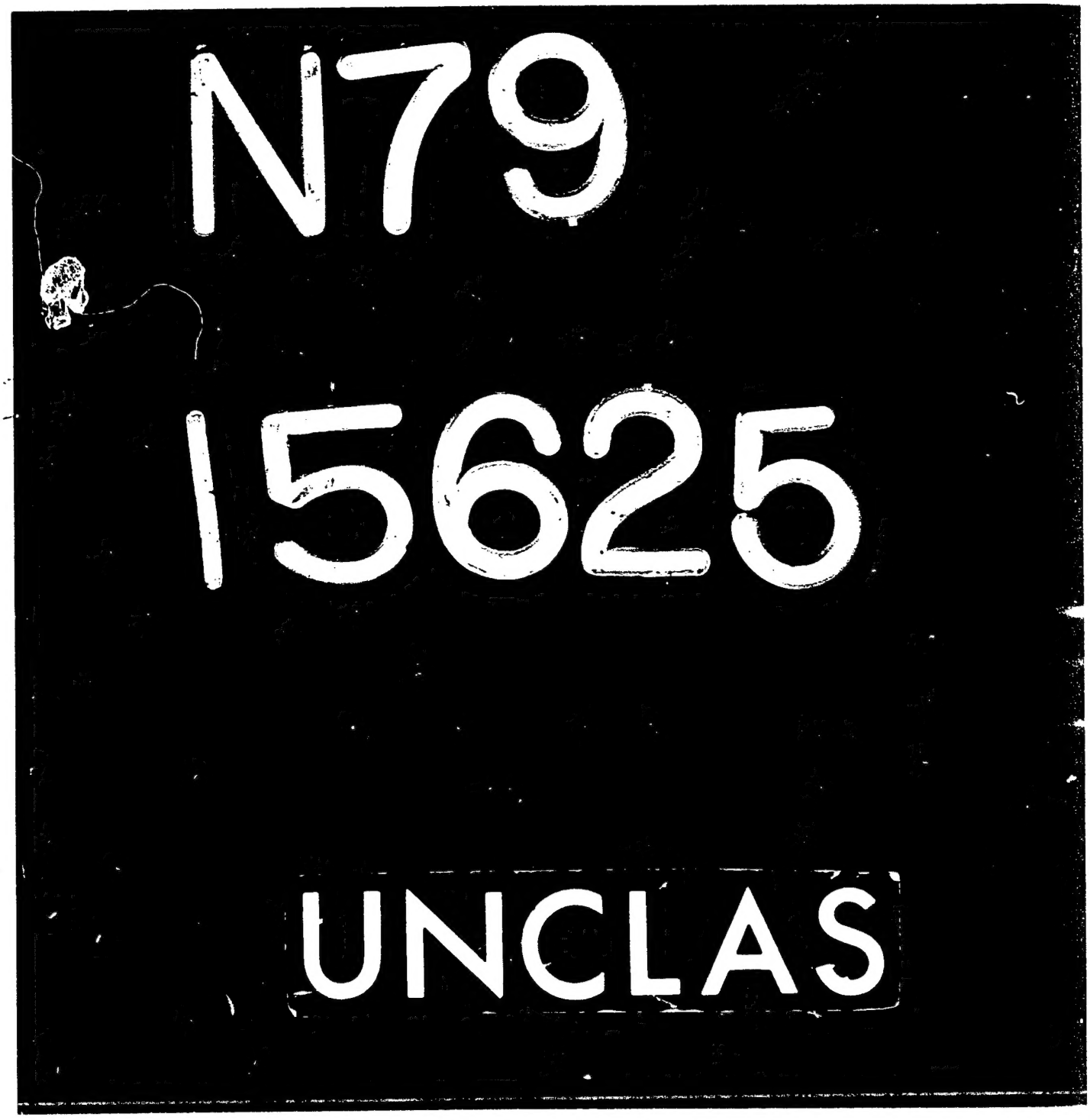
N79
15625
UNCLAS

A THEORETICAL AND EXPERIMENTAL ANALYSIS OF THE OUTSIDE WORLD PERCEPTION PROCESS

by P.H. Wewerinke
National Aerospace Laboratory NLR
the Netherlands

SUMMARY

The outside scene is often an important source of information for manual control tasks. Important examples of these are car driving and aircraft control. This paper deals with modelling this visual scene perception process on the basis of linear perspective geometry and the relative motion cues.

Model predictions utilizing psychophysical threshold data from base-line experiments and literature of a variety of visual approach tasks are compared with experimental data. Both the performance and workload results illustrate that the model provides a meaningful description of the outside world perception process, with a useful predictive capability.

INTRODUCTION

Many manual control tasks depend on the visual perception of the outside scene. In the context of aircraft control, the most important example is the visual approach scene. So, in order to investigate a great many flight situations in the approach and landing, it is mandatory to take into account this visual scene perception process which has often a major impact on mission performance.

Based on a concise inventory of the most important characteristics (cues) of the visual scene the visual scene perception process is described (modelled) on the basis of the linear perspective geometry and the relative motion cues. This involves mathematical relationships between these visual cues and the aircraft state variables. After linearization this model can be integrated in the existing framework describing piloted aircraft behavior (the optimal control model). This is the subject of the next chapter.

The visual scene perception model involves assumptions concerning perceptual thresholds of the various cues, noise levels associated with observing these cues and interference among them. Values for these parameters are derived from baseline experimental data supplemented by the psychophysical literature. Based on these values a theoretical analysis is performed dealing with a variety of visual approach conditions.

Furthermore, the results of an experimental program are compared with the model predictions. In addition, model predictions of pilot workload are compared with subjective ratings.

VISUAL SCENE PERCEPTION MODEL

One of the earliest studies of visual scene perception directly related to flight control problems has been performed by Gibson (Refs. 1 and 2). According to Gibson, the most important visual cues which can be derived from the visual field are related to

- the linear perspective geometry
- relative motion or motion parallax
- the apparent size of objects whose real size is known
- a far object covered by a near one
- the distribution of flight and shade over an object
- aerial perspective and the loss of detail with distance.

Of these, the linear perspective geometry provides a variety of cues. This is illustrated by the schematic version of the visual scene in figure 1a which can be thought of to consist of lines and points (textural elements). This involves not only the linear and angular position of the observer with respect to the outside world but also (dynamically) the relative motion. The point of the visual field toward which the observer is moving appears to be stationary ("focus of expansion"). All other textural points move with respect to the observer which can be indicated by velocity vectors ("streamers"). This is shown in figure 1b for the case of rectilinear motion. Various other references mention visual cues which can be conceived as examples of the afore-mentioned basic elements. Most of them are related to the landing approach scene (Refs. 3-5).

From the foregoing it can be derived that a reasonable approach is to model the visual scene perception process on the basis of the linear perspective geometry and the relative motion cues. Following reference 6 this involves a description of the cues which can be derived from the visual scene and their functional relationships with linear and angular positions and velocities of the observer. When, in addition, the relationships between the moving observer and the visual scene can be linearized about a nominal condition, the perception process can be described in standard estimation theoretical terms and included in the optimal control model structure in the following manner.

Let the observer (aircraft*) moving with respect to the outside world be described by the system state $x(t)$. This involves the common linear and

*) Although the following applies to a variety of man-machine situations, this analysis is directed at the aircraft control problem.

angular positions of the aircraft as well as additional parameters to describe relevant characteristics of the moving visual scene (with respect to the aircraft). After linearization about a nominal path the result will be a set of linear, (in general) time-varying equations given by

$$\dot{x}(t) = A(t)\, x(t) + E(t)\, w(t) \qquad (1)$$

where A(t) describes the process of the aircraft moving with respect to the outside world, and w(t) represents system disturbances (e.g. turbulence). Furthermore, the visual cues will be described by the display vector y(t). The relationships between these displayed variables and the system state is given by

$$y(t) = C(t)\, x(t) \qquad (2)$$

The perception of these variables is accompanied with an equivalent time delay, perceptual thresholds and observation noises. Also the interference between the various visual cues, a.o. arizing from the necessity to scan the visual field and to divide the attention among the various cues, has to be considered (Refs. 7 and 8). Now, these observations of the visual scene are dealt with in the same fashion as observations from other sources (e.g. displays, motion cues, etc.). The system state is estimated optimally (by means of a Kalman-Bucy filter) on the basis of the known (learned) dynamics involved and the observations. This state estimation process can be considered as an internal representation of the task environment.

Relationships between visual scene characteristics and the system state

A schematic version of the visual scene (Fig. 1) can be assumed to comprise textural elements and known objects. Both provide linear perspective geometrical cues (basically, the inclination of lines) and impressions of relative position and velocity.

The inclination Ω, of a line element of the visual scene is given by

$$\Omega = \tan^{-1} Y/H \qquad (3)$$

where Y is the distance between the observer and the pertinent line element perpendicular to the looking direction and H is the vertical position of the observer. Assuming small perturbations (y, h and ω) around the trim condition (Y_o, H_o and Ω_o) results after some manipulation (to a first order) in the linear expression

$$\omega = C_h\, h + C_y\, y \qquad (4a)$$

where

$$C_h = -\sin 2\Omega_o / 2H_o \qquad (4b)$$

Differentiating eq (4a) yields the expression for the inclination rate

$$\dot{\omega} = C_h \dot{h} + C_y \dot{y} \qquad (4c)$$

The small perturbations of the relative position and velocity of an element of the visual scene is simply given by

$$\alpha_h = h/R \; ; \; \alpha_y = y/R$$

and (5)

$$\dot{\alpha}_h = \dot{h}/R \; ; \; \dot{\alpha}_y = \dot{y}/R$$

where α is the visual angle and R is the distance between the object and the observer.

Furthermore, when the attitude of the observer (aircraft) is taken into account (with attitude angles φ, Θ and σ) eqs. (4) and (5) become

$$\begin{aligned} \omega &= C_h h + C_y y + \varphi \\ \alpha_h &= h/R + \Theta \\ \alpha_y &= y/R + \sigma \end{aligned} \qquad (6)$$

and the corresponding time-derivatives $\dot{\omega} = \ldots$, etc.

Next, these expressions are utilized to describe the cues which can be derived from the visual approach scene.

Visual approach scene

A schematic version of the visual approach scene is shown in figure 2. The cues which are assumed to be derived from this scene are indicated.
The most important cue for lateral guidance is derived from the inclination of the runway sides and/or centerline. The lateral deviation y, is zero if the inclination of both runway sides is the same ($\omega_r = \omega_l$) and the inclination of the centerline is zero ($\omega_c = 0$).
Vertical guidance has to be based on the (average) inclination of the runway sides when no runway end and no horizon is visible. In that case, the observer has to know the nominal inclination (Ω_o), which is range-varying. The following model analysis and experimental results will show that a better indication of the vertical position is obtained when the length of the runway α_h (or, almost equivalently, the depression of runway threshold with respect to the horizon) is visible. Also in that case, the observer has to know the nominal depression which is, however, constant during a standard approach (e.g., 3 deg).
Glide slope information requires also the estimation of the distance to touchdown. This can be based on the apparent size of ground objects, of which the most important is often the runway width.
Aircraft attitudes provide "inner-loop" information and can be derived from the relative position and inclination of (e.g.) the horizon and any aircraft reference. The pitch angle Θ, which has to be estimated with respect to its (non-zero) nominal value and the bank angle φ are indicated in figure 2.

MODEL ANALYSIS

The linear visual scene perception model (VSPM) can be implemented in the optimal control model (Refs. 6 and 7). Based on the foregoing discussion, a variety of visual approach conditions are selected to analyze theoretically. In addition, an experimental program has been conducted to provide a critical test for the hypotheses (assumptions) underlying the model results. In order to obtain detailed information concerning the information processing involved in the manual approach task, no range-varying effects are considered in the following analysis. In other words, it is assumed that the aircraft is "frozen" at a fixed point of the approach path corresponding with a nominal altitude of 200 ft for a 3° approach ("hovering"). The consequence is a stationary process involved allowing frequency domain measures such as human describing functions and observation noise spectra. Especially the latter will provide a sensitive check on the exactness of the values used for the model parameters under investigation. The primary model parameters are the perceptual thresholds of the various visual cues (display elements) involved because these represent the most uncertain model parameters. The results of several previous experimental studies suggest reasonable accurate values for the remaining model parameters.
Therefore, base-line experiments have been conducted and relevant psychophysical literature have been searched resulting in reasonable reliable estimates for the perceptual thresholds involved. Finally, the last section contains the model analysis proper and the resulting model predictions.

Visual scene configurations

Referring to the foregoing discussion the configurations given in figure 3 were selected for the following model analysis and formal experiment.

Vertical control on the basis of the inclination of the runway sides can be compared with the condition that the depression of the runway threshold below the runway end (α) or below the horizon is visible (configurations 1 and 2). Furthermore, the effect of an aircraft reference providing explicitly pitch information is of interest (configuration 3).

Lateral control utilizing the inclination of the centerline is represented by configuration 4. In case the runway sides are available, the inclination of both sides has to be estimated and compared with each other (configuration 5). A simple model analysis shows that this process is associated with the same observation noise as in the case of a center line. Only the perceptual thresholds involved are different (next section). This will be tested against the experimental results. Again the effect of explicit roll information provided by the aircraft reference is considered by including configuration 6. Configuration 7 concerns roll tracking based on the aircraft reference. This (presumably) easy task is included to evoke some variation in workload in order to yield additional experimental evidence for the workload model of reference 8 and to test the perceptual threshold assumptions involved.

Configurations 8 and 9 are selected to investigate the interference between vertical and lateral control. It is assumed that the pilot has to divide his attention between the various display variables (visual scene cues) involved. This interference is assumed not only within a control task (e.g. attention has to be divided between pitch angle and altitude) but also between vertical and lateral control when performing both tasks simultaneously. This represents a crucial hypothesis which will be tested in the following as the visual scene is widely assumed to represent integrated information and it is a non-trivial question whether the visual scene can be "broken down" into separate elements. Finally, configuration 10 is included to investigate the effect of additional texture. This has, in principle, its implications for the information contents of the visual scene which turned out to be of no interest but also for the psychological aspects (perspective illusion and realism).

Perceptual thresholds

It was anticipated that perceptual threshold phenomena could be important for the foregoing visual scene cues. Thresholds can be accounted for in the optimal control model by modifying the observation noise covariance associated with a particular visual cue.

Although the psychophysical literature reports a wealth of emperical threshold data, these data are known to be affected by numerous experimental conditions which easily explains the typical scatter in "comparable" data. Therefore, a baseline experiment has been conducted to determine the position thresholds of the display elements involved in the visual scene configurations shown in figure 3. These thresholds are primarily due to the lack of explicit visual references concerning zero or nominal, visual scene conditions.

This involves that learning (experience) and temporal cues (memory functioning) are important in measuring and interpreting thresholds.

Experimental details are given in reference 9. The resulting measurements are "translated" to values suitable for (as required by) the describing function representation for the assumed dead-zone non-linearity. The results are summarized in table 1.

As discussed in reference 9 thresholds associated with the perception of motion in the visual field can be related to resolution properties. This implies that the motion detection thresholds can be inferred from the foregoing discrimination data. The result is also contained in table 1.

Apart from these (nominal) threshold estimates, in table 1 it is also indicated how reliable these estimates are assumed to be. A sensitivity analysis in the following will serve to relate this incertainty in threshold values to a confidence interval associated with the system performance predictions of the model.

Model predictions

A block diagram of the control task(s) is given in figure 4. System disturbance enters the system parallel to the control input. The resulting

output is displayed to the human operator as the pitch and roll angle (for the pertinent configurations) representing K-dynamics. The integral of these outputs are the altitude (or approach angle) and lateral deviation (or center line inclination), respectively (K/s-dynamics). The disturbances are white noise processed by two first order filters with poles at one rad/sec and two rad/sec. The disturbance levels are for the vertical task given by a resulting pitch variance of 0.068 deg^2 and for the lateral task given by a resulting roll variance of 10.5 deg^2 (corresponding with the values used for the experimental program). Details concerning sensitivities and gains involved are contained in reference 9.

Model parameters can be divided in parameters which are constant for all configurations and parameters which are considered as the remaining model variables. Also the experimental results of the next chapter will be related to these (dependent) variables. The key variables are the perceptual thresholds. The nominal values of table 1 are assumed for the model predictions. Furthermore, the effect of the upper- and lower threshold values on the system outputs is also determined and discussed in the following chapter. The overall level of attention (P_o) is also, to same extent, variable, although this value has been shown in previous studies to be relatively constant. A nominal value of -20 dB is assumed and the effect of $\pm$ 3 dB on the system outputs is considered.
The constant model parameters are: a neuro-motor time constant of 0.1 sec, a perceptual time delay of 0.2 sec and a motor noise ratio of -30 dB.

Now, assuming that the human operator divides his attention among the visual cues (position and velocity of all display elements) optimally, i.e., minimizing the given cost functional* (Ref. 8), system performance can be predicted for the various configurations. The results are given in table 2.

Vertical control is superior for the condition that the runway depression angle and the pitch angle can be observed (conf. 3). The contribution of the pitch information amounts to a 20 % reduction of the approach angle variance (σ_α^2 of conf. 2). When the viewing condition is such that no horizon or runway end is visible and control has to be based on the runway sides (ω_c and/or ω_r) and runway threshold variation ($\dot{d}$) the vertical approach performance is degraded substantially. This clearly demonstrates the contribution of the various visual cues involved. Furthermore, in the case of both vertical and lateral control, the vertical approach performance is predicted to deteriorate with 30 % to 50 % (due to the assumed interference between both tasks). The last column of table 1 contains the (optimal) fractions of attention dedicated to the various cues.

The best lateral approach performance is obtained when the runway centerline inclination (ω_c) cue is available (conf. 4). Lateral control utilizing the runway sides is substantially degraded (conf. 5) due to the larger perceptual threshold of this cue. The bank angle provides useful

* According to the instructions given to the subjects in the experiment the system output is assumed to be minimized. In addition the control rate is weighed yielding the neuro-motor time constant of 0.1 sec.

inner loop information (conf. 6). When performing the vertical and lateral task simultaneously, the model predicts a deterioration in lateral performance (confs. 8 and 9) of about 100 %. The model predicts that the effect of the texture (conf. 10) on system performance is negligible.

The effect of the model parameter variations (thresholds and overall attention) on the system scores and additional theoretical results will be discussed in the next chapter where the model predictions will be compared with the experimental results.

EXPERIMENTS

The first objective of the experimental program was to test the foregoing model results with respect to both the fundamental hypotheses involved (optimality in control and attention allocation, interference between cues) and the assumed numerical values of the key model parameters. Secondly, in case significant discrepancy occurs between model and experimental results the appropriate adjustments can (hopefully) be made in the model assumptions underlying the model results.

Experimental procedures

The same 10 configurations as discussed previously are investigated in the experimental program. These configurations were four times presented to the (four) subjects (general aviation pilots) in a random order. Each run lasted 200 sec. Between the runs the subjects were asked to give their impression of the exerted workload (Reference 9 contains the rating scales used and additional experimental details). The subjects were instructed to minimize the mean-squared system output. They were trained on the ten configurations in a random order till a relatively stable performance level was reached. All together, about 250 training trials were performed.

An analog computer was used to simulate the vehicle dynamics and to generate the visual scene characteristics. This visual scene was presented to the subjects on a TV monitor located 2.5 m in front of their point of regard, They manipulated a two-axis isometric hand control. The system parameters were recorded on FM magnetic tape for off-line mean-squared scores and frequency domain computations*.

Comparison of experimental results and model scores

In this section the experimental results in terms of mean-squared performance scores are compared with the model predictions. Based on the results of table 2 firstly the approach angle (α)- and centerline inclination (ω_c) scores are considered (the model predicts attitude- and control scores which are relatively insensitive over the configurations).

* Unfortunately, these frequency domain data were not available in time to include in this paper. These results will be included in reference 9.

Apart from the nominal model predictions (of table 2) the effect of the uncertainty in underlying assumptions (i.e., numerical values of the thresholds and overall attention) on system performance is determined. For the upper- and lower threshold values given in table 1 and, in addition, + 2 dB and -2 dB variation in overall attention the corresponding performance scores are determined. It is hypothesized that the experimental scores lie within the resulting performance interval.

In figures 5 and 6 both the experimental means and standard deviations (of 16 runs) and the model predictions are given. For all single-axis tasks the experimental scores lie well within the predicted interval. This indicates not only that the model is "right" but also that the assumed numerical values for the thresholds and overall attention are close to the "real" values.

For the dual-axis tasks the experimental results do clearly not match the model predictions. The experimental data of configuration 9 and 10 have been pooled because both the model predictions and the experimental results for both configurations indicate that the only effect of the texture information is the enhancement of the perspective illusion. This was also apparent during the learning phase. An adjustment of the model parameter values (which has to be appropriate for the single-axis tasks as well) does not result in a good agreement with the experimental scores. Therefore, it is tentatively concluded that the assumed hypothesis of interference between the two tasks has to be rejected. Instead, the following hypothesis is considered: the visual scene stimulates the human operator to perform the dual-axis task just as well as the single-axis task (thus, vertical control is not degraded when the lateral control task is added, and vice versa). So, it is assumed that there is no performance interference. This will be further discussed in the following.

Comparing also the attitude scores (ϑ and φ) and the control scores (δ_e and δ_a) of the model predictions in table 1 and the measured scores given in table 3 it is apparent that both the measured attitude scores and the measured control scores are much lower than predicted. This indicates that the subjects (being pilots) performed the - to some extent realistic appearing - "approach" tasks in a much smoother fashion than the model predicts on the basis of an assumed neuromotor time constant of 0.1 sec. This is confirmed by pilot commentary indicating that the pilots were reluctant to make rapid control movements and "chase the needles".
Based on this observation the neuromotor time constant was adjusted to a value of 0.25 sec. This value which was kept constant in the following analysis is apparently more representative for outer-loop control behavior. In addition, figure 5 suggests that for the vertical control tasks a better agreement between measured and model results will be obtained when the lower threshold values given in table 2 will be assumed (0.2 ^{o}/sec and 0.4^{o}). This is the only minor adjustment of the model variables.

The resulting model scores are compared with the measured mean-squared values in table 3. In general, the agreement between the measurements and the refined model scores is quite good. Now (with a neuromotor lag of 0.25 sec) the control scores match, on the average, very well. The same can be

said of the system outputs α and, to less extent, ω_c.
A comparison of the pitch attitude scores shows that the pilots were somewhat more conservative in making pitch corrections than the model predicts (apart from configuration 1). These lower pitch scores (and the corresponding somewhat lower control scores) could easily be duplicated by the model, however, by an appropriate weighting of the pitch angle. The mean-squared roll angles match again, rather well*.

The system output scores are summarized in figure 7. For the dual-axis configurations, both the scores corresponding with the assumption that there no performance interference between the two axes and the "full interference" scores are indicated. The results strongly support the hypothesis that there is no interference between the vertical- and lateral axis thanks to the visual scene.

In summary, it can be concluded that for the relatively realistic, outer-loop control tasks under investigation a neuromotor time constant of (say) 0.25 sec is appropriate. Furthermore, only one minor adjustment of the nominal model variables was required to yield, on the average, a good agreement between model results and measurements: a position threshold for α and ϑ of 0.4° and a velocity threshold for $\dot{a}$ and $\dot{\Theta}$ of 0.2°/sec (the same value as found in reference 10). Finally, the experimental results provided convincing support for the hypothesis that the visual scene perception process can be described on the basis of the, mutually interfering, various (separate) visual cues considered. There is no performance degradation (interference) when both the vertical and lateral control task are performed simultaneously.

Workload model results and subjective ratings

Using the foregoing model results human operator workload can be computed. The workload model (a.o. discussed in reference 8) involves not only the level of attention, P_o, dedicated to the task in accordance with the model of reference 11, but also the aspect of arousal ("uncertainty").

The model predictions are compared in figure 8 with subjective ratings on the workload scale given in references 8 and 9. Apart from configuration 1 the linear correlation between subjective ratings and workload model predictions is quite good ($r = 0.88$). This result provides additional support for the workload model.

The model predicts a much lower workload level for configuration 1 than reflected by the subjective ratings. The explanation for this is that for this configuration the subjects were not sure what the right (nominal) vertical position was. Not only they learned slowly on this configuration (somewhat discouraged by their varying performance) but also they clearly did not like the uncertainty involved in performing the task which can also be related to training. So, the model, not including this learning aspect, predicts that the workload corresponding with this configuration will

* For the roll-only task (conf.7) an overall level of attention, P_o, of -18 dB had to be assumed in order to match the measured scores.

substantially reduce when the subjects are more trained on (familiar with) this task.

CONCLUSIONS

The visual scene provides a variety of perspective geometrical and relative motion cues. The experimental results have supported that these characteristics can be considered as separate cues among which the human operator has to divide his attention. The commonly accepted idea that pictorial information is better integrated (less interfering) than separate display elements is in the present study specifically demonstrated in that there is no performance interference between the vertical and lateral task. Both the workload model results and the subjective ratings indicate that the workload is increased indeed when performing both tasks.

In the case of guidance control tasks (e.g., the visual approach task) pilots are reluctant to make rapid control movements. This is represented in the optimal control model by a weighting on control rate corresponding with a neuromotor time constant of about 0.25 sec. This outer-loop control behavior is distinguished from attitude (inner-loop) control tasks which can be modelled with a neuromotor time constant of 0.1 sec (Ref. 7).

Furthermore, the assumptions concerning the key parameters of this investigation, i.e. the perceptual thresholds, could (indirectly) be checked against the experimental data. Apart from one minor adjustment the a priori assumed threshold values yielded a good agreement between model scores and measurements. The sensitivity analysis visualized in figures 5 and 6 indicates that this result allows a reasonable accurate verification of the underlying model parameters (thresholds and level of attention).

Finally, the workload model predictions have been confirmed convincingly by subjective ratings. Apart from configuration 1 (the performance of which task must have been dominated by a psychologigal effect not included in the model) the linear correlation between model predictions and subjective ratings was 0.9.

REFERENCES

1. Gibson, J.J. The perception of the visual world. The Riverside Press. Cambridge, Mass. 1950.

2. Gibson, J.J. et al., Parallax and perspective during aircraft landings. Amer.Journ. Psych. 68 (1955).

3. Havron, M.D., Information available from natural cues during final approach and landing. Human Sciences Research Inc., HSR-RR-62/3-Mx-X, March 1962.

4. Bronw, J.L., Visual elements in flight simulation. Rochester University TR 73-2, December 1973.

5. Naish, J.M., Control information in visual flight. Seventh annual conference on manual control, NASA SP-281, June 1971.

6. Baron, S. and Berliner, J., Manmod 1975: Human internal models and scene-perception models. US Army Missile Command, TR RD-CR-76-3, September 1975.

7. Baron, S. and Levison, W.H., Display analysis with the optimal control model of the human operator. Human Factors, 1977, 19(5).

8. Wewerinke, P.H., Performance and workload analysis of in-flight helicopter missions. Paper presented at the 13th Annual conference on manual control, MIT, June 1977. (also NLR MP 77013 U).

9. Wewerinke, P.H., Visual scene perception process involved in the manual approach. NLR TR 78 (forthcoming).

10. Levison, W.H., The effects of display gain and signal bandwidth on human controller remnant. AMRL-TR-70-93, March 1971.

11. Levison, W.H., A model for mental workload in tasks requiring continuous information processing. Nato symposium on mental workload, Mati, Greece, September 1977.

Table 1 Thresholds

PAR	DISPLAY	THRESHOLD	CONFIDENCE INTERVAL
	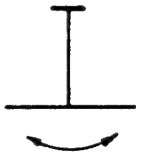	1° $1^{\circ}/s$	- $0.5 - 2^{\circ}/s$
ω_c $\dot{\omega}_c$		5° $3^{\circ}/s$	$4 - 6^{\circ}$ $2 - 4^{\circ}/s$
	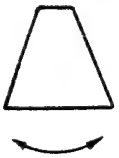	2° $2^{\circ}/s$	- $1 - 3^{\circ}/s$
Φ $\dot{\Phi}$	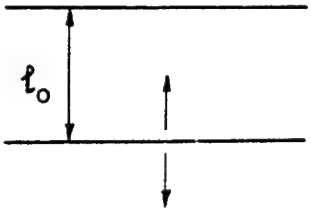	0.5° $0.3^{\circ}/s$	$0.4 - 0.6^{\circ}$ -
α $\dot{\alpha}$		0.5° $0.3^{\circ}/s$	$0.4 - 0.6^{\circ}$ $0.2 - 0.4^{\circ}/s$
φ $\dot{\varphi}$	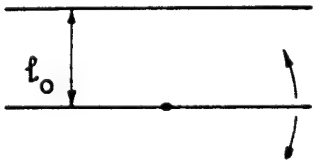	0.7° $1^{\circ}/s$	- -

Table 2 Model predictions

a) VERTICAL CONTROL

Configuration	$\sigma_\alpha^2(\text{deg}^2)$	$\sigma_\theta^2(\text{deg}^2)$	$\sigma_{\delta_e}^2(\text{N}^2)$	attention allocation f_i
1	0.211	0.242	57.6	f_{ω_1} = 0.55 $f_{\dot{\alpha}}$ = 0.45
2	0.121	0.239	57.3	f_α = 0.6 $f_{\dot{\alpha}}$ = 0.4
3	0.103	0.247	58.8	$f_{\dot{\alpha}}$ = 0.6 f_θ = 0.4
8	0.156	0.319	70.2	f_α = 0.42 $f_{\dot{\alpha}}$ = 0.58
9	0.157	0.331	72.4	f_α = 0.36 $f_{\dot{\alpha}}$ = 0.27 f_θ = 0.38

b) LATERAL CONTROL

Configuration	$\sigma_{\omega_c}^2(\text{deg}^2)$	$\sigma_\varphi^2(\text{deg}^2)$	$\sigma_{\delta_a}^2(\text{N}^2)$	attention allocation f_i
4	1.86	9.68	13.1	f_{ω_c} = 0.37 $f_{\dot{\omega}_c}$ = 0.63
5	4.22	14.7	15.7	f_{ω_c} = 0.42 $f_{\dot{\omega}_c}$ = 0.58
6	2.96	9.35	12.9	f_{ω_c} = 0.35 f_φ = 0.65
8	8.01	24.8	20.9	f_{ω_c} = 0.27 $f_{\dot{\omega}_c}$ = 0.13
9	6.71	19.6	18.2	f_{ω_c} = 0.22 f_φ = 0.22

Table 3 Comparison of measured scores and model results

VERTICAL CONFIGURATION		$MS_{\alpha}(deg^2)$	$MS_{\theta}(deg^2)$	$MS_{\delta_e}(rad^2)$
1	model	0.189	0.095	26.7
	measured	0.193	0.098	26.4
2	model	0.082	0.096	26.0
	measured	0.077	0.054	23.0
3	model	0.072	0.091	26.4
	measured	0.081	0.047	21.2
5	model	0.085	0.110	28.4
	measured	0.083	0.061	24.6
9, 10	model	0.072	0.095	26.9
	measured	0.065	0.040	20.1

LATERAL CONFIGURATION		$MS_{\omega_c}(deg^2)$	$MS_{\varphi}(deg^2)$	$MS_{\delta_a}(rad^2)$
1	model	2.78	5.82	9.70
	measured	3.62	7.82	10.9
2	model	5.42	8.40	10.6
	measured	4.72	7.90	10.9
3	model	3.40	5.46	9.62
	measured	3.99	5.40	9.43
7	model	-	2.89	4.54
	measured	-	2.99	4.99
8	model	6.37	10.0	11.2
	measured	6.20	12.1	14.0
9, 10	model	4.14	6.66	10.8
	measured	4.52	6.90	10.8

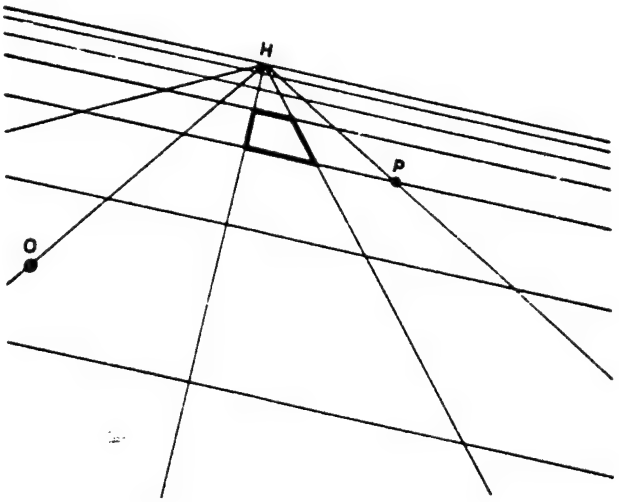

1a OUTSIDE VIEW

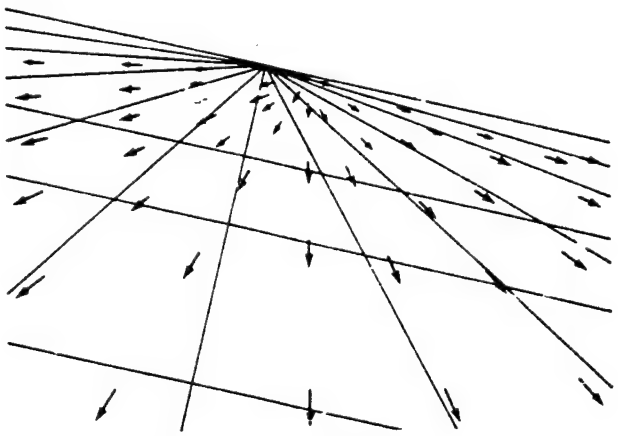

1b RELATIVE MOTION OF THE VISUAL FIELD

Fig. 1: Visual scene

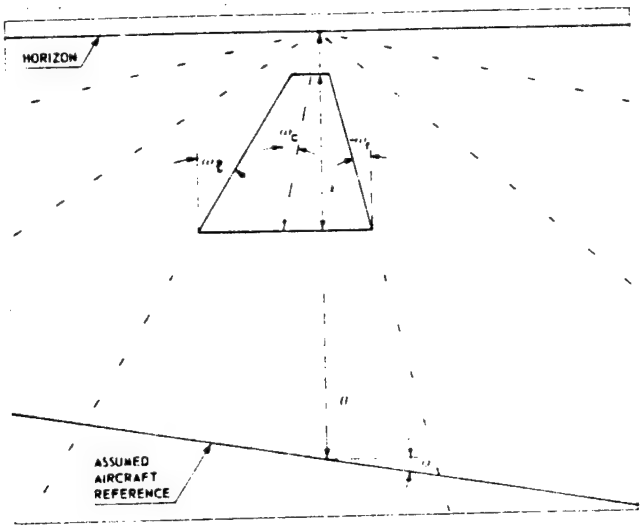

Fig. 2: Cues derived from the visual scene

VIEWING CONDITION	CONTROL		
	VERTICAL	LATERAL	BOTH
	1		
		4	
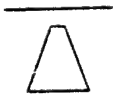	2	5	8
	3	6	9
			10

N.B. CONFIGURATION 7 CONCERNS ROLL TRACKING BASED ON ROLL BAR ONLY

Fig. 3: Viewing conditions and selected configurations

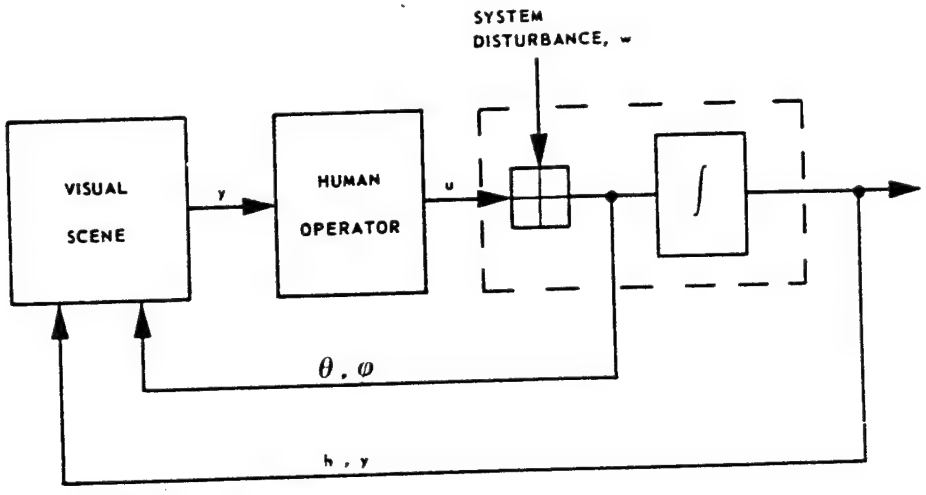

Fig. 4: Control task

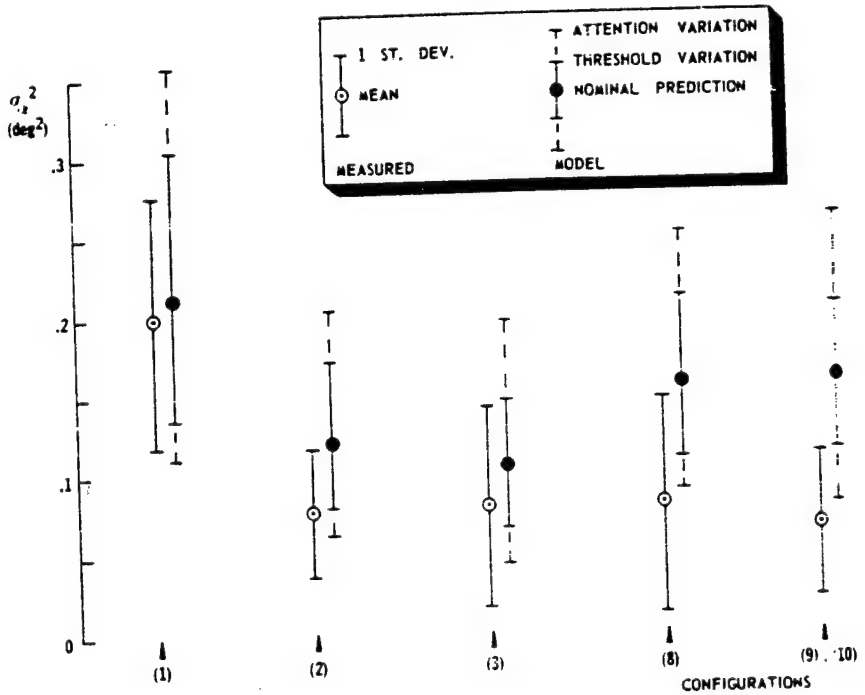

Fig. 5: Comparison of experimental scores and model predictions - vertical control

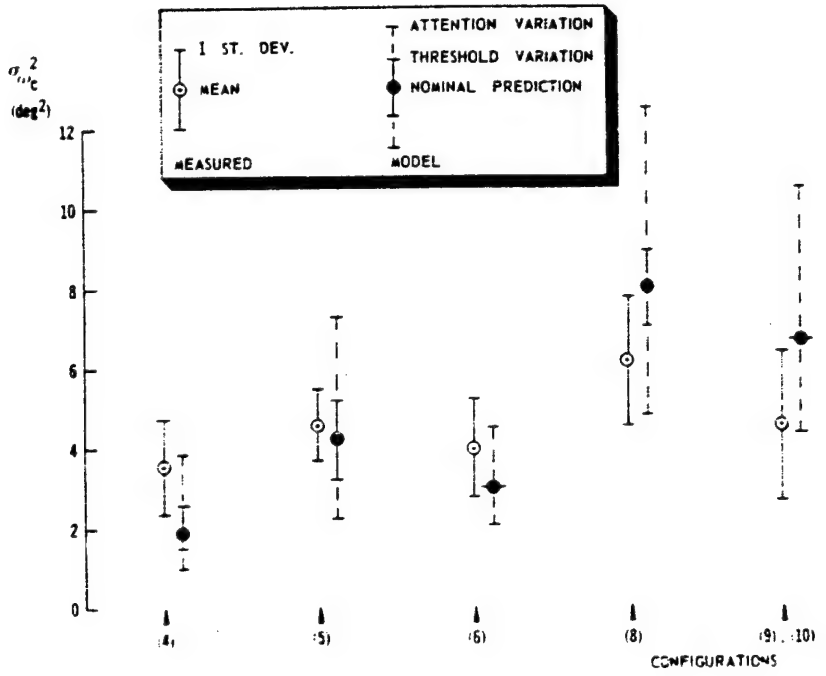

Fig. 6: Comparison of experimental scores and model predictions - lateral control

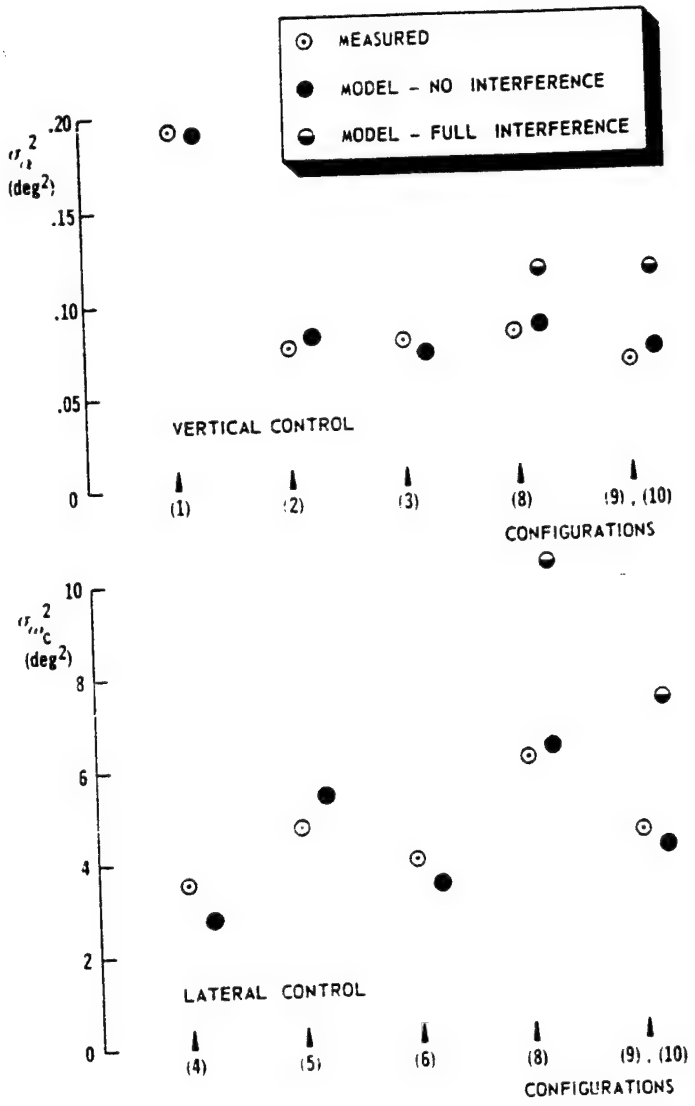

Fig. 7: Refined model scores and experimental results

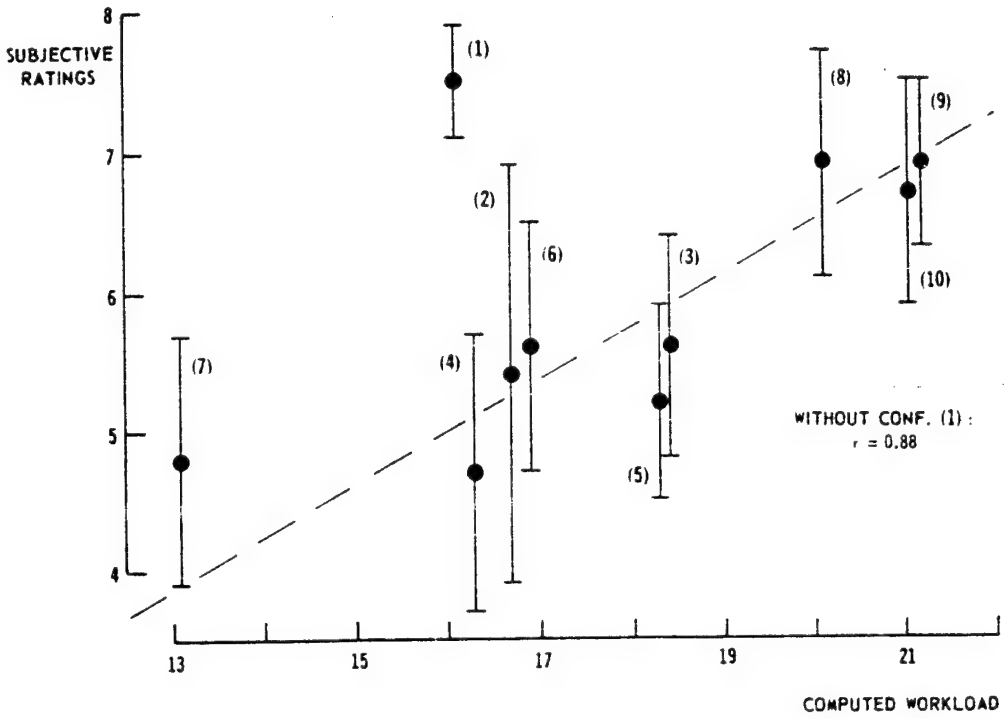

Fig. 4: Subjective workload ratings and computed workload

N79-15626

LINEAR MODELLING OF ATTENTIONAL RESOURCE ALLOCATION[1]

by Byron Pierce[2] and Christopher D. Wickens

University of Illinois Department of Psychology

SUMMARY

Eight subjects time-shared performance of two compensatory tracking tasks under conditions when both were of constant difficulty, and when the control order of one task (designated primary) was varied over time within a trial. On line performance feedback was presented on half of the trials. The data are interpreted in terms of a linear model of the operator's attention allocation system, and suggest that this allocation is strongly suboptimal. Furthermore the limitations in reallocating attentional resources between tasks, in response to difficulty fluctuations were not reduced by augmented performance feedback. Some characteristics of the allocation system are described, and reasons for its limitations suggested.

INTRODUCTION

A common requirement imposed upon the human operator engaged in time-sharing performance under time-varying environmental conditions results when changes occur in the difficulty of one of two concurrently performed tasks, as its performance constraints are held constant. Such changes thereby force a reallocation of attentional resources toward the task whose difficulty is increasing. Thus for example in precision flight, an increase in lateral air turbulence will require re-allocation of resources away from tasks of lesser demand (communications, pitch control) toward control along the lateral axis.

The entire process of task demand evaluation and resource allocation can be conceptualized as a two stage process. The operator must first evaluate the error, or discrepancy between desired and actual performance on the task or tasks required (error evaluation). If such an error is perceived to exist, the attention allocation system then must respond by shifting resources in a manner to restore the desired level of performance and nullify the original error (resource allocation). This closed feedback loop describing the resource allocation system is analogous in some respects to a compensatory tracking task, in which position error is evaluated and a manual control response is executed to nullify the error. Because of this similarity, modelling techniques borrowed from manual control will be utilized in

[1]This research was supported by a grant from Air Force Office of Scientific Research Life Sciences directorate. AFOSR77-3380. Dr. Alfred Fregly was the contract monitor.

[2]Now at Williams Air Force Base.

the current investigation to describe and evaluate the human's attention allocation system.

Delp and Crossman (Reference 1) have provided an analytical framework for describing the linear relation between time-varying task parameters and single task performance in terms of a higher level "meta transfer function." The objective of the present research is to apply similar procedures to analyze the meta transfer function of the resource allocation system to task demand (difficulty) changes in the dual task environment. In the paradigm employed, subjects perform two concurrent tracking tasks. One task is designated as primary--a high priority task whose performance is to be maintained at or above some criterion for the duration of a trial. During the trial, the difficulty of the primary task is varied in a semi-periodic fashion. It is assumed that, to the extent that he is capable, the subject follows the priority instructions, and primary task performance remains constant in the face of varying primary task difficulty. To achieve this optimal allocation behavior, the subject is therefore required to withdraw processing resources from performance of the secondary task, and its performance should then vary, more or less phase-locked to the difficulty variations of the primary task.

An hypothetical example of this "optimum allocation response" to a ramp increase in primary task difficulty is depicted by the solid lines of Figure 1. The time-varying performance on both tasks is portrayed, along with the inferred allocation of processing resources between the tasks. Note the differential sensitivity of primary vs. secondary task performance to the increase in primary task difficulty, and the corresponding optimum allocation of resources. Naturally, other varieties of allocation responses may be observed as well. The dashed lines in Figure 1 depict that of a non-optimum allocator in which resources are not at all redistributed, and primary task performance varies with its difficulty. Naturally a hybrid response between that of the optimal and nonoptimal allocator is possible, in which there is some reallocation of resources, but in insufficient degree to meet the new primary task demands.

The model that will be employed to describe the allocation system is portrayed in Figure 2. Here the allocation system is assumed to be a linear dynamic system in the sense that it receives inputs (task demands and subjectively assessed performance) and generates outputs in response (mobilized processing resources). While these outputs cannot be directly observed, they may be inferred from an appropriately filtered on-line performance measure. Thus in dual task performance, depicted in Figure 2, the dynamic relation between the four inputs to the allocation system (difficulty and performance demands on both tasks) and the two outputs (task performance on each task) can be evaluated to determine the extent to which these are described by a linear transfer function or orderly mathematical relation. Such a procedure is analogous to the analysis of dual axis tracking (Reference 2).

When analyzing dual task performance, one may examine for each task, the sensitivity of its allocated resources (inferred from performance) to changes in its own difficulty (D_1P_1 and D_2P_2 in Figure 2) and to changes in the difficulty or performance of the concurrent task (D_1P_2 and D_2P_1). In the

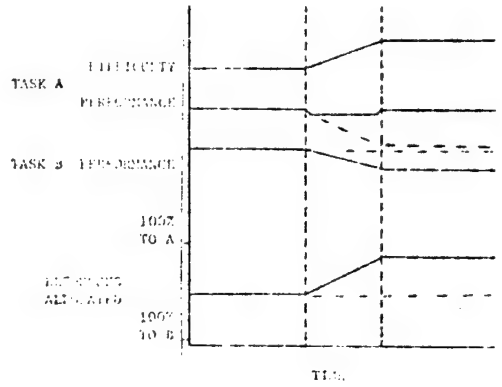

Figure 1. Hypothetical response depicting optimal allocation adjustment (solid lines) and nonoptimal allocation (dashed lines)

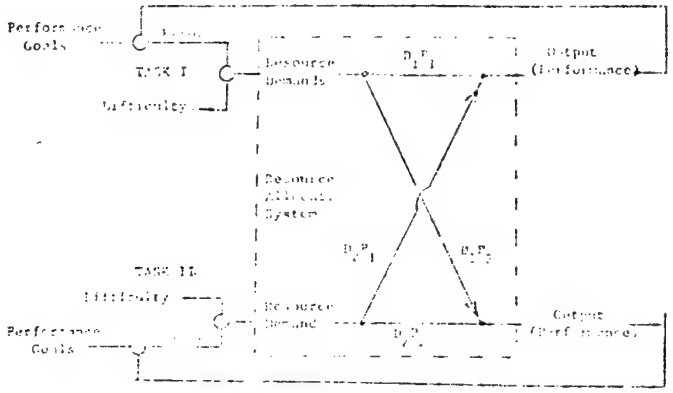

Figure 2. Schematic representation of dual task performance

current study Fourier analysis will be employed to determine the relations between time-varying inputs (tracking task difficulty) and time-varying outputs (filtered performance). To the extent that the resource allocation system is sensitive at all to these variations, the linear coherence measure, correlating variations over time between the input and output signals, should be non-zero. More specifically the cross-channel (D_1P_2 and D_2P_1) and like-channel (D_1P_1 and D_2P_2) coherence measure will be examined as a means of determining the optimality of the allocation system. For a highly optimal system, the like channel coherence (D_1P_1) should be a low (near 0), with the crosschannel coherence (D_1P_2) high (near 1.0). For the non-optimal allocator the values should be reversed, and for the hybrid case both coherence values should be relatively high.

If suboptimal allocation is observed in the present results, then an important question that can be asked relates to the source of the limitation in the allocation system. In terms of the two-phase description of the allocation process as shown in Figure 2, one may ask whether the limitation results from the operator's inability to perceive discrepancies between desired and actual performance (failure of error evaluation), or from the inability to reallocate resources in response to an accurately evaluated error. In an analogous manner it is possible to ask whether inadequate performance in a compensatory tracking task results from poor perceptual evaluation of the displayed error, or from an inability to execute an appropriate control response.

To investigate the source of potential limitations, a separate set of experimental conditions were included in which the conventional instantaneous tracking error display was supplemented by augmented performance feedback that displays the discrepancy between the desired level of primary task performance, and the running average of that performance (e.g., Reference 3). To the extent that limitations in the allocation system result from inadequate error evaluation, rather than limits of allocation, then the explicit display of the discrepancies in performance should produce a corresponding approach toward optimality of allocation (i.e., an increase in the cross-channel, and decrease in the like-channel coherence).

METHOD

Tasks. Subjects performed two compensatory tracking tasks, displayed one above the other with a slight horizontal offset. The left display was controlled by left-right manipulation of a spring loaded controller held in the left hand. The right display was similarly controlled with the right hand. The total visual angle subtended by both displays was 4^{o} (horizontal) x 1^{o} (vertical). Disturbance inputs consisted of band-limited white noise with an upper cutoff frequency of .32 Hz. Separate uncorrelated disturbances were employed on each task and were added to the output of the control dynamics. Control dynamics were of the form:

$$Y_c = K\left(\frac{1-\alpha}{s} + \frac{\alpha}{s^2}\right)$$

On trials of constant difficulty, the value of the difficulty parameter alpha was set at .50. On variable difficulty trials, the value of alpha on one task, designated primary, was driven by the function: $\alpha = .50 + \text{Sin}\ (.1884\ t) + \text{Sin}\ (.0628\ t)$, $(0 < \alpha < 1)$. This produced a system that varied continuously between second order unstable dynamics, first order stable dynamics, and intermediate levels in a series of spikes and ramps (see Figures 3 and 4). Secondary task difficulty was always held constant with alpha = .50.

Supplementary performance feedback of the primary task, used in variable difficulty trials, appeared as a bar graph varying in height to reflect changes in performance (Reference 3). The performance bar represented in-

tegrated primary task error, averaged over a sliding 5-second window. The desired performance level, indicated by a short horizontal line positioned about half the distance from the zero point (no bar graph showing) to the top of the display, reflected the subject's average performance assessed for trials of constant difficulty. By tracking so that the bar graph remained at or above the desired performance line, the subject attained desired standards of primary task performance.

Root mean squared error (RMSE) was computed on line for each task and recorded at the end of each trial. Control stick and cursor error positions were sampled and recorded on tape every 120 msec. Experimental control was governed by a Raytheon 704 computer.

Design and Procedure. Eight right-handed male students at the University of Illinois participated in the experiment and were paid for participation. A within-subjects design was employed so that all subjects performed all experimental conditions. Following one day's session of practice on the dual axis tracking tasks, four experimental sessions were conducted. Within each session, subjects performed 24 two minute dual task trials. These consisted of 8 trials of constant difficulty, of which the final 4 were used for data analysis (Phase I), followed by 12 trials of variable difficulty, of which the final 8 were used for data analysis (Phase 2). Finally the subjects received four more trials of constant difficulty (Phase 3). During constant difficulty trials subjects were instructed that the two tasks were of equal priority, while in Phase 2, the task of variable difficulty was designated as primary--its performance to be held constant. On alternating Phase 2 trials, either the left hand task or the right hand task was primary (and was therefore variable). Similarly on alternating pairs of Phase 2 trials, supplemental feedback was either present or absent.

RESULTS

RMS Error. Two 1-way repeated measure analyses of variance were performed on the RMS tracking errors, one for primary and one for secondary task performance. The four levels of each ANOVA consisted of Phase 1, Phase 2 feedback, Phase 2 no-feedback, and Phase 3. The effect of condition on the performance measures in both ANOVAs was highly reliable (Primary Task, $F_{3,21} = 107.98$, $p < .001$; Secondary Task, $F_{3,21} = 54.93$, $p < .001$). The mean values of primary and secondary task error for the four conditions are shown in Table 1. It is apparent that large differences in both tasks

Table 1: RMS Error (Proportion of Scale

	Phase 1	Phase 2 Feedback	Phase 2 No Feedback	Phase 3
Primary Task	.1164	.1808	.1869	.1166
Secondary Task	.1206	.2058	.1806	.1147

were evident between the variable (Phase 2) and constant difficulty (Phases 1 and 3) trials, a difference substantiated by the experimental contrast of Phase 1 with Phase 3 no-feedback (Primary Task, $F_{1,7} = 153.0$, $p < .001$; Secondary Task, $F_{1,7} = 31.8$, $p < .001$). The effect of feedback, however, examined in the contrast between the two Phase 2 conditions, was only reliable for the Secondary Task ($F_{1,7} = 59.03$, $p < .001$).

Coherence Analysis. The response of performance to the time-varying changes in task difficulty is illustrated in Figures 3 (feedback) and 4 (no-feedback). The error measures were smoothed by averaging tracking RMS error within a sliding 2.4 second window. These smoothed performance records were then ensembled over trials and subjects to produce the data portrayed in Figures 3 and 4. It is evident in these figures that to some extent performance on both tasks "tracked" the time-varying difficulty parameter, an observation that was born out by the analysis of linear coherence.

The linear coherence analysis employed a Fast Fourier Transform algorithm (Reference 4) to transform time variations of primary task alpha and within trial error measures to power spectra in the frequency domain. From these transformed measures, linear coherence values (Reference 5) were computed correlating variations over time between Primary Task difficulty (alpha level) and the performance measures (within trial error averages) on both tasks.

Obtained linear coherence values, assessed at the six lowest frequency values that best account for variations of the task one alpha signal, are displayed in Figure 5. It is evident in Figure 5 that linear coherence is reasonably high in both conditions for both measures. However, primary task difficulty fluctuations seem to induce greater variation in primary task than in secondary task performance. Similarly feedback demonstrated little effect on primary task coherence but a small but consistent effect on the coherence with the secondary task.

DISCUSSION

The most striking aspect of the data relates to the marked deterioration in performance on both tasks that results when the difficulty of one is made variable. This was manifest in a 60-70% increase in RMS error, despite the fact that the average value of the difficulty parameter alpha (= .50) in the variable difficulty tasks was equivalent to its value in the constant condition.

A reasonable explanation for this difference can attribute the performance decrement to the higher level cognitive process required to deal with varying task demands, in an effort to meet performance requirements. In short, the operation of the attention allocation system itself requires processing resources in order to function in continuously reevaluating and responding to resource demand changes.

ORIGINAL PAGE IS
OF POOR QUALITY

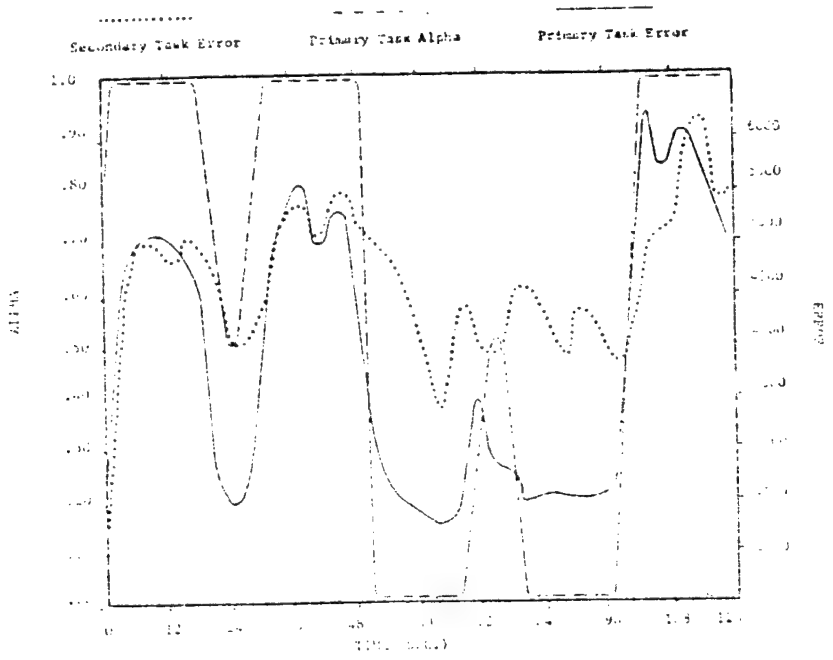

Figure 3. Average time history of within trial dual task error

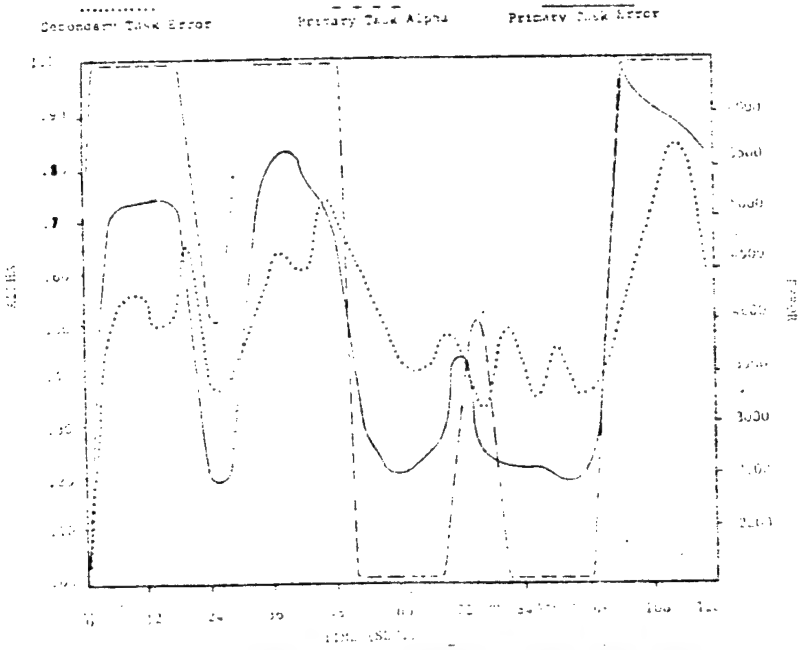

Figure 4. Average time history of within trial dual task error and primary task alpha--no-feedback condition

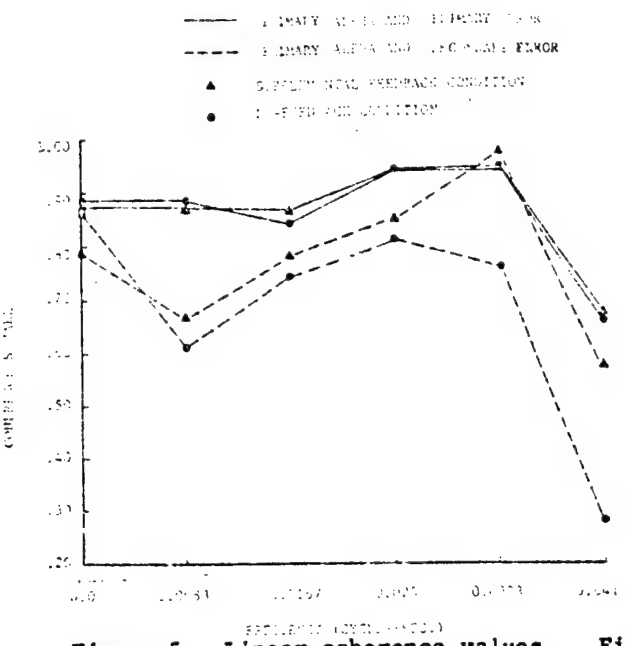

Figure 5. Linear coherence values between alpha and tracking error measures

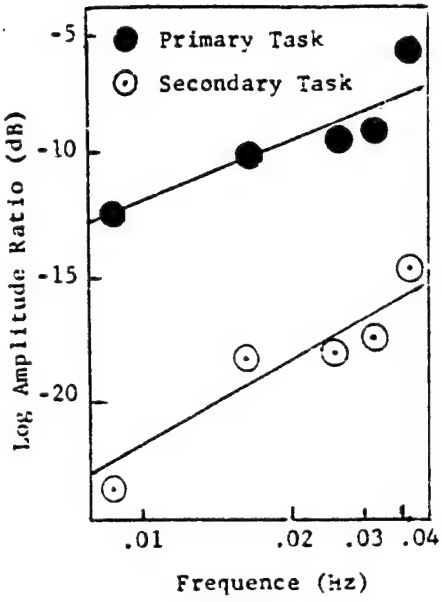

Figure 6. Gain plot of transfer function. Ratio of tracking error (range 0-1.0) to alpha.

Properties of the Allocation System. The proposition that the system may be modelled approximately as a linear dynamic system received some support in the current results, both from the relatively high linear coherence values obtained at the frequencies corresponding to difficulty variation, and on the basis of visual examination of Figures 3 and 4. In addition to the general responsiveness of performance on both tasks to the difficulty fluctuations described above, two additional characteristics of these figures that are not revealed by the coherence analysis are particularly relevant.

1. The transfer function of the alpha-performance data was computed, and the amplitude ratio data are plotted in the gain portion of the Bode plot shown in Figure 6. While the linear correlation of this slope is not high, and the number of points (6) is too few to allow any strong conclusions, the implication of these data is that the response of the allocation system, as inferred from subjects' performance is to lead the difficulty variation as a KS system. That is, performance is sensitive to the rate of change or first derivative of difficulty, rather than to the absolute level of difficulty itself. This behavior is graphically illustrated in the response of primary task performance to the spike increase in alpha at time t = 72 in Figures 3 and 4. This result is in contrast to that observed by Delp and Crossman (Reference 1), who modelled the performance response to difficulty changes (their "meta"-transfer function) as a first order, K/S, or integral system.

The source of this difference is not immediately apparent; it may be attributable to either the repeated nature of the difficulty function employed in the current study that allowed the subjects some degree of anticipation, to the discrete steplike changes of that function, or to the dual task environment used here.

2. Both figures indicate the presence of relatively high frequency oscillations in secondary task performance that do not correspond to variations in alpha. While these oscillations might at first be described as "noise," it should be noted that they correspond very closely, point-for-point in time between the separate and independent replications depicted in Figures 3 and 4. A close correspondance of this nature would not be predicted from random variability in the two replications. Instead, these oscillations bear a resemblance to the frequency response that a second order physical system with spring loading might show to a step or impulse input, approximating the nature of the difficulty changes presently employed. While the precise nature or source of these oscillations cannot be established, their presence nevertheless provides supportive evidence for the linearity, and invariant properties of the allocation mechanism, and encourages further investigation.

Optimality of the Allocation System. The coherence analysis performed indicated clearly that subjects did not behave as the optimum allocator of Figure 1. In marked contrast to the instructions delivered to the subjects, primary task performance was highly sensitive to primary task difficulty. It is therefore important to ask why, in the present results, subjects appeared unable to follow the imposed priority instructions. Wickens and Kessel (Reference 6) showed that when the difficulty of a task (instability tracking) is increased between sessions in a dual task environment, it is possible for subjects to hold that task performance constant--at the expense of secondary task performance. Why then, when difficulty was manipulated within a session in the current experiment, was the severe limitation observed?

It appears unlikely that subjects simply ignored the instructions, as resources clearly were withdrawn from the secondary task to deal with the difficulty increase and were returned when demands were lowered, thus producing the high secondary task coherence measure. Instead it appeared that either the resources withdrawn were not delivered to the primary task, or alternatively that the changes in difficulty were sufficiently abrupt that smooth resource modulation could not occur (i.e., resource adjustment did not have sufficient time to operate). This second hypothesis is supported by visual inspection of Figure 3. Note following the difficulty step increases at times $t = 24$-28 and $t = 96$ seconds that in both instances primary task error begins gradually to reduce as secondary task error undergoes a corresponding increase, as if at this point the subject begins a gradual and appropriate reallocation of processing resources away from the secondary task toward the primary, in accordance with instructions. In fact a rough estimate of the lag between difficulty increases and secondary task error increases places this lag at approximately 2-3 seconds, a value that corresponds reasonably well to the 2.8 second lag observed by Delp and Crossman.

The implication of this observation is that the appropriate resource mobilization might be within the capabilities of the operator to a greater extent, had the difficulty transitions been of the more gradual nature employed by Delp and Crossman.

Feedback. The contrast in performance measures between the augmented feedback and no-feedback conditions indicated further that the operator's limits were manifest in the second stage of the closed loop allocation system--the reallocation of resources--rather than in the first stage--the error evaluation process. When this evaluation process was presumably aided by explicit presentation of the discrepancy between desired and obtained performance, no reliable improvement in allocation behavior was observed, either in the form of a reduction of primary task error, or a reduction in its linear coherence function with alpha. In fact, the only effect of feedback that was observed was a reliable increase in secondary task error, and a corresponding increase in the secondary task coherence measure, as this task apparently became more responsive to the changes in primary task difficulty.

While augmented feedback did not prove to be useful in the current investigation, the conclusion drawn must of necessity be limited. It is quite likely that the difficulty changes were sufficiently dramatic that their presence, and the resulting performance changes, were easily observable by the subjects. Changes of a more subtle nature might have produced a sub-threshold deterioration in performance that could only be detected with the aid of the augmented feedback.

CONCLUSION

The major limitations of human performance in the variable difficulty paradigm, demonstrated in the present results, suggest that this area warrants further exploration. Research is needed to determine the effect on allocation ability of such variables as training, the nature of the difficulty time functions, and the qualitative similarity between the time-shared tasks. Through this research a better appreciation can be gained not only of the mechanism by which attentional resources are allocated, but of the fundamental nature of those resources themselves.

REFERENCES

1. Delp, P. and Crossman, E. Transfer Characteristics of Human Adaptive Response to Time-varying Plant Dynamics. Proceedings 8th Annual Conference on Manual Control. Wright Patterson Air Force Base. AFFDL-TR-72-92. June 1972.

2. Damos, D. and Wickens, C. A Quasi-linear Control Theory Analysis of Time-sharing Skills. Proceedings 13th Annual Conference on Manual

Control. U.S. Government Printing Office, 1977.

3. Wickens, C. and Gopher, D. Control Theory Measures of Tracking as Indices of Attention Allocation Strategies. Human Factors, 1977, 19, 349-366.

4. Shirley, R. Application of a Modified Fast Fourier Transform to Calculate Operator Describing Functions. Proceedings 5th Annual Conference on Manual Control, NASA, SP-215, 1969.

5. Sheridan, T. and Ferrell, L. Man-machine Systems. Cambridge, Mass.: MIT Press, 1974

6. Wickens, C. and Kessel, C. The Effect of Participatory Mode and Task Work-load on the Detection of Dynamic System Failures. Proceedings 13th Annual Conference on Manual Control. U.S. Government Printing Office, 1977.

D39

N79-15627

A MODEL FOR DYNAMIC ALLOCATION OF HUMAN ATTENTION AMONG MULTIPLE TASKS +

Thomas B. Sheridan and M. Kamil Tulga
Man-Machine Systems Laboratory
Department of Mechanical Engineering
Massachusetts Institute of Technology
Cambridge, Massachusetts 02139

Abstract

This paper consists of two parts. The first part describes the problem of multi-task attention allocation with special reference to aircraft piloting, the experimental paradigm we use to characterize this situation and the experimental results obtained in the first phase of our research. A qualitative description of an approach to mathematical modeling, and some results obtained with it are also presented to indicate what aspects of the model are most promising. The second part of the paper consists of two appendices which (1) discuss the model in relation to graph theory and optimization and (2) specify the optimization algorithm of the model.

1. Introduction

We think that an increasingly crucial aspect of piloting an aircraft is "multi-task allocation of attention". The pilot must monitor many more systems than before, most of which are growing in complexity. In earlier days flying the aircraft "by the seat of the pants" was difficult, but piloting was, more or less, a constant task. It was obvious that the pilot could keep track of what was being controlled at what time and how well that was working because he was doing it; he was in the loop and could see or feel it directly.

As systems become automatic the pilot himself tends to lose track of what signals are coming into what subsystem and what response that subsystem is making. Most of the time when everything is normal the automatic systems do just fine. Indeed if we demanded that the pilot actually perform all functions which are now automated it is clear he couldn't do a fraction of such tasks. Yet we expect him to monitor all such functions, and at the first overt alram or even subtle evidence of failure we expect him to be able to render a quick accurate diagnosis of the problem and set it straight.

We call the pilot a "flight manager" or "supervisory controller" and we see him in the image of a corporation manager with legions of dutiful automatic servants doing his will and bringing him information as he desires it. The problem is that the corporate manager has time to ponder and investigate and weigh evidence and consider his decisions. He operates

+ research supported by NASA Grant NSG 2118.

568

PAGE INTENTIONALLY BLANK

on a human time scale: if the corporation manager sees his "production vehicle" about to go bankrupt he has at least a few minutes to decide what's wrong and what to do about it. The flight manager doesn't.

The general research questions implied are:

a) What are the expected behaviors and what are the limits of a person's capability to allocate his attention among many simultaneous tasks of varying importance and varying urgency, as a function of the number of tasks, the general pace at which they occur and other salient parameters?

b) If there is a normative or optimal way a person should perform such a task, can it be specified as a quantitative model, and how close does a trained person come to behaving optimally?

c) What are the implications for improving the design of the man-machine systems in which the pilot must perform such multi-task allocation decisions?

2. Experimental Paradigm

To characterize such a multi-task decision-making situation we have developed a very general experimental paradigm and an associated model. The experimental paradigm requires the subject (or decision-maker DM) to select one at a time from among a number of blocks ("tasks") of different heights and widths displayed simultaneously on a CRT (Figure 1). His selection, made by holding a cursor even with the block "attended to" is in order to maximize his reward, where the earning rate is proportional to the displayed "importance" (indicated by the height of each block) and the "productivity rate" (the rate at which the block decreases in width when "attended to"). Blocks appear at random distances from a "deadline" and move at constant velocity toward that deadline, disappearing when they first touch it. Various task parameters have to do with the frequency at which new blocks appear, the speed with which they move toward the deadline, the variability in importance, the variability in how far from the deadline they first appear, and so on. The toal is to "remove" as much block area as possible.

In one experiment blocks continually appear with exponential distribution in time. In a second experiment all blocks appear at the start of the run; no new ones appear thereafter.

An important feature of the experiment is that blocks do not queue up for service, i.e., if a block reaches the deadline the opportunity to earn its reward is lost. We cannot say for sure, however, whether blocks queue in the operator's mind for attention in correspondence to the fact that at any one instant of time there may be some blocks which are far from the deadline and others which are close. The close ones, of course, may be of little importance, so often it is better to attend to more important tasks which are farther from the deadline in order to ensure that all of the really important ones do get attended to before the deadline.

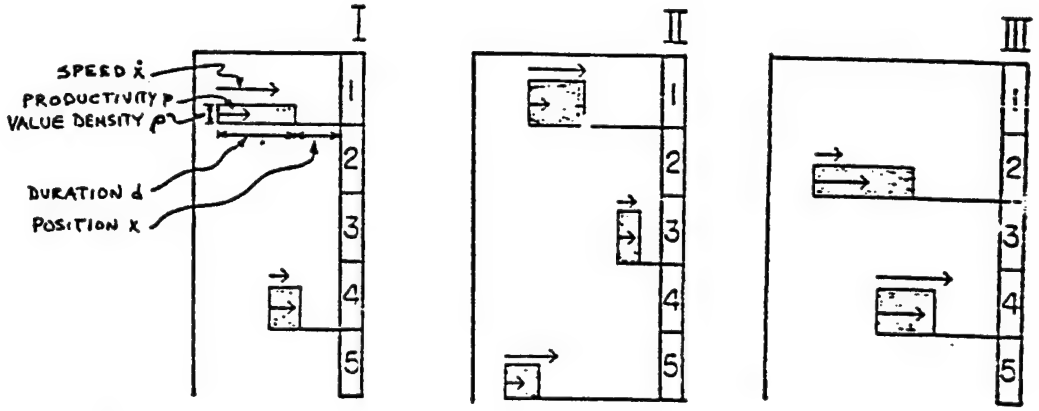

Figure 1. Experimental Computer Display of Moving Blocks Representing Tasks

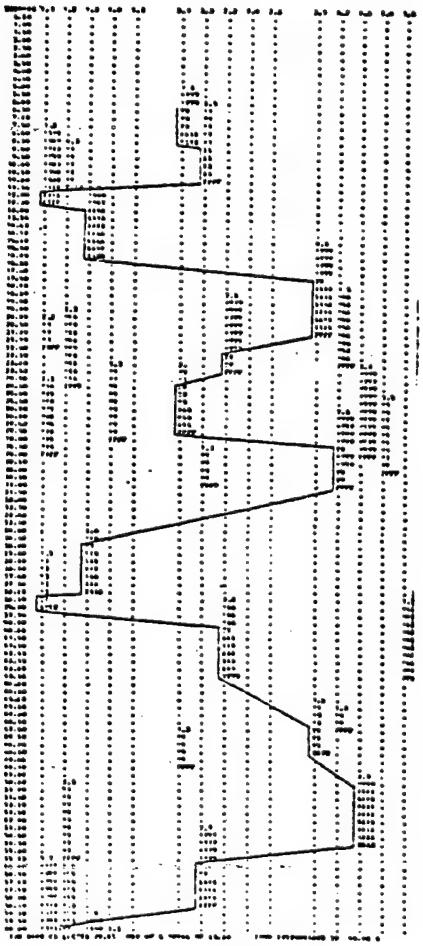

Figure 2. Record of D.M.'s Action Trajectory in Real Time

Figure 2 illustrates a means we have used to obtain a time-plot of which block the subject selects in which queue (column headings). Printed symbols in each column tell the service time the block requires, the time the block will be available, and the value to be obtained.

Having informally experimented with this situation with a variety of parameter combinations we are now in a position to claim that the experiment does seem to simulate various attentional demands which are placed on the pilot. These vary considerably in duration. Some tasks are urgent, but of modest importance; some are urgent and of great importance; some are not urgent and of modest importance; some are not urgent but of great importance to be done before the deadline.

3. Experimental Results

As the first phase of the second author's doctoral thesis, experiments with human subjects have been run with various experimental parameter combinations. Because the number of such possible combinations is so large we have investigated the effects of changing one parameter at a time, relative to a "baseline condition". Table 1 indicates that for all runs the subject worked with 3 queues of blocks (tasks) and runs lasted 400 seconds. The baseline parameters are given above. Seven changes in parameters are indicated below, made one run at a time, all other parameters matching the baseline condition in each case. For each the values gained by each of three subjects, the range of their data, the average, and the total possible are given.

In Table 1 it is seen that a considerably higher speed of blocks moving toward the deadline (2) reduces the score, but not much, compared to the baseline (1). Greater variation in block speed (3) makes little difference. A reduction of interarrival time (4) of blocks means more blocks become available - more opporunity is there for earning a score - but a smaller fraction of these are completed. As the height of blocks (task value densities) become more variable (5) the net earnings are little affected, though the presence of a few very lucrative blocks doubles the total possible score. Giving partial credit (6) for productivity (allocation) on a task when it hits the deadline increases the earnings little more than one percent, which is surprising. Lowering productivity (7) has the most significant effect, as seems intuitively reasonable - but the reduction in score is not quite in proportion to the forced reduction in rate of doing tasks.

4. A Mathematical Modeling Approach

To accompany the experimental task, we have developed a mathematical model which can be run on the computer immediately after any human data run. (The relationship of the model to graph theory in general and the full specification of the model algorithm given in Appendices 1 and 2 respectively).

COMMON CONDITIONS

3 queues, 400 sec duration

BASELINE CONDITION

Task Interrival time, exponential distribution, mean = 20 sec/queue

all tasks appear 5 units away from the deadline

all tasks 2.5 units in duration

all tasks speed toward deadline at 0.1 units/sec.

productivity on all tasks 0.5 units per sec.

value density rectangular distributor 0 - 1 utiles/sec

No partial credit was given in the baseline case.

	CONDITION	% AVAILABLE VALUE GAINED BY SUBJECTS				AVG.	TOTAL POSSIBLE VALUE (UTILES)
		DY	KT	SJ	RANGE		
1	Baseline, B	.913	.931	.942	.029	.929	98.7
2	More speed (2.5 B)	.917	.880	.873	.061	.891	98.7
3	Variable speed (rect, .05-2.5)	.934	.907	.912	.027	.918	98.7
4	Less interarrival time (0.75B)	.803	.809	.795	.014	.802	122.2
5	More varied value density (rect dist 0-2)	.946	.940	.902	.044	.929	197.6
6	Baseline, but with partial credit	.943	.949	.926	.023	.940	98.7
7	Less productivity (0.5B)	.642	.660	.650	.018	.650	98.7

Table 1

Some Experimental Results

The model is essentially a dynamic program which calculates an optimal "attention allocation trajectory" for all the blocks present, and then takes the first step of that trajectory. As soon as each new block appears, the dynamic programming calculation is repeated. The model is constrained by three parameters to make it human-like. The parameters may be adjusted according to various criteria until the model best fits experimental data. One parameter is a time delay τ, simply adjusted to match human motor reaction time plus decision time.

A second parameter is a linear discounting of importance of later blocks in various alternative trajectories which the dynamic programming algorithm compares to determine which trajectory costs least. This discount rate we call β. Zero β means that, in present evaluation of alternative trajectories for future action, what the model earns in the more distant future weights just as heavily as what it earns in the very next step. Large β means the model discounts the future completely and only considers alternative next steps.

A third parameter, γ, is a linear discount rate on distance of blocks (tasks) from the deadline, determined anew at each successive model iteration. Zero γ means that, in deciding what to do next, blocks far from the deadline are just as heavily weighted as those close to it (multiplied by the blocks' individual importance). Large γ means the model only attends to what is close to the deadline. It is a "putting out bonfires" strategy.

It may seem at first reading that β and γ mean the same thing, but this is not true, and in fact it was our experiments which led us to see this distinction: this aspect of the model grew out of the research. The point is that time into the future, with respect to alternative sequences of (planned) action, is quite different from opportunity time available. In other words, the task which is far from the deadline can be done first, and the one which is close to the deadline done later. The only absolute constraint, of course, is that no task can be "done" after it crosses the deadline.

5. Results from the Model

We now have experimented with the model itself on various multi-task situations. In those situations cited above where all blocks appear at the outset we have verified, as expected, that zero β and zero γ are best. All information is known from the start, and an optimal trajectory as determined by dynamic programming is optimal in an absolute sense.

Curiously, this is not true of the experiment where blocks appear continually. Let us recall that the dynamic programming algorithm computes an optimal trajectory based on what blocks are in view at the time, then commits itself to the first step of that optimal trajectory. Thus, if there is discounting in "planning time", optimal may be to do a relatively unimportant but about-to-disappear task, since there is just time

then to complete an important task which is the only one available. But, while doing the unimportant task, suppose a new important task appears with the same opportunity time as the other important one. A choice must be made between the two important tasks, since only one task can be attended to at a time; one important task must be lost. Had the model expected the new important task was coming it would have attended first to the available important task, ignoring the unimportant close-to-dead-line one, and then had time available for the new important one. Instances of this effect are revealed in simulation runs described below.

Our model runs thus far had been made with varying τ values (reaction times) and either varying β or varying γ. τ values have been matched to average reaction times of experimental subjects on a one-run-at-a-time basis.

We have let the computer compare human DM results with computer results separately on the basis of five different criteria: 1) percent value gained for the given run out of the total possible value obtainable; 2) percentage of all completed tasks independent of duration or importance; 3) percentage of time both model and human subject acted on the same tasks at the same time; 4) squared differences between cumulative value gained by model and human, summed over the entire run; 5) squared differences between incremental value gained by model and human for brief time interval, summed over the entire run.

Figures 3 through 7 show examples of five model runs. Figure 3 is for subject KT for the baseline experimental conditions. Figure 4 is for the same subject for a speed 2.5 times as great as the baseline. Figures 5, 6, and 7 are for three different subjects for a productivity half that of the baseline. On each page are ten plots, each plot representing a series of model runs at different values of β (left column, see abscissa below for value of β) with $\gamma = 0$, or model runs at different values of γ (right column) with $\beta = 0$. Points symbolized by X are model runs. The horizontal lines represent human data for the given experimental condition. Circles are comparisons between human and model. Each row is for measures according to a different criterion, as indicated. Thus all points on any vertical slice represent the same model run. Ordinate values of the performance criteria are shown at the right.

Thus, considering the plots in order from top criterion to bottom, the top one is to be maximized (or matched to the line for best fit to human). The X plot of the second one is to be maximized (or matched to the line for best fit to human); the circles on this plot represent % of tasks which are common to model and human, and are to be maximized. The third plot is to be maximized, the fourth and fifth are to be minimized.

For the first criterion (% value gained) it is evident that the model closely approximates the human, at lower values of β or γ doint slightly better (as one would expect for little or no discount) while at higher values doing slightly worse (where the model is not allowed to "plan ahead", i.e., β is large, or is not allowed to consider blocks

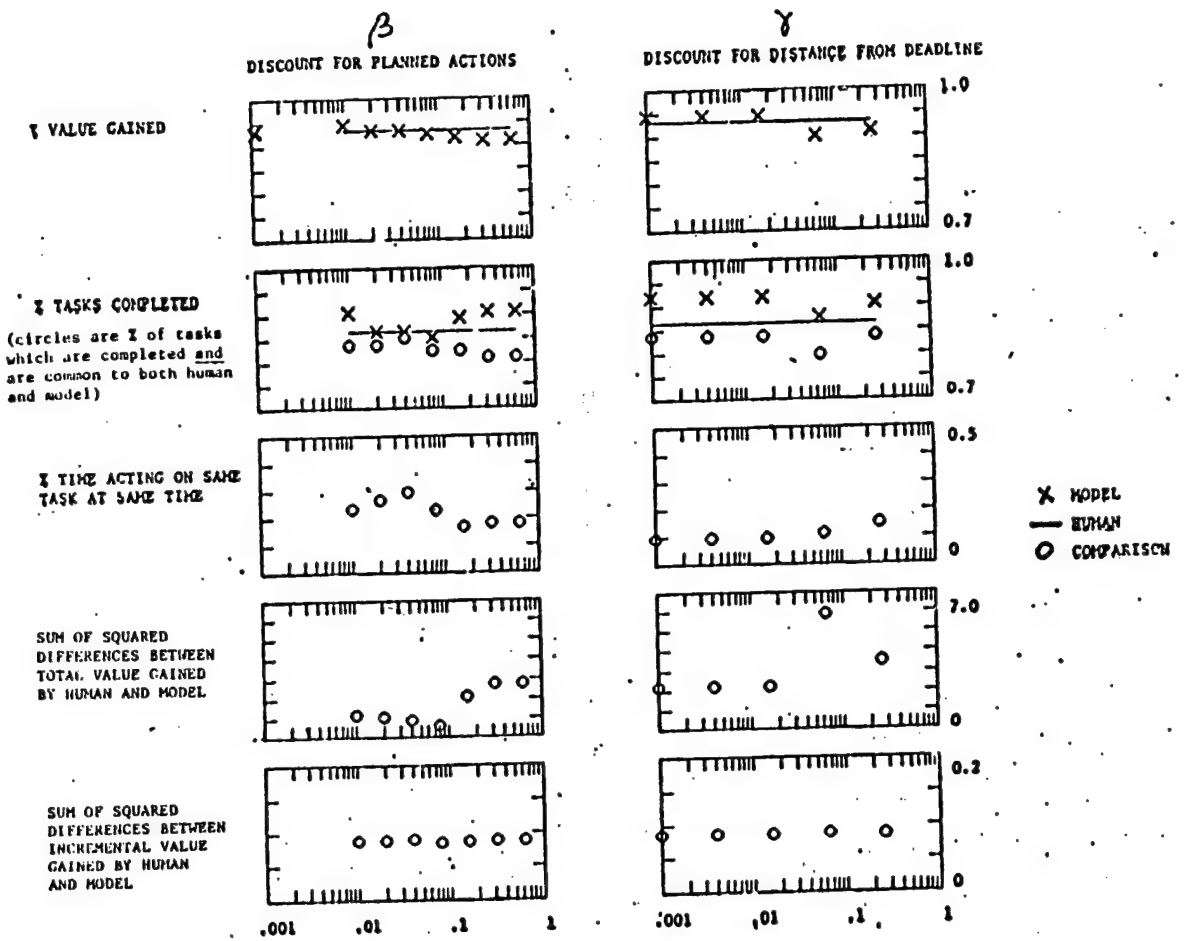

Figure 3. Condition 1. BASELINE:
interarrival 20 sec/queue
speed 0.1 units/sec
productivity 0.5 units/sec
Subject: KT

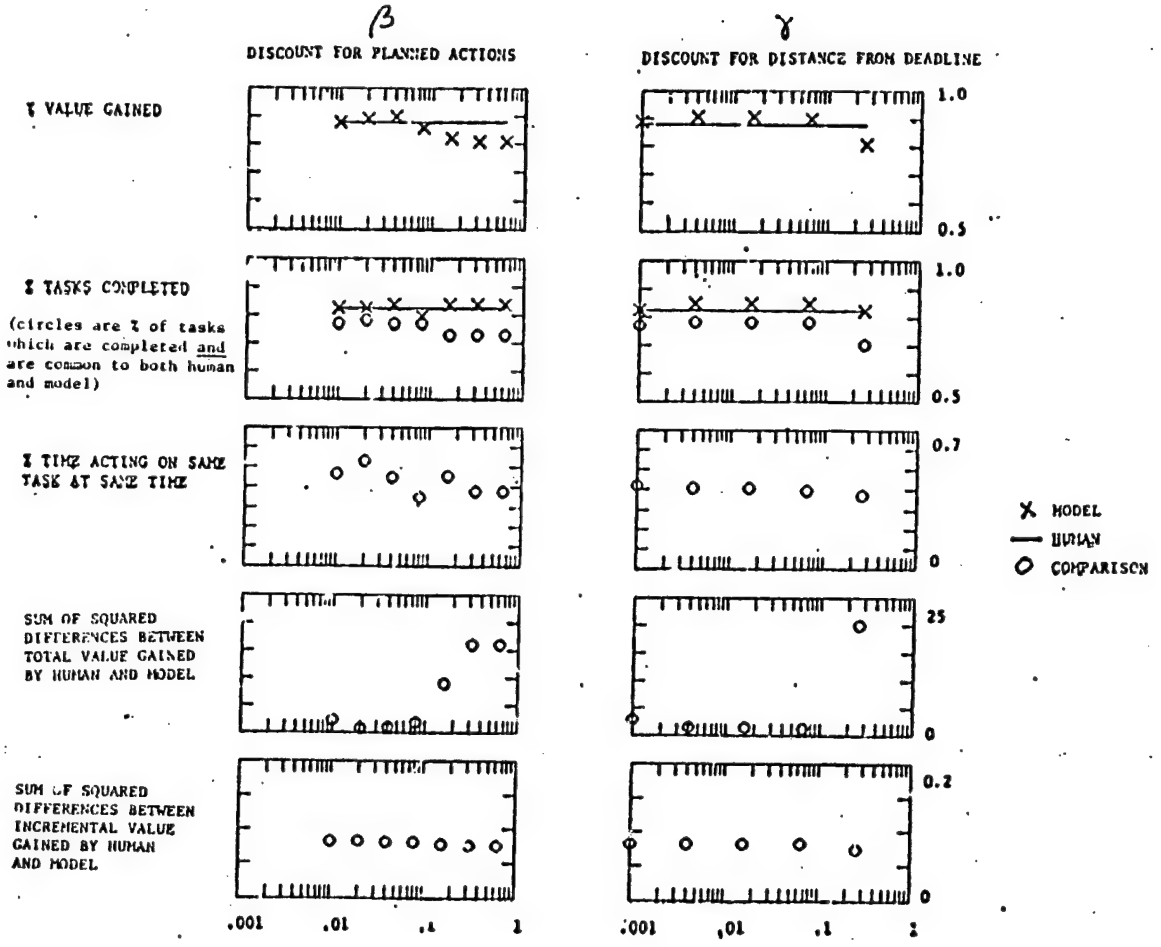

Figure 4. Condition 2
Interarrival 20 sec/queue
speed 0.25 units/sec
productivity 0.5 units/sec
Subject: KT

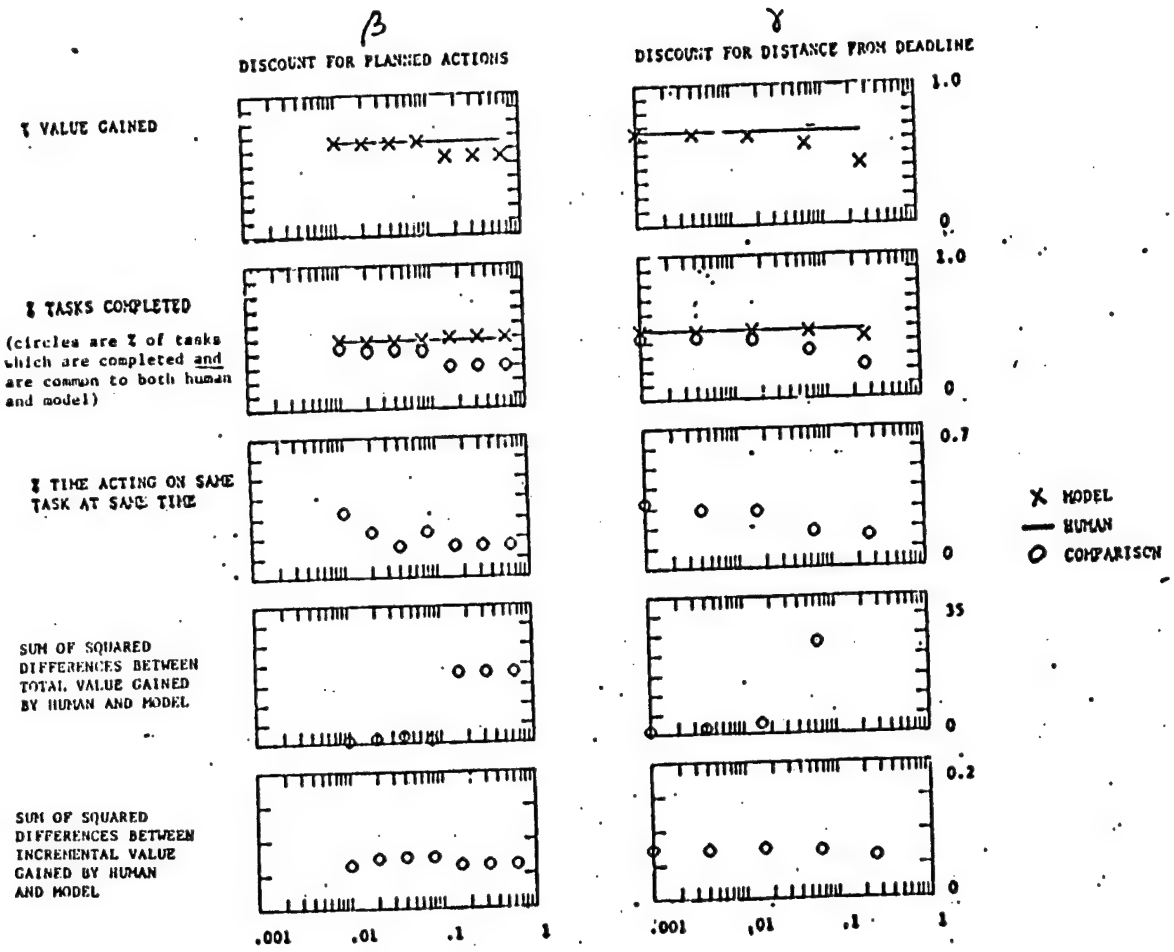

Figure 5. Condition 7
interarrival 20 sec/queue
speed 0.1 units/sec
productivity 0.25 units/sec
Subject: KT

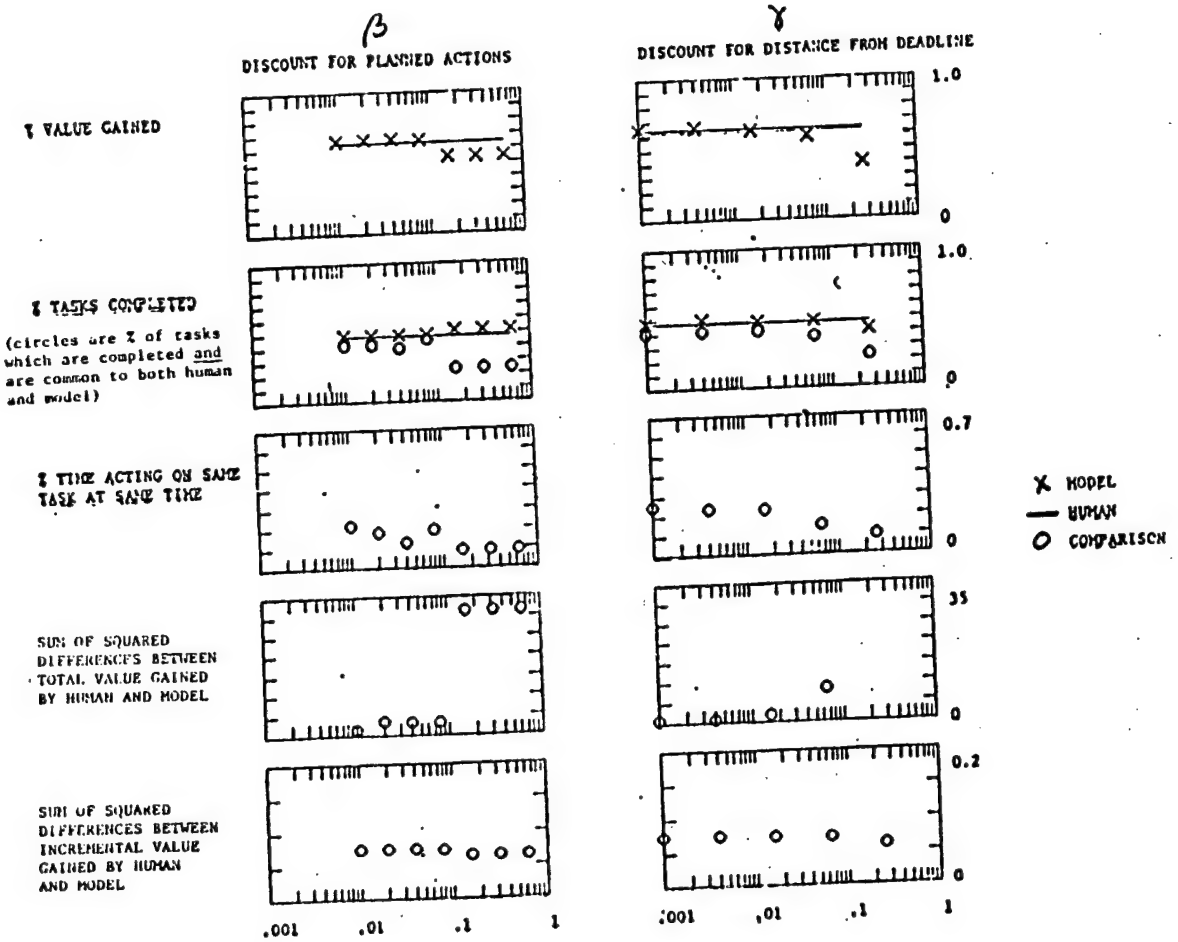

Figure 6. Condition 7.
interarrival 20 sec/queue
speed 0.1 units/sec
productivity 0.25 units/sec
Subject; DY

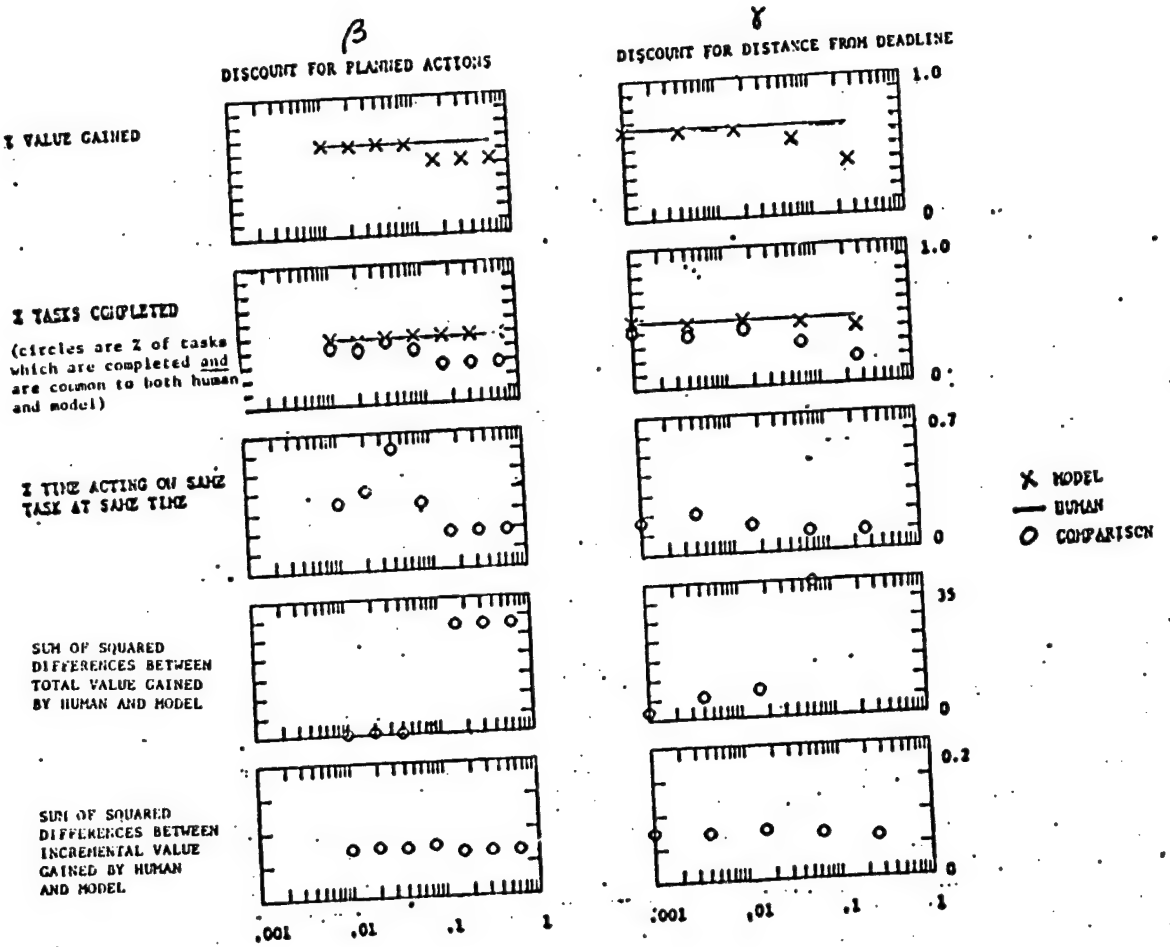

Figure 7 ndition 7.
int ival 20 sec/queue
sp 0.1 units/sec
productivity 0.25 units/sec
Subject: SJ

far from the deadline, i.e., γ is large). Interestingly, however, for data on the first two pages zero β is not quite as good as a slightly larger β. The theoretical reason for this was discussed above, i.e., with a slight discounting of the future the model is more apt to do the most important block first, and be more open to new blocks which have high payoff.

In everyday terms, this suggests that a person with lots to do, little time to do it, and new tasks continually popping up with relatively short deadlines, should not plan too far ahead. Mostly he should do the most important thing first, ignoring the closest-to-deadline factor. As he has time to see what's coming farther into the future and doesn't expect many new opportunities to be popping up, he should plan ahead.

With respect to the second criterion (% tasks completed) it is interesting that the model and human match precisely in a mid range of β which is also the best match of model to human for tasks which are common to both model and human. This suggests (1) that a β in this range is a good candidate for a model, (2) that the higher task completion capability of the model in other β ranges, without concommitant increase in total value gained, meant it was wasting time on unimportant tasks. The γ fits for this criterion are not so good or so consistent, and we begin to see that γ seems not to be a very meaingful parameter.

As for the next parameter, % of time acting on the same task at the same time, it appears that the β curve peaks at approximately the same value for several of the subjects, but again the γ curve is not very interesting.

The curves for the final two criteria seem to have little to offer, except that the fourth curve consistently takes a jump (gets worse) for β values at 0.1 or larger.

Further experiments will seek to refine the model, the fitting criteria, and possibly add an estimator of future tasks to the optimization algorithm.

Appendix 1. The Model in Relation to Graph Theory*

The paradigm described in the paper will result in a graph $G_T(t) = G(N;A)$ with N nodes and A arcs, where each node represents a task and arcs represent the transfer properties between these tasks. Note that rewards associated with different nodes can be different and delay-(time-) dependent. Also the processing (or service) and availability times of the nodes and the transfer times between them can be different. Therefore in a reward-time (r-t) coordinate framework we have graph $G_T(t)$ as shown in Figure A1.

Note that in Figure A1 τ values represent transfer times between nodes, which incidentally can be direction-dependent, such that precedence constraints can be imposed. t^R, t^D and t^P are "ready-time", "deadline time and "processing time", respectively. Note that when the rewards associated with the tasks are constant until they hit the deadline, the r-t curve associated with a node will be as shown in Figure-A2a. For the case in which the DM can get partial credit, however, the rewards, rather than being Fixed-Loss, will be as shown in Figure-A2b.

In the Figure A2 t^S is the slack time, i.e. the latest time; if, during which the task is completed all the reward associated with the task can be gained. Note that "time available" is deadline-time minus ready-time:

$$t^A = t^D - t^R.$$

One interesting observation that can be made from Figure-A1 is that in $G_T(t)$ graphs there may not be enough time to get the rewards of all nodes N. In fact, we can infer from the same figure that the best schedule that can be chosen in the particular graph $G_T(t)$ is $\Pi = (2,1,4)$ which does not include node (task) 3.

At this point we digress and consider this sequencing problem in relation to other common combinatorial problems like Job-Shop Scheduling, Traveling Salesperson, etc. (Golden and Magnanti, 1977).

We can differentiate the sequencing problems listed in Table-A1 according to the following criteria:

1) Will multiple journeys between the nodes be counted multiple?
2) Can we add extra nodes?
3) Can the rewards associated with the nodes be delay-dependent?
4) Can the transfer delays between different pairs of nodes be different?
5) Is it imperative to return to the base node?
6) Is it necessary to satisfy the above requirement before a certain delay, T_R?
7) Can the graph G, desribing the problem change dynamically in time?

*See list of symbols at end of Appendix 2.

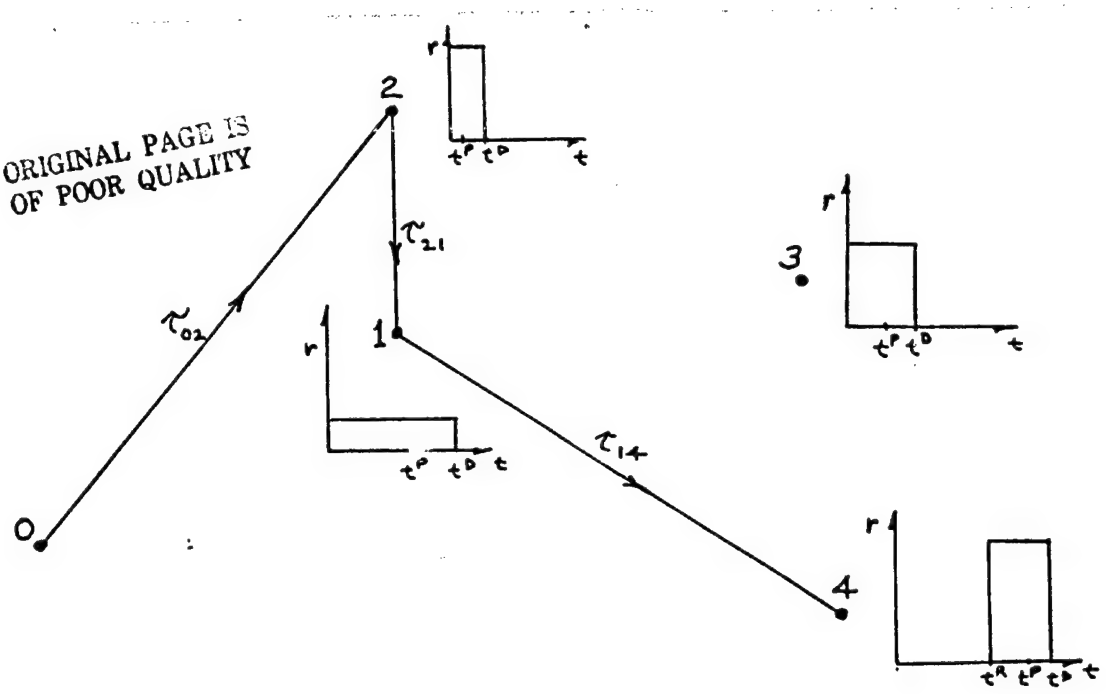

FIGURE A1. A Schedule π = (2,1,4) for Multi-Task Attention Allocation on Graph $G_T(t) = G (N ; A)$.

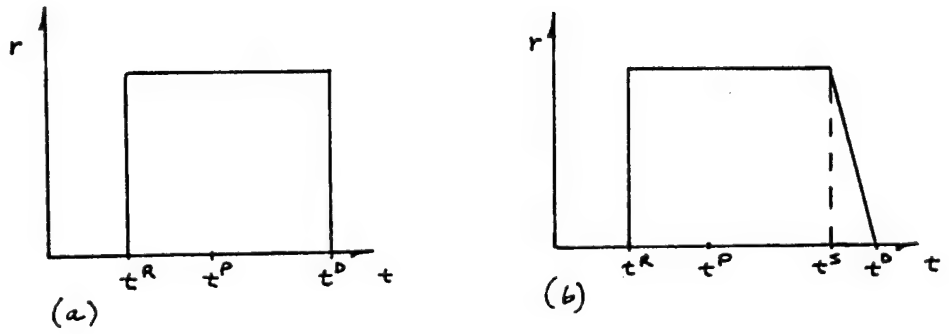

FIGURE A2 Reward-Time Curves for a Task (a) when no Partial Credit is Given, and (b) when Partial Credit is Given.

Using these criteria we have listed some common combinatorial optimization problems with two new ones:

a) Minimum Spanning Trees, MST (Kruskal, 1956)

b) Steiner Tree Problem, STP (Nijenhuis & Wilf, 1975)

c) Job-Shop Scheduling, JSS (Elmaghraby, 1968 and Sahni, 1976)

d) Hamilton Cycle, HC; alias the Traveling Salesperson Problem (Held & Karp, 1962)

e) Open Tulga-Path, OPT; alias Multi-Task Attention Allocation,

f) Closed Tulga-Path, CTP

Note that in Table-A1 the indicator '0' means that the particular criterion need not be satisfied for the problem at hand, while indicator '1' is for the opposite case, with 'N/A' indicating that the criterion is not applicable for the problem. Figure-A3 is a schematic representation of some of the problems. OTP describes Multi-Task Attention Allocation.

Problems vs. Criteria:	MST	STP	JSS	HC	OTP	CTP
1	0	0	1	1	1	1
2	0	1	N/A	N/A	N/A	N/A
3	0	0	1	0	1	1
4	1	1	0	1	1	1
5	0	0	0	1	0	1
6	0	0	0	0	0	1
7	0	0	0	0	1	1

Table-A1. Properties of Various Sequencing Problems.

Before returning to the Multi-Task Supervisory Control, the reader can observe from Figure-A3 that, if the requirement was to serve all the nodes (tasks) with minimum number of controllers (or processors or vehicles or people, etc.) another controller might have been assigned to node-3 in Figure-A3(iii), and the OTP problem will become an advanced version of the 'Bin-Packing Problem'. (Johnson, 1974) The reader may note here the case of computer aiding (2nd. controller) of the human operator (1st. controller). (Rouse, 1977) Similarly in Figure-A3(iv) an extra vehicle can serve node-3 and come back to the base node before T_R; however, unless the return time T_R is sufficiently large, node-4 cannot be served whatever the number of vehicles, but as T_R increases 3, then 2 vehicles will be enough to serve all the nodes: the CTP then becomes an advanced 'Vehicle-Routing Problem". (Golden, 1976)

We can see from Figure-A3 that Multi-Task Attention Allocation Paradigm is representable by the OTP Combinatorial Problem when we consider that node 0 (base node) is where the DM currently is, and 4 tasks

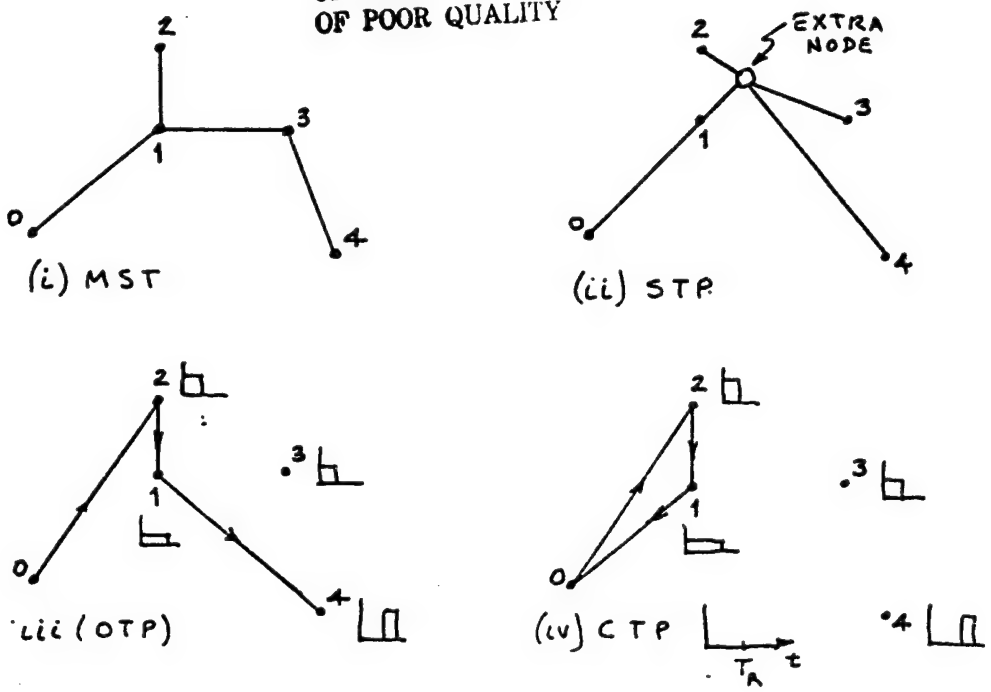

FIGURE A3 Graphical Representation of Some Sequencing Problems

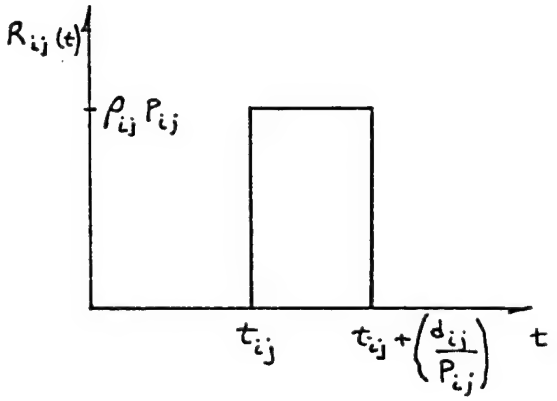

FIGURE A4. The Return, for a Task, as a Function of Time for the Partial Credit Mode

are (or will be) available with different properties. The DM will then act on the first task of the optimal schedule, $\Pi^\circ = (2,1,4)$, i.e. task 2.

Note however, that new tasks may appear on this graph $G_T(t)$ probabilistically according to the interarrival rates and with the task parameters explained in the paradigm section, and the thing to be maximized is the reward gained at the end of the experiment, so that tasks that are going to appear cannot be ignored. That is to say: since graph $G_T(t)$ is time-dependent, then the optimal schedules $\Pi^\circ(t)$ on them are time-dependent too.

Appendix 2. Optimization Algorithm of the Model

In choosing his control, i.e., which task to at upon, we can model the DM as an optimal controller who maximizes his expected returns over a planning horizon. (Koopmans, 1964). In particular, the DM will act to maximize his expected total returns over a finite planning horizon, T, with a discount function $B(\beta, t)$:

$$\max_{\Pi} \quad r(\Pi) = E\left[\int_0^T R_\Pi(t)\,dt \right]$$

where $$R_\Pi(t) = \sum_{(i,j)\in\Pi} R_{ij}(t) \cdot B(\beta, t)$$

in which the summation is over all the tasks (i,j), which collectively make up the ordered task set, schedule Π, that the DM expects to act upon over his planning horizon. $R_{ij}(t)$ is the return he gets for acting on (or completing) the task (i,j) during (or at) time t.

For the case in which the DM gets credit continuously while acting on a task, the $R_{ij}(t)$ will be as shown in Figure-A4.

In Figure-A4, t_{ij}, P_{ij}, d_{ij}, p_{ij} represent the time at which the DM plans to start acting on the task, the value density of the task, the duration of the task, and the productivity of the DM for the task (i,j), respectively.

If however, the DM is going to get (full) credit only after successfully completing a task, then the $R_{ij}(t)$ will be as shown in Figure-A5.

The DM, in effect, will choose at each decision point a schedule $\Pi^\circ = (\Pi_1^\circ, \Pi_2^\circ, \ldots)$ that he intends to act upon to maximize his expected returns, and then he will actually act upon the first task Π_1°, in this ordered set of tasks.

It is probable and acceptable that he might have to give up on acting on some tasks when their 'available times' are small - due to their high speed and/or due to their proximity to the deadline - or when they have comparatively low value densities, especially in compe-

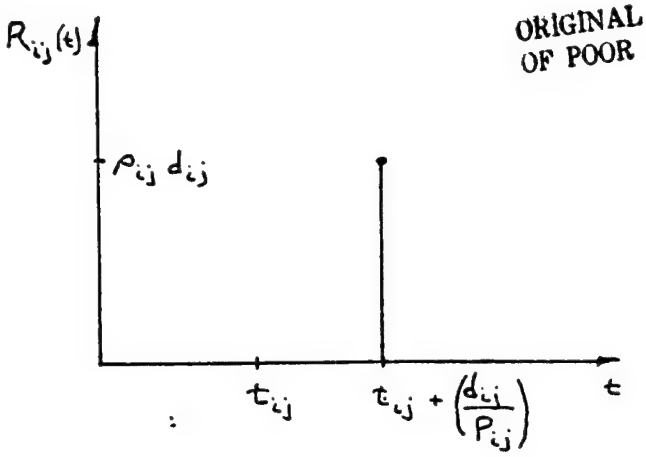

FIGURE A5. The Return, for a Task, as a Function of Time for the No-Partial Credit Mode.

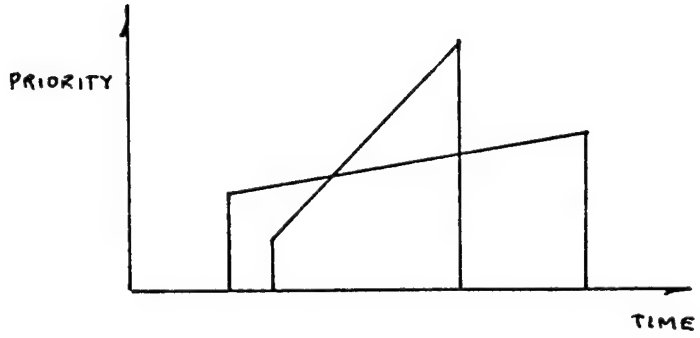

FIGURE A6. Increasing Priorities of Different Tasks as They Wait to be Served.

tition with other simultaneously available tasks which are preferred in these respects. Another important parameter, of course, is the transfer time $\tau_{ii'}$, between the queues. He has to consider the fact that he will end up getting no credit for a period of time when he transfers his control from the i.th queue to the i'.th one.

The algorithm for finding the optimal schedule of tasks Π°, to act upon is:

Algorithm T_PATH

Input (usage, T_R, $\tilde{X}_{ijk}$, $\tau_{ii'}$, B, G)

The input parameter 'usage' indicates whether an OTP or a CTP is desired, and if it is a CTP, T_R is used as the required return time to the base node. τ is the transfer-delay time matrix between the queues of tasks and B, and G are discount functions on future returns and on tasks away from the deadline-tasks with larger slack-times -, respectively.

Note that the system state tensor $\tilde{X}_{ijk}$ specifies the various task parameters for each given instant of time like:

1) whether the task is available (display) or not, L_{ij} (=1 or 0)
2) the return associated with the task as a function of time, $R_{ij}(t)$
3) the processing/service time of the task $t^{P}_{ij}(t)$
4) the 'available time' of the task, $t^{A}_{ij}(t)$

Output optimal schedule Π°, and discounted present value $r(\Pi^{\circ})$ and completion time $c(\Pi^{\circ})$ associated with it.

Step-1 [Initialize]

for i = 1 to I do
for j = 1 to J_i do
while L_{ij} = 1 do /* is the task available ? */
transform (i,j) to ℓ and
generate the tuple ($r(\ell)$, $c(\ell)$)

$r(\ell) = R_{\ell}(t = 0)$
$c(\ell) = \tau_{o\ell} + t^{P}_{\ell}(t = 0)$

end
end

Note that $R_{\ell}(t) = \int_{\tau=t}^{\infty} R_{ij}(\tau), B(\beta, \tau) \cdot d\tau$

Furthermore, the tasks currently available are summed to give N, which is also the maximum number of stages, M, the optimal schedule can have.

Step-2 [Generate schedules that are m stages deep]

for m = 2 to M do

generate all m-member-subsets = S

and for each task $\ell \in S$
generate the $(r(\Pi)\ ,\ c(\Pi))$ tuple(s)
-where $\Pi = \{\Pi'\ ,\ \ell\}$, i.e. schedule Π is schedule Π' with task ℓ at stage m.
-for each $\Pi' = \text{order}\{S-\ell\}$, i.e. for each $\Pi' \overline{\overline{=}} \{S-\ell\}$,
-where the '$\overline{\overline{=}}$' operator tests whether each member of one set is also contained in the other. (Weinberg, 1971)

$$r(\Pi) = r(\Pi') + R_{\ell}(t = c(\Pi'))$$

$$c(\Pi) = c(\Pi') + \tau_{\ell'\ell} + t^{P}_{\ell}(t = c(\Pi'))$$

where ℓ', is the last task - task at stage (m-1) in schedule Π'.

Eliminate schedules according to the rules:

1) Eliminate the tuples which are infeasible, that is credit cannot be obtained from the last task ℓ in schedule Π before it reaches the deadline; or if usage is CTP, before $(T_R - \tau_{\ell o})$, where $\tau_{\ell o}$ is the transfer time between the queue of task ℓ and the base node 0.

2) Eliminate schedule Π^1, if there is a schedule Π^2, such that:

$$\Pi^1 \overline{\overline{\subseteq}} \Pi^2$$

and $\ell^1 = \ell^2$ or queue of ℓ^1 = queue of ℓ^2

-ℓs are the last tasks -at stage m- in the respective schedules-

and $r(\Pi^1) \leq r(\Pi^2)$

and $c(\Pi^1) \geq c(\Pi^2)$

3) Eliminate the schedules that are less than (m-1) stages deep.

end

Step-3 [Return to the base node if usage is CTP]

if usage = Closed Tulga-Path then
for all schedules Π do

$$r(\Pi) = r(\Pi) + R_{o}(t = c(\Pi))$$

$$c(\Pi) = c(\Pi) + \tau_{\ell o}$$

with ℓ being the last task of schedule Π.

end

Step-4 [Optimal]

The optimal schedule Π° is the one with the property:

$$r(\Pi^\circ) > r(\Pi) \quad \text{for all } \Pi \neq \Pi^\circ.$$

and if

$$r(\Pi^\circ) = r(\Pi) \quad \text{then } c(\Pi^\circ) < c(\Pi)$$

Note that when the rewards of nodes are delay-independent then this algorithm reduces to the dynamic programming formulation of the Traveling Salesperson:Problem. (Held & Karp, 1962). On the other hand, when transfer delays between all tasks are equal and when rewards of all tasks are Fixed-Loss, i.e. constant up to a certain delay (time) and then zero, then the solution will reduce to Job-Shop Scheduling with Deadlines. (Elmaghraby, 1968 and Sahni, 1976).

Several things should be clarified at this point. First, if the model is permitted to get partial credit, as in Figure-A4, then the tasks which will hit the deadline before they can be complted will also be included in the optimization, although with their returns $R_{ij}(t)$ appropriately adjusted to reflect the gain that can be obtained from them before they disappear.

Another point that should be emphasized is that, since all the dynamics of the tasks are known a-priori by the algorithm (and also by the human), there is no need to repeat the optimization unless there is a new task arrival; when no new information is presented, the optimal plan, i.e., the currently optimal schedule will be followed in real time as the tasks in this linked list are compieted. It has also been proven theoretically (McNaughton, 1959) that there is nothing to be gained by shifting attention from one task to another and back again, even in the case of no time penalties for doing so. On the other hand, if after a new task arrival the first task in the new optimal schedule is not the task that is currently being attended, then the model will pre-emptively leave the current task to serve the first task in the new optimal schedule. However, the task that was pre-emtively abandoned might still be in the new schedule, and conditions permitting may eventually be re-attended.

The effect of $G(\gamma, t^s)$ will be to adjust the return $R_{ij}(t)$ for acting on task (i,j), by changing the effective value density of the task (i,j) as:

$$R_{ij}(t) = R_{ij}(t) \cdot G(\gamma, t^s_{i,j})$$

where t^s_{ij} is the slack-time of the task, i.e., $t^s = \max.\{0, \lfloor (x/\dot{x}) - (d/p) \rfloor\}$, with $x, \dot{x}, d, p$ representing the current position, speed, current duration and the productivity associated with the particular task, respectively.

Note that the idea of weighing tasks according to their initial priorities plus incremental priority increases as they wait in a queue (Carbonell, 1966 and Jackson, 1965), as shown in Figure-A6, corresponds to the $G(\gamma, t^s)$ function, where the initial priority is determined by the initial proximity of the task to the deadline, and this priority increases as the task approaches the deadline.

It is interesting to note also that, as the speeds of the tasks approach zero, i.e., the deadlines are at infinite future time - and if the transfer times between all the tasks are equal, then the DM is modeled to choose the new task to act upon, according to:

$$\max_{(i,j)} \rho_{ij} p_{ij}$$

This, of course is the familiar result from the Queueing Theory (Smith, 1956) when we consider the productivity of the DM, p_{ij}, as the service rate μ_{ij} and the value density of the task (i,j) ρ_{ij} as the negative cost per unit time delay c_{ij}:

$$\min_{(i,j)} c_{ij}\mu_{ij} \text{ where } c_{ij} < 0$$

List of Symbols

G	graph
t	time
τ	transfer time
$\boldsymbol{\tau}$	dummy time
r	reward available at a node (task)
R	reward gained for a given plan
Π	a schedule — $r(\Pi)$ total discounted return of a schedule; $c(\Pi)$ completion time of a schedule
Π°	that schedule which is optimal
T_R	deadline time for return to base node
T	planning horizon
B	discount function on future returns
β	discount parameter (rate in this case) on future returns
G	urgency discount function
γ	urgency discount parameter (rate in this case)
I	total number of queues
J_i	total number of tasks in queue i.
ℓ	combination of i & j for any task
M	maximum number of stages that optimal schedule can have
m	stage index
d	duration
$\dot{x}$	speed
ρ	value density
p	productivity
x	position

t^P processing time

t^R ready time

t^D deadline time

t^A available time

t^S slack time

References

Elmaghraby, S.E., "The One Machine Sequencing Problem with Delay Costs", J. Ind. Eng., Vol. 19, No. 2, p. 105-108, February 1968.

Golden, B.L. and Magnanti, T.L., "Deterministic Network Optimization: A Bibliography",Networks, Vol. 7, No. 2, p. 149-183, Summer 1977.

Golden, B.L., Ph.D. Dissertation, Sloan School of Management, M.I.T., 1976.

Held, M. and Karp, R.H., "A Dynamic Programming Approach to Sequencing Problems", J. SIAM, Vol. 10, No. 1, p. 196-210, March 1962.

Johnson, D.J., Ph.D. Dissertation, Mathematics Department, M.I.T., 1974.

Koopmans, T.C., "On Flexibility of Future Preference", in Human Judgements and Optimality", (eds. M.G. Shelly II and G.I. Bryan), John Wiley 1964.

Kruskal, J.P., Jr., "On the Shortest Spanning Subtree of a Graph and the Traveling Salesman Problem", Proc. Amer. Math. Soc., Vol. 7, No. 1, p. 48-50, February 1956.

McNaughton, R., "Scheduling with Deadlines and Loss Functions", Management Sci., Vol. 6, No. 1, p. 1-12, October 1959.

Nijenhuis & Wilf, Combinatorial Algorithms, Academic Press, 1975.

Rouse, W.B., "Human-Computer Interaction in Multitask Situations", IEEE Trans. Syst. Man and Cybern., Vol. SMC-7, No. 5, p. 384-392, May 1977.

Sahni, S.K., "Algorithms for Scheduling Independent Tasks", J.ACM, Vol. 23, No. 1, p: 116-127, Jan. 1976.

Smith, N.E., "Various Optimizers for Single-Stage Production", Naval Res. Logist. Quart., Vol. 3, No. 1, p:59-66, Mar. 1956.

Weinberg, P., "Betriebswirtschaftliche Iogik", Bertelmans Universitaetsverlag* Duesseldorf, 1971.

D40

N79-15628

PERCEPTUAL FACTORS INVOLVED IN PERFORMANCE OF AIR TRAFFIC CONTROLLERS USING A MICROWAVE LANDING SYSTEM

Gary Gershzohn*
San Jose State University Foundation
San Jose, Calif.

SUMMARY

This study investigated performance of air traffic controllers using a Microwave Landing System (MLS). Eight professional radar air traffic controllers acted as subjects and performed their normal duties within the constraints of the experimental design and simulation. The task involved the control of two simulated aircraft targets per trial, in a 37.0-km (20-n. mi.) radius terminal area, by means of conventional radar vectoring and/or speed control. The goal was to insure that the two targets crossed the Missed Approach Point (MAP) at the runway threshold exactly 60 sec apart. The effects on controller performance of the MLS configuration under wind and no-wind conditions were examined.

The data for mean separation time between targets at the MAP and the range about that mean were analyzed by appropriate analyses of variance. Significant effects were found for mean separation times as a result of the configuration of the MLS and for interaction between the configuration and wind conditions. The analysis of variance for range indicated significantly poorer performance under the wind condition. These findings are believed to be a result of certain perceptual factors involved in radar air traffic control (ATC) using the MLS with separation of targets in time.

INTRODUCTION

This study was designed to investigate some of the perceptual factors which affect performance of air traffic controllers using an MLS to control the landing of aircraft. The MLS is a new type of landing guidance aid and is still in an experimental phase. When fully operational its primary purpose will be to facilitate the safe an expeditious flow of a new generation of aircraft into airports with an efficiency that cannot be duplicated today. The implementation of the MLS will require an alteration of the physical structure of airways and the ATC system.

A radar scope was simulated on a cathode-ray tube (CRT) and displayed

---

*This author's research was supported by NASA Grants NGL 05-046-002 and NSG-2269 to San Jose State University.

a terminal area with the MLS. The controllers were presented with several air traffic situations and were required to separate targets. The experimental goal was to identify some of the perceptual factors involved in and the performance of controllers using the MLS.

Although the MLS is one of the most recent developments in ATC, and as such has not been the subject of lengthy investigation, research in aeronautics has placed considerable emphasis on developments in human factors aspects of ATC. The literature contains numerous reports on topics such as mental processes of controllers (1), workload (11), and the role of automation (10). The general picture of the evolution of ATC responsibilities and required performance has also been outlined (8, 9). By and large, data on basic human perceptual processes specifically involved in ATC has received only scant attention. Therefore, this study, in part, examined pertinent psychological literature on visual motion perception in order to analyze performance of controllers using the MLS.

METHOD

The geometric arrangment of the MLS as viewed on the radar scope is significantly different from conventional Instrument Landing Systems. Whereas current Instrument Landing Systems employ a single, straight course to the runway, the complex MLS in this experiment was composed of five courses, both straight and curved. In order to evaluate the effects of this particular configuration on controller perception and performance, a specific task was developed.

Subjects

Eight professional air traffic controllers served as paid participants. All had extensive experience in radar ATC either with the military or FAA at high traffic density locations.

Apparatus

A 25.4- by 25.4-cm (10- by 10-in.) CRT display was generated by an Evans & Sutherland Line Drawing System interfaced with a Digital Equipment Corporation PDP 11/40 computer. Figure 1 illustrates the simulation that represented the ATC scope with the MLS. The scale of 2.9 km/cm (4 n. mi./in.) was close to standard usage.

Aircraft targets were represented by triangles measuring .45 cm (.18 in.) on each side. Each symbol was labeled by a single alphanumeric tag for use by the controller in identifying and tracking targets. The targets appeared to move in a manner not unlike those on conventional radar ATC scopes. Simulated aircraft had several basic movement capabilities: (a) entry along an MLS route at the periphery and complete tracking to the MAP, (b) automatic landing and exit from the display at the MAP, (c) heading change at a rate of 3°/sec, and (d) acceleration at a rate of 3.7 km/hr

(2 knots)/sec (equivalent to .0003 cm/sec^2 on the CRT). Altitude information was not required for this experiment.

The computer generated movement of targets was controlled by the subject. His verbal commands were transmitted by a standard microphone. Receiving and acknowledging these ATC instructions was the experimenter in the role of pilot of the simulated aircraft. Communication between the controller and experimenter reflected standard ATC operations and phraseology. Upon receipt of the controller's commands, the experimenter input the information to the PDP 11/40 computer via a high speed interface device which then altered the flight dynamics of the simulated aircraft accordingly.

Procedure

The task required that the controller control two targets per trial in order to achieve the desired goal of 60-sec separation between targets at the MAP. At the beginning of each trial one target appeared at the start of the VIKING route at the 37.0-km (20-n. mi.) hash mark at an airspeed of 464 km/hr (250 knots). It was followed approximately 60 sec later by a second target at the same airspeed which entered either along the VIKING route or one of the other four MLS routes. Since the second target traversed one of the five routes in following the first target, there were five different perceptual relationships between the two targets. These will be called path combinations of target movement. For example, a target entering on the VIKING route followed by a target on the GEMINI route would be called the VIKING-GEMINI (V-G) path combination.

The controller was instructed to adjust the movement of one or both targets by use of speed and/or directional control in order to insure that the two targets crossed the MAP exactly 60 sec apart. Each target automatically reduced its airspeed to 167 km/hr (90 knots) by the time it reached the 9.3-km (5-n. mi.) fix; this was in keeping with normal aircraft operating limitations. The airspeed of 167 km/hr (90 knots) was then maintained to the MAP. As the controller perceived the continuing relationship between the targets, he had to make a decision to issue or not to issue ATC instructions to change the relative movement or position of one or both in order to reach the goal of 60-sec separation. The airspeed and heading of either target could be changed only during the time that target was between the 37.0-km (20-n. mi.) fix and 9.3-km (5-n. mi.) fix; the controller had received instructions that no control was to be applied to a target after it had passed the 9.3-km (5-n. mi.) fix. When the second target reached the MAP the trial was at an end. The actual separation in seconds was recorded by the computer and used as the raw data for that trial. In order to measure performance in several situations, trials were conducted under wind (360^0 at 46 km/hr (25 knots)) and no-wind conditions.

An introductory session familiarized the controller with the general nature of the experimental purposes and MLS. Written instructions were supplied. Three practice trials with no-wind and three with wind before the respective experimental trials were used for the purpose of acquainting the controller with the appearance of the MLS and movement dynamics of targets. At the conclusion of each practice trial, the controller was told exactly how much separation in time existed between the two targets as they successively

crossed the MAP. This gave the controller an indication of the spatial and temporal relationships between targets under his control. This feedback, however, was not given during experimental trials.

Experimental Design

Two dependent variables were studied: (a) the mean separation time between targets at the MAP, and (b) the average range about that mean. A 5 X 2 X 2 factorial design for repeated measures was used to analyze the data. The five path combinations served as five levels of one independent variable. Two wind conditions constituted conditions of a second independent variable and the order of presentation of wind conditions was the third independent variable. The wind treatment condition was presented first to one half of the controllers and the reverse order was administered to the other half. There were 15 experimental trials under the no-wind condition and another 15 under wind. The same path combination was administered to each controller three times.

RESULTS AND DISCUSSION

The mean of the three separation times for each controller was calculated and constituted the data on which the analysis of variance was performed. For the purpose of noting the variability of controller performance, a second analysis of variance was performed on the range of the separation times per subject. Results of the analysis of variance for means are shown in Table 1 and for range in Table 2. A summary of the means and average ranges for each condition is presented in Table 3 and Table 4, respectively.

The effect of the order of presentation of wind conditions was not statistically significant. Therefore, for the purpose of analysis of other results, these data were combined.

The analysis of variance for means showed a significant difference between path combinations ($F = 3.84$; $df = 1, 10$; $p < .05$). This indicated that controller performance in attaining 60-sec separation between targets was affected by the different path combinations. The analysis of variance for range did not indicate any significant effects ($F = .98$; $df = 4, 24$; $p > .05$) due to different path combinations (fig. 2).

The mean separation times between targets under the no-wind condition (60.6 sec) and under the wind condition (57.0 sec) were close to the 60-sec target value, yet the magnitude of the average range of times about these means was quite large (fig. 2 and 3). Under the no-wind condition, the average range was 19.6 sec, and under wind, 43.2 sec. The analysis of variance for range showed a statistically significant difference in controller performance as a function of wind condition ($F = 12.42$; $df = 1, 6$; $p < .05$). The analysis of variance for means revealed no significant results ($F = .48$; $df = 1, 6$; $p > .05$). While the overall mean separation time between targets under the no-wind and wind condition were not significantly different, the average ranges about these means were. Both the no-wind and wind mean times indicated a high degree of accuracy on the average in attaining the 60-sec

target value. But the 19.6 and 43.2 sec ranges showed the accuracy reflected in the mean times to be a result of the high separation times between targets cancelling out the low separation times, especially under the wind condition.

These results will be discussed from three points of view: (a) the perceptual factors involved in performance of controllers using the MLS, (b) controller performance using time as a relevant separation criterion rather than distance, and (c) the implications of the findings for future development of the ATC system with the MLS.

The controller's perception of the ATC situation constitutes an important factor in understanding the results. Three primary perceptual factors are considered to be of importance in the controller's task in this experiment: (a) spatial separation of targets, (b) figure-ground (map overlay) effects, and (c) the perception of wind-generated accelerated motion. The latter point appeared to be most significant in evaluating the data and requires special consideration.

The mean separation time under the no-wind condition was closer to the 60-sec target value than under the wind condition. This was due primarily to the controller's difficulty in taking into account the differential effects of wind on ground speed as the target changed heading. The difficulty in perceiving the onset of of accelerated motion had several consequences for controller performance. First, the reduction of the ground speed of a target, either in the automatic speed reduction phase of the approach or as a result of the wind, altered the separation between it and the other target. Should the velocity change have gone undetected, the result would have been a new amount of separation between targets of which the controller was completely unaware. Obviously, a continuous series of such changes by one or both targets would lead to inaccurate and erratic performance such as was evident under the wind condition. Second, the perception of acceleration of one or both targets required an evaluation by the controller of the actions necessary to maintain or change the relationship between the targets. This necessitated the ability to make an accurate prediction of the future progress of the target undergoing acceleration. It has been shown by Gottsdanker (4-6) and Gibson (3) that future target position during constant velocity motion can be predicted with considerable accuracy. However, predicting target position during accelerated motion was found to be generally inaccurate and appeared to be based on the last perceived velocity rather than on acceleration (2, 7). The apparent inability of the controller to successfully predict the accelerated motion of targets, and hence future positions in time, was associated with high variability in performance. Third, the changes in ground speed of a target traversing that part of the MLS course that curved toward the airport were difficult to assess. The controllers reported that the point in time when the ground speed began to slow was not immediately apparent nor was it possible to accurately predict the future motion of targets. The large magnitude of the change in ground speed in those MLS courses with long curved segments made accurate perceptions difficult and inaccurate performance most evident in the results. The accelerations that occurred within the curving courses were most significant under the wind condition and posed a situation which the controllers were unable to gauge precisely.

On the basis of discussions with the controllers after the experiment, it would appear that the controllers' attempt to separate the two targets by

60 sec at the MAP was not accomplished merely by estimating time. Rather, they used a time-distance conversion (distance = airspeed x time). This was not surprising since controllers perform their normal ATC duties using mileage not time as the separation criterion, and consequently they were faced with a novel and difficult task.

Two factors involving time and distance conversions were involved. The first concerned a principle that specific separation in time between two targets will remain constant if the ground speeds of the two targets remain unchanged. Secondly, separation in time will remain constant when ground speeds change if, and only if, the place and rate of change of ground speed of one target is identical to that of the other. The realization of these phenomena led to another point. Since time separation was held constant between the targets during the automatic speed reduction (under conditions heretofore described), the establishment of 60-sec separation between targets prior to the commencement of the speed reduction (which entailed accelerated motion) was seen as desirable. Once the automatic speed reduction began, the controller had no means of adjusting the airspeed of a target. This required action to be taken earlier in order to have control capability of a useful and realistic magnitude and to set up a relationship between the two targets when they proceeded at a constant velocity. Since the judgment of constant velocities is more accurate than accelerated velocities, the controller was able to judge the separation in time more precisely when targets moved at constant rates.

The results of the present experiment indicate that the control of aircraft using an MLS with curved courses and temporal separation may be subject to a number of limiting factors. The different path combinations had an effect on both the mean separation between targets and the variability of the controller's performance under the wind condition. Under the no-wind condition, there was little difference in performance by path combination. The controllers' comments indicated that they attributed this to their careful and precise attention to the position of the targets with reference to hash marks and the calculation of time-distance equations. The wind condition posed more serious difficulty since the use of hash marks and the time-distance equation did not provide information which could be used to compensate for the perceptual factors associated with the wind.

In consideration of the perceptual factors involved in controller performance, it seems unlikely that the addition of any appreciable workload (in the form of more targets) would permit positive and accurate control. One of the most important influences on performance is workload. It may be measured by the number of targets a controller has to deal with at one time. By current standards in the current ATC system, with complicating intersecting and converging routes, a light workload might be five targets; a heavy workload might reach as high as 15 targets. In this experiment, which employed only two targets at one time, the workload was minimal yet the variability in performance with wind was high. This was true in spite of the fact that the controller had enough time to calculate time-distance relationships for the two targets. With more than two targets, it is not likely that the controller would be able to maintain the mental strategies of control found in this experiment. Furthermore, an increase in workload that would reflect a busy terminal area would make accurate and successful separation between aircraft, with time as the separation criterion, a most unlikely occurrence.

Yet, innovations in ATC systems, cockpit displays, and possible alterations of the MLS configuration may alleviate some of the problems that faced controllers in this simulation. Such improvements may allow conventional radar ATC using the MLS with a real world workload.

REFERENCES

1. Bisseret, A.: Analysis of Mental Processes Involved in Air Traffic Control. Ergonomics, vol. 14, 1971, pp. 565-570.

2. Filion, R. D. L.: On the Visual Detection of Accelerated Motion. Unpublished doctoral dissertation, Princeton Univ., 1964.

3. Gibson, J. J.: Research on the Visual Perception of Motion and Change. In Second Symposium on Physiological Psychology. Office of Naval Research: 1958.

4. Gottsdanker, R.: The Accuracy of Prediction Motion. J. Exp. Psych., vol. 43, 1952, pp. 26-36.

5. Gottsdanker, R.: A Further Study of Prediction Motion. Amer. J. Psych., vol. 68, 1955, pp. 432-437.

6. Gottsdanker, R.: The Ability of Human Operators to Detect Acceleration of Target Motion. Psych. Bull., vol. 53, 1956, pp. 477-487.

7. Gottsdanker, R; Frick, J.; and Lockard, R.: Identifying the Acceleration of Visual Targets. Brit. J. Psych., vol. 52, 1961, pp. 31-42.

8. Litchford, G.: Aeronautics and Air Traffic Control. NASA CR-1833, 1971.

9. Roberts, L.: Future Trends in Air Traffic Control Technology. Paper presented at the 19th Conference of the International Air Transport Association (Dublin, Ireland), 1972.

10. Secretariat of the 19th Conference of the International Air Transport Association: An Assessment of the Expected Aircraft Movement Demand on Typical Air Routes and for Representative Terminal Areas, and the Consequent Impact on Air Traffic Handling Capabilities. Paper presented at the 19th Conference of the International Air Transport Association (Dublin, Ireland), 1972.

11. Sperandio, J.: Variations of Operator's Strategies and Regulating Effects on Workload. Ergonomics, vol. 14, 1971, pp. 571-577.

TABLE 1

Analysis of Variance for Mean Separation Time Between Aircraft Targets at the MAP

Source	df	MS	Error Term	F
Order of presentation of wind condition (A)	1	18.15	D	.03
Path combination (B)	4	589.68	B X D	3.83[a]
Wind condition (C)	1	258.13	C X D	.48
Subjects (D)	6	555.18		
A X B	4	46.23	B X D	.31
A X C	1	200.66	C X D	.37
B X C	4	532.82	B X C X D	6.48[b]
B X D	24	163.66		
C X D	6	542.16		
A X B X C	4	63.02	B X C X D	.77
B X C X D	24	82.19		

[a] $p < .05$

[b] $p < .01$

TABLE 2

Analysis of Variance of Range About Mean Separation Times between Aircraft Targets at the MAP

Source	df	MS	Error Term	F
Order of presentation of wind condition (A)	1	68.45	D	.07
Path combination (B)	4	556.32	B X D	.98
Wind condition (C)	1	11,092.05	C X D	12.42[a]
Subjects (D)	6	929.25		
A X B	4	451.45	B X D	.80
A X C	1	344.45	C X D	.39
B X C	4	551.98	B X C X D	1.03
B X D	24	565.02		
C X D	6	892.91		
A X B X C	4	178.89	B X C X D	.33
B X C X D	24	536.10		

[a] $p < .05$

TABLE 3

Summary of Mean Separation Times (in seconds)
between Aircraft Targets at the MAP by
Path Combination and Wind Condition

Path combination	Wind condition		
	no-wind	wind	across no-wind/wind
V-V	62.6	71.5	67.1
V-G	58.1	56.2	57.1
V-A	59.1	41.4	50.2
V-P	65.4	52.4	58.9
V-M	57.7	63.4	60.6
Across all path combinations	60.6	57.0	58.8

TABLE 4

Summary of Average Ranges (in seconds) about Mean Separation Times between Aircraft Targets at the MAP by Path Combination and Wind Condition

Path combination	Wind condition		
	no-wind	wind	across no-wind/wind
V-V	19.1	24.8	21.9
V-G	20.9	54.5	37.7
V-A	20.1	42.9	31.5
V-P	24.0	45.1	34.6
V-M	14.1	48.8	31.4
Across all path combinations	19.6	43.2	31.4

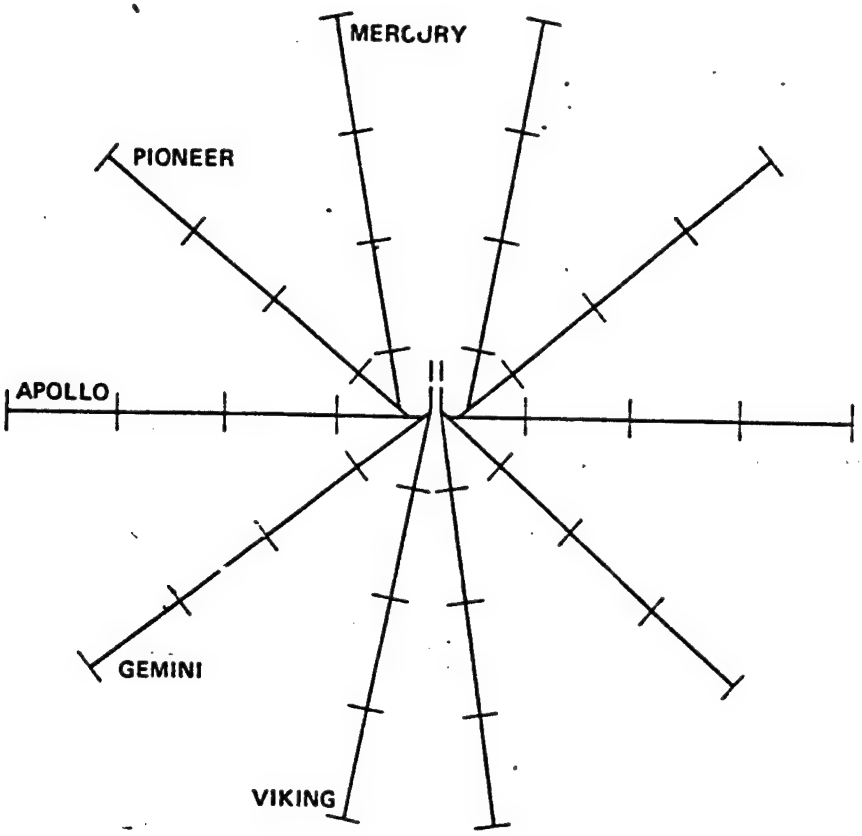

Figure 1.- MLS route configuration as seen on controller's display.

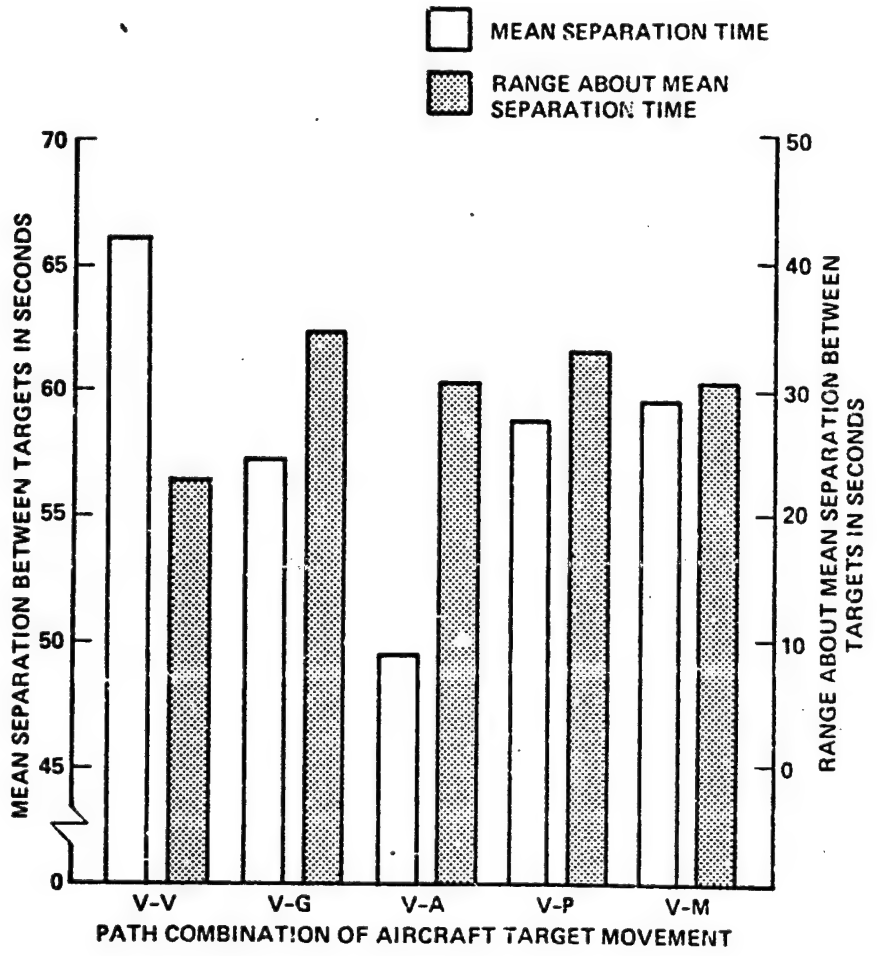

Figure 2.- Mean separation time and range about mean separation time between aircraft targets at the MAP by path combination.

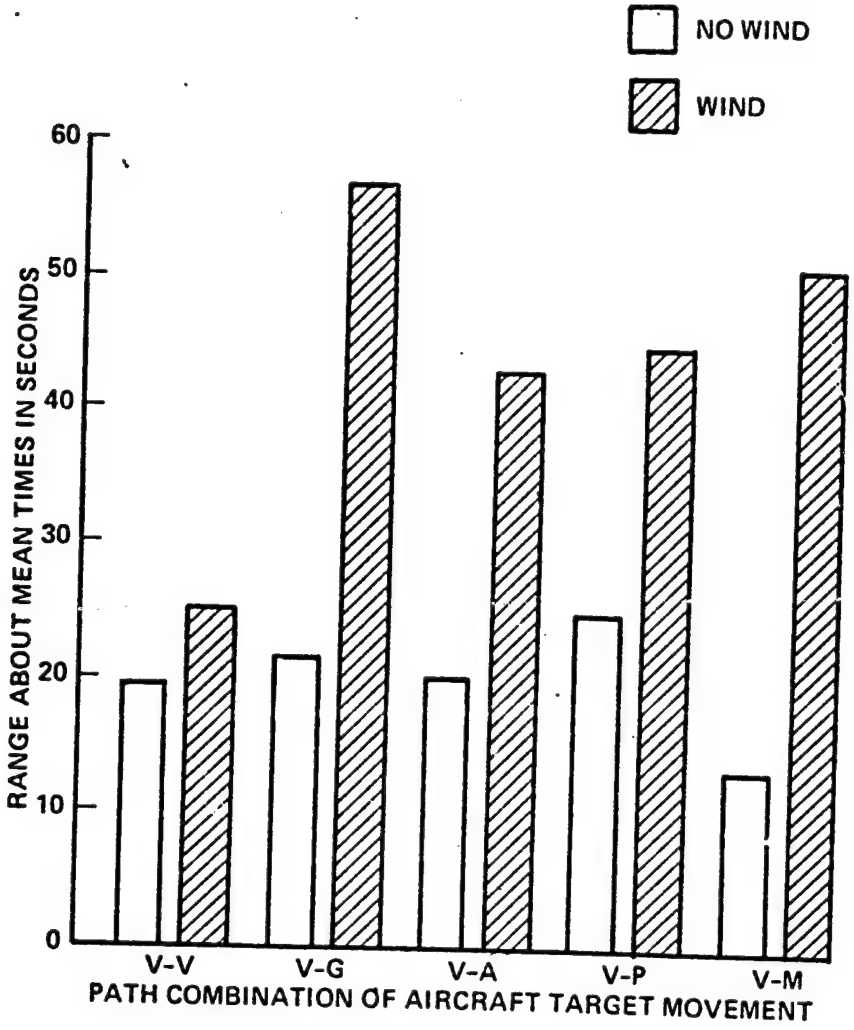

Figure 3.- Average range about mean separation time between aircraft targets at the MAP by path combination and wind condition.

SESSION K: DECISION-MAKING BEHAVIOR AND MODELING

Chairman: R. Curry

D41

N79-15629

THE EFFECTS OF ALCOHOL ON DRIVER PERFORMANCE IN A DECISION MAKING SITUATION*

By R. Wade Allen, Stephen H. Schwartz,
Anthony C. Stein and Jeffrey R. Hogge

Systems Technology, Inc.
Hawthorne, California

ABSTRACT

This paper reviews the results of driving simulator and in-vehicle field test experiments of alcohol effects on driver risk taking. The objective was to investigate changes in risk taking under alcoholic intoxication and relate these changes to effects on traffic safety.

The experiments involved complex 15 minute driving scenarios requiring decision making and steering and speed control throughout a series of typical driving situations. Monetary rewards and penalties were employed to simulate the real-world motivations inherent in driving. A full placebo experimental design was employed, and measures related to traffic safety, driver/vehicle performance and driver behavior were obtained.

Alcohol impairment was found to increase the rate of accidents and speeding tickets. Behavioral measures showed these traffic safety effects to be due to impaired psychomotor performance and perceptual distortions. Subjective estimates of risk failed to show any change in the drivers' willingness to take risks when intoxicated.

INTRODUCTION

Alcohol has been shown to be overrepresented in accident statistics (Refs. 1 and 2). Recent surveys have subdivided accident causation into a variety of factors including vehicle, environmental and driver factors (Ref. 3). Driver behavior can be further subdivided roughly into perception, psychomotor skill and higher cognitive factors including decision making. Alcohol effects on driver psychomotor skill in steering control have been previously studied in some detail (Ref. 4), and the objective of the work reported here was to investigate the alcohol impairment in driver decision-making situations.

*This work was supported by the Office of Driving and Pedestrian Research, National Highway Traffic Safety Administration, Department of Transportation. The views expressed in this paper are those of the authors and do not necessarily represent those of the National Highway Traffic Safety Administration.

608

An important aspect of this research was to determine whether driver risk taking changes with Blood Alcohol Concentration (BAC) and, further, to partition the changes in risk taking into changes in driver perception, psychomotor factors and the acceptance of risk. These three factors combine to determine performance in a decision-making task and, singly or in combination, give rise to performance that we objectively observe as risk taking. Take, for example, the situation where a driver has run a red light. This could be due to the driver's having misperceived his speed or the time interval of the amber light; it could also be due to the fact that he took too long in making a decision and thus his reaction time for accelerating or braking to a safe stop was delayed; or the driver may merely have elected to accept the risk of running a red light because he was motivated to minimize the delays caused by stopping.

In previous research on driver risk taking, no consistent approach has been used to differentiate between the various factors contributing to decision task performance. Several studies have measured driver risk taking, which has been found to increase with BAC (blood alcohol concentration) (Refs. 5-7). More recently, however, it was found in a gap acceptance task using significant rewards and penalties that intoxicated subjects did not consciously accept greater risks (Ref. 8). Impaired psychomotor skill did result in degraded performance, however.

The inconsistency in past research has been in the definition and simulation of driver risk taking, the analysis of all behavior components in risk taking, and the use of tangible risks. Based on a review of the literature, the following elements were felt to be essential to adequately determine the effects of alcohol on driver decision making: 1) division of driver behavior into perceptual, psychomotor and cognitive components; 2) use of rewards and penalties to simulate real-world risks (e.g., accidents, tickets, lost time); 3) use of tasks which simulate the temporal pressure of normal driving. The experimental methods for accomplishing these goals are discussed below.

EXPERIMENTAL METHODS

Approach

This research was accomplished in two separate experiments, the first a simulator study and the second involving field validation trials. The two experiments were designed to be as similar as possible in order to allow direct comparison of results. The specific setup for each was as follows.

Simulation. The simulation was configured to present a plausible driving scenario, requiring both steering and speed control in driving decision-making situations. The functional details of the simulation have been described previously (Ref. 9). Basically, the simulator consisted of an actual car cab and controls with a two lane roadway drawn on a 0.25 x 0.32 m

(10" x 12")* CRT mounted on the cab cowl 0.76 m (30 in.) in front of the driver as illustrated in Fig. 1. Equations of motion for the car steering and speed control were solved on an analog computer, which generated car heading angle, lateral position, and forward speed in response to steering wheel, accelerator and brake commands. The car motion variables drove special purpose electronic circuits which generated a dashed line two lane roadway [3.65 m (12 ft) lane width] with 0.76 m (2.5 ft) shoulders. The roadway was presented in correct perspective, but reduced scale (roughly two-thirds) in order to fit on the CRT and yet subtend a 22 degree perceptual field of view.

Driving events were controlled by a paper tape programmer at a rate proportional to forward speed. From a cross section of the many typical driving decision-making situations three events were selected that could be easily implemented in a laboratory simulation. The functional details of each event and related measurements are described further on.

Field Validation. This study was conducted in an instrumented vehicle described elsewhere (Ref. 10). Special equipment was added to allow the car to interact with the test course. A photo detector mounted on the vehicle sensed reflective strips on the test course and triggered a programmer which controlled event sequences in the field course driving scenario. Instrumentation was also added to allow experimenter feedback in scenario conditions and subject progress. Details of the field setup are illustrated in Fig. 2.

Driving Tasks and Measurements

The driving scenario was designed to allow implementation both in the simulator and on the field course. A variety of events were considered, and events that could be conveniently mechanized were selected for each experiment as indicated in Table 1 (Ref. 11). A signal light situation was selected as a classical single stage decision event. Vehicle control in a curve was selected to investigate the large number of single vehicle loss of control accidents that occur with alcohol involvement (Ref. 12). The remaining situations selected from Table 1 involve divided attention, a driver behavior factor which has been shown to be sensitive to alcohol impairment (Ref. 13). Details of the driving tasks and overall scenario were as follows.

Signal Light. A model signal light was mounted directly above the horizon of the roadway display in the simulator (Fig. 1a), and an actual signal light was set up on the test course in the field validation study (Fig. 2a). Signal timing was controlled as a function of car speed and distance from the intersection in order to control the time-to-go to the intersection. Several timing conditions were used ranging from a sure stop to a sure go. Details of the signal timing and task kinematics have been presented elsewhere (Ref. 11).

*Customary units were used for the measurements and calculations of this study.

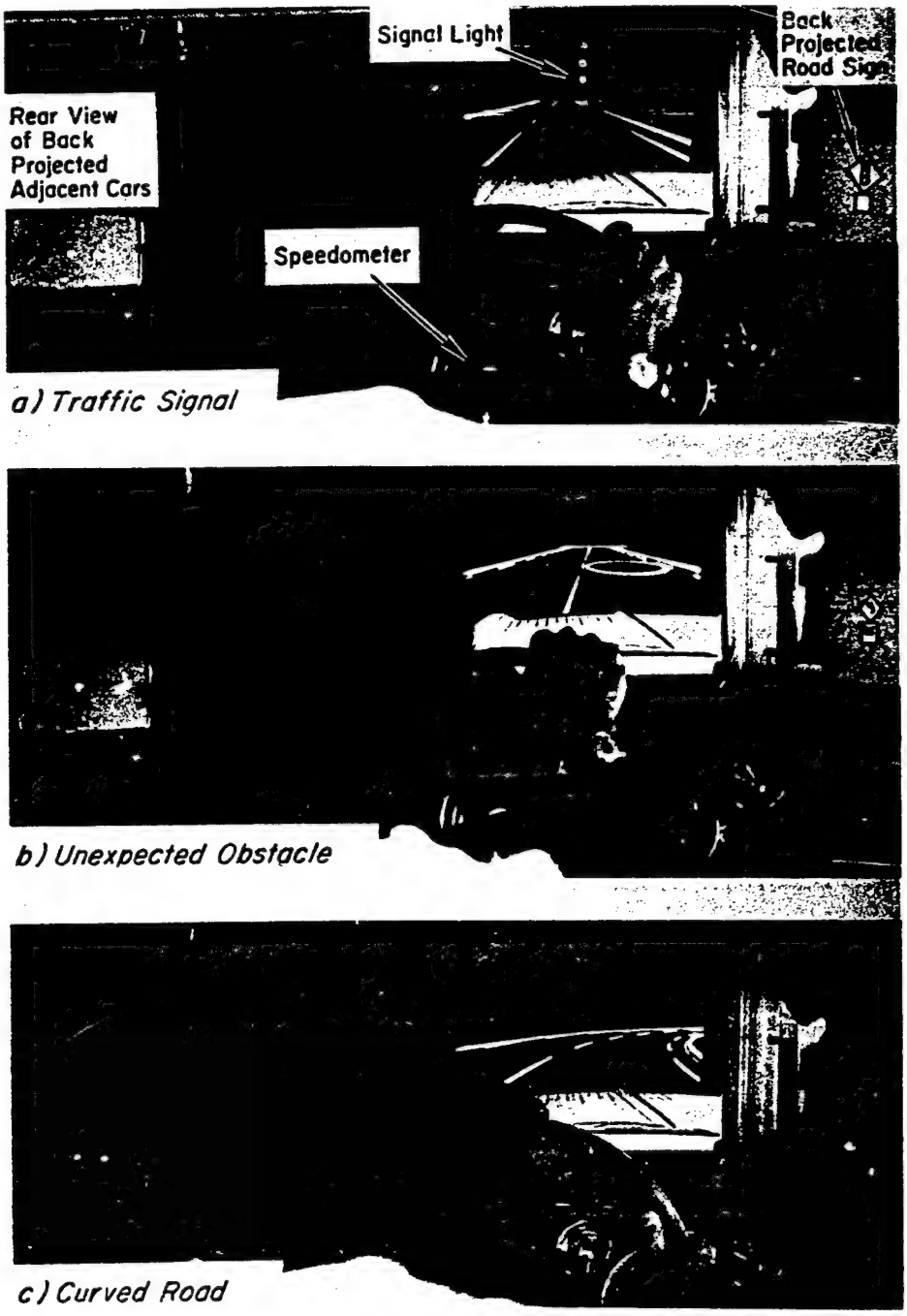

Figure 1. Simulation Setup

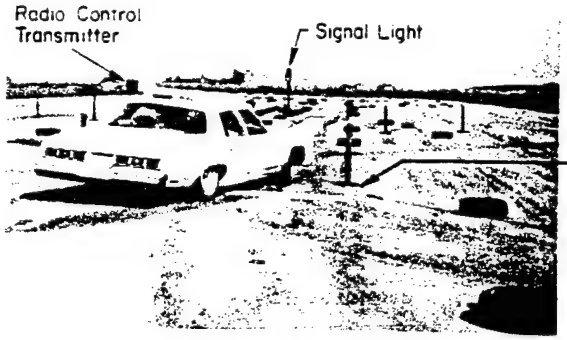

a) Course Layout Showing Car Approaching Signal Light

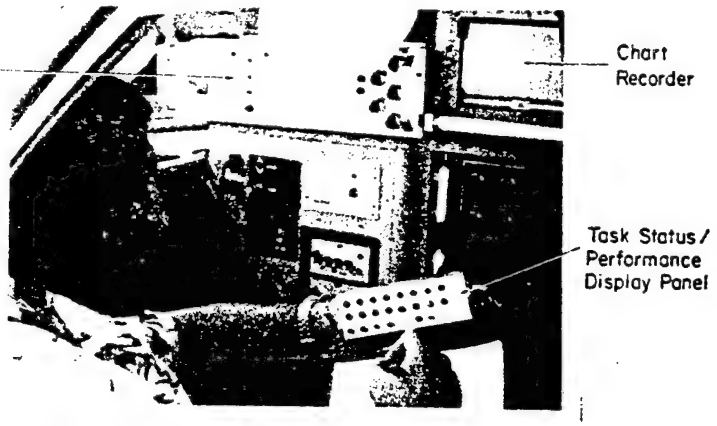

b) Back Seat Experimenter's Station

c) Front Seat Experimenter's Station

Figure 2. Equipment Setup for the Field Validation Study

TABLE 1. DRIVING DECISION-MAKING SITUATIONS

DECISION CLASS	BASIC TYPE	SPECIFIC SITUATIONS	SELECTED TASKS	
			SIMULATION	IN-VEHICLE
Single Stage	Traffic Control	• Signal light	X	X
		• Course navigation		X
	Unexpected Threats	• Car, pedestrian, object unexpectedly enters roadway	X	
		• Object in/on roadway	X	X
Sequential	Maneuvers	• Speed and steering control in a curve		
		• Lane changing and merging		
		• Road entry and merging		
		• Overtaking and passing		

The perceptual requirements of this task were to estimate car speed and distance to the intersection which the driver then uses to determine the probability of making the light. Driver perception is based on motion of the dashed lines and the intersection, auditory feedback of car speed, and position of the intersection when the light changes from green to amber. The driver does not separately estimate speed and distance, but makes a "Gestalt" estimate of the chance of entering the intersection before the light turns red. The amber light interval was held constant at 3 seconds which is typical of urban signal timing.

Driver signal timing perception was measured by having the subjects verbally report their chance of failing to make a given signal situation immediately after passing through the intersection. Failure was defined as entering the intersection after the light had turned red. This amounts to measurement of a subjective probability in decision theory context, and care was taken to insure that these estimates were unbiased by task performance (Ref. 11). Psychomotor performance was measured in terms of brake reaction times in the situations where the driver stopped.

Curve. The curved portion of the simulation and field test driving scenarios (Figs. 1c and 2a, respectively) required specific steering and speed control in order to avoid loss of control. Tire forces were limited in the simulator equations of motion such that peak curvatures could not be negotiated at speeds greater than about 45 km/h (28 mph) although the

scenario legal speed limit was set at 72 km/h (45 mph). Also 40 km/h (24 mph) speed advisory signs were displayed to the simulator drivers in advance of the curves.

In the field test a special circuit was set to activate an alarm at greater than 0.5 g lateral acceleration in order to simulate a loss of control accident. The car was capable of 0.7-0.8 g turns but actual loss of control had to be avoided for safety reasons. The field course speed limit was 40 km/h (25 mph) and the curve radii were such as to require significantly lower speeds in order to avoid exceeding the imposed g limit.

The critical perceptual task in the curve situation was speed judgment. Speed was represented by visual field motion and auditory feedback, as in the signal event, plus quantitative readout on the speedometer. Use of the speedometer is more appropriate here than for the signal event because of the quantitative nature of the curve limit speed and a lower time pressure on perception and psychomotor action. Perception in this task was again measured by driver-reported subjective probability of crashing which was solicited directly after curve exit. Speed at peak curvature was obtained as an objective measure of risk, i.e., the higher the speed, the greater the risk. Comparison of subjective risk estimates with speed then gives a measure of driver risk perception in the curve situation.

Divided Attention. In the simulator the divided attention situation involved obstacle avoidance. This task consisted of a circular object at the right side of the displayed roadway which sometimes remained stationary at the side of the road or, more frequently, moved laterally into the subject's (right) lane (Fig. 1b), requiring either stopping or steering avoidance. The subject also had to contend with adjacent cars in the left lane which were simulated by a projected slide viewed in the side view mirror (Ref. 9). Changing lanes in the presence of an adjacent car led to a crash as simulated by a buzzer and display jitter. Crashes also resulted from striking the obstacle or running off the road shoulder.

The obstacle avoidance task was a conflict situation. The subject was encouraged by a time reward to continue going if possible, but was penalized for crashing as described further on. This task primarily provided a measure of the driver's visual monitoring and steering control. Comments were solicited from subjects on monitoring behavior in the event of an adjacent crash.

Mechanization of the obstacle avoidance task was deemed too difficult for the field study so a simple route guidance task was substituted. A dashboard mounted indicator was used to direct the subject either left, right or straight after he had passed the signal light intersection. The course layout and timing were such that the route decision was made under a reasonable amount of time pressure.

Driving Scenario and Reward/Penalty Structure

Each run in the simulator and field tests consisted of an approximately 15 minute drive which included a pseudo-random sequence of the above tasks. Program starting points were varied and counterbalanced between subjects in order to avoid learning the event sequences. Circuits for detecting red light and speeding violations were activated at approximately 30 percent of the events to simulate occasional police surveillance.

Audio alarms were activated when violations were detected, and when the lateral g limit for loss of control was exceeded in the field test. A crash buzzer was activated in the simulator when subjects exceeded the road shoulder limits, or ran into obstacles or adjacent cars. Accidents in the field test were further defined by striking the tires and cones used to define the edge of the course (Fig. 2a). Thus subjects were given complete feedback on traffic safety related variables (accidents and tickets) as they would in the real world. In addition the number of accidents and tickets were used as traffic safety measures on the overall driving scenario and were also accounted for in the reward/penalty structure as described below.

Subjects were instructed to behave as they normally would in a driving situation with a reasonable motivation for timely progress while avoiding traffic violations and accidents. In addition, the monetary reward/penalty structure given in Table 2 was used to simulate real-world driving motivations and risks (Ref. 14), and provide a quantitative value structure for expected value modeling of decision-making behavior (Ref. 15). The overall

TABLE 2. REWARD/PENALTY STRUCTURE FOR SIMULATING REAL-WORLD MOTIVATIONS IN DRIVERS

COMPONENT	LAB SIMULATION	FIELD VALIDATION
Run completion bonus	$10	$10
Time saved reward	$2/min	$2/min
Low ticket penalty group	$1/ticket	$1/ticket
High ticket penalty group	$2/ticket	$4/ticket
Accident penalty	$2/crash	$2/crash
Route error penalty	—	$0.50/error

scaling of the structure was made large enough to be meaningful and comparable to the subjects' hourly wages. The run completion bonus was included to insure subjects completing each run, and the time saved reward was set to encourage the subjects to make timely progress on the drives and not become excessively cautious. Penalties were assessed for tickets, accidents and route errors (traffic safety factors). Ticket penalties are one factor that can be manipulated in the real-world (i.e., traffic court fines) and a between group comparison was included for two levels of this variable. Results of the simulator study showed no significant differences between the $1 and $2 penalty groups so the high ticket penalty was increased to $4 for the field experiment. Results on the ticket penalty variation are fully discussed in Ref. 14.

Design, Treatments and Procedures

Subjects were selected from the male licensed driving population through a newspaper ad and screened to insure heavy drinking tendencies (defined as the capability for reaching a peak BAC of 0.15). Based on age and scores on a hostility test (Ref. 16) and betting test (Ref. 17), subjects were matched and divided into the two penalty groups. During training sessions subjects were given several one-half hour exposures to the simulated driving scenarios and reward/penalty structure in order to minimize learning effects during the formal data sessions.

The experimental design shown in Fig. 3 was completed by 12 subjects in the simulator experiment and at a later date by a different group of 14 subjects in the field tests. Session order was counterbalanced between subjects. Performance was measured in four separate runs during sessions of nominally eight hours in length. During alcohol days runs were administered at sober, ascending, peak and descending levels of Blood Alcohol Concentration (BAC) in the simulator tests. The ascending BAC runs were subsequently dropped in the field tests based on minimal differences in simulator performance levels on the ascending and descending portions of the BAC curve. During placebo days runs were administered at roughly the same times as on the alcohol days. Thus subjects served as their own controls for alcohol effects, and penalty structure was between group effect.

Actual times and blood alcohol levels are illustrated in Fig. 4. BAC was measured with a gas chromatograph breath analyzer. Placebo drinks were made by floating a small amount of liquor on top of mixer. Subjects were allowed to select their own mixed drinks in order to maximize subject morale; however, combinations which would not allow credible placebos were tactfully avoided. Alcohol was administered proportional to body weight in three drinks.

The facility layout and personnel assignments were designed to maintain subject motivation and experimental efficiency. Recreational areas were set up adjacent to the simulator and included a bar, breath test area, lounge and dining area, and a restroom. This provided a relaxing atmosphere for the

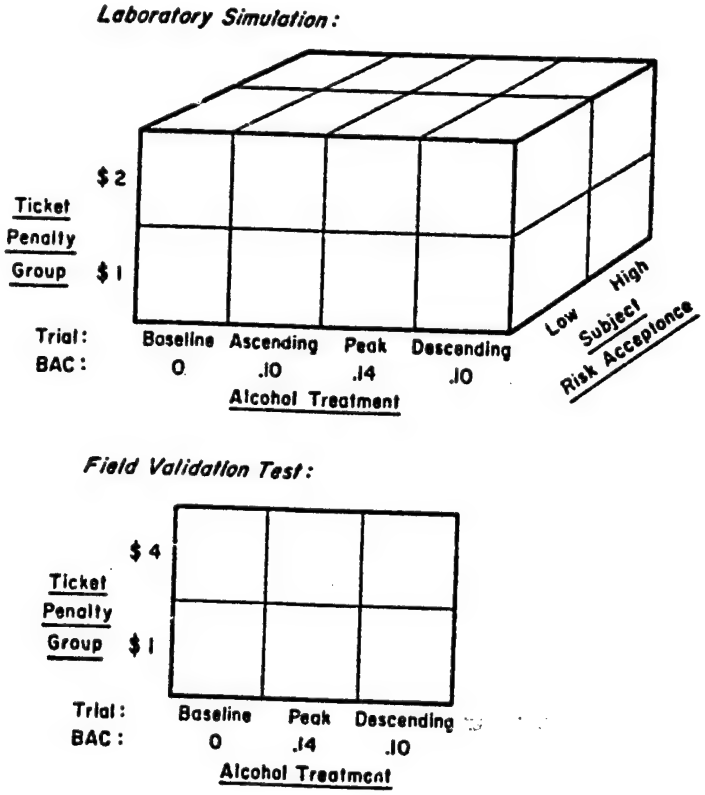

Figure 3. Experimental Design

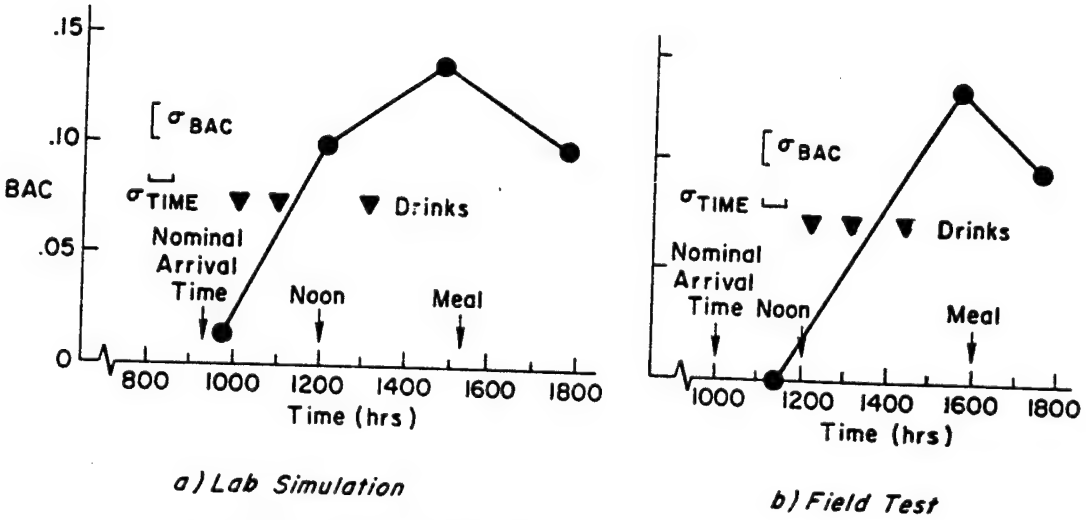

Figure 4. Alcohol Treatment Procedure Summary

subjects between experimental trials and isolated them from laboratory activity other than when they were being tested.

RESULTS AND DISCUSSION

Overall Performance

Performance measures accumulated over the whole driving scenario are plotted in Fig. 5, which show excellent agreement between the simulation and field test experiments. The total payoff per run gives an overall combined performance measure of the reward/penalty structure components. Average payoff was appreciably affected by BAC as illustrated in Fig. 5a. Sober subjects were making an average $12.50 per run, which dropped to $5 at the peak BAC condition. Analysis of variance procedures (ANOV) proved these results to be reliable ($P < 0.01$), but showed no significant difference between the two ticket penalty groups. The payoff levels were quite substantial, as the average sober subject made roughly $30-50 during his placebo session, and subject comments indicated these payoff levels motivated performance.

Component measures of the reward/penalty structure are also given in Fig. 5. Average driving time to complete the driving scenario (Fig. 5b) was remarkably insensitive to BAC, while speeding tickets and accidents were appreciably elevated with BAC (Figs. 5c and 5d). Since driving completion time was constant, the increased incidence of speeding tickets with BAC implies increased speed variability. Subjects were well aware of the speed limit and speeding penalty, and feedback of speed was available both visually and aurally. Thus, increased speed variability suggests decrements in perception and/or speedometer monitoring.

Considering a speed versus accuracy paradigm, it is apparent here that these subjects maintained average speed levels (and thus average rate of event occurrence) under alcohol impairment at the expense of accuracy (increased tickets and accidents). Thus risk taking increased with BAC, but the question remains as to whether the drivers were aware of the increased risk and thus were willingly accepting greater risk.

The simulator driving scenario provided for three types of accident exposure, and these accident results are plotted in Fig. 6. Crashes on the curve resulted from excessive speed and/or poor steering control and were the most prevalent accident. The adjacent car crashes arose from the driver not monitoring his rearview mirror when he decided to steer around the obstacle (subject reported). This result is consistent with previously reported monitoring failures in driving situations (Ref. 4). Observations during the experiment indicated that obstacle crashes occurred either because the driver took too long to decide to stop and then hit the obstacle, or tried to steer around and clipped it from the side.

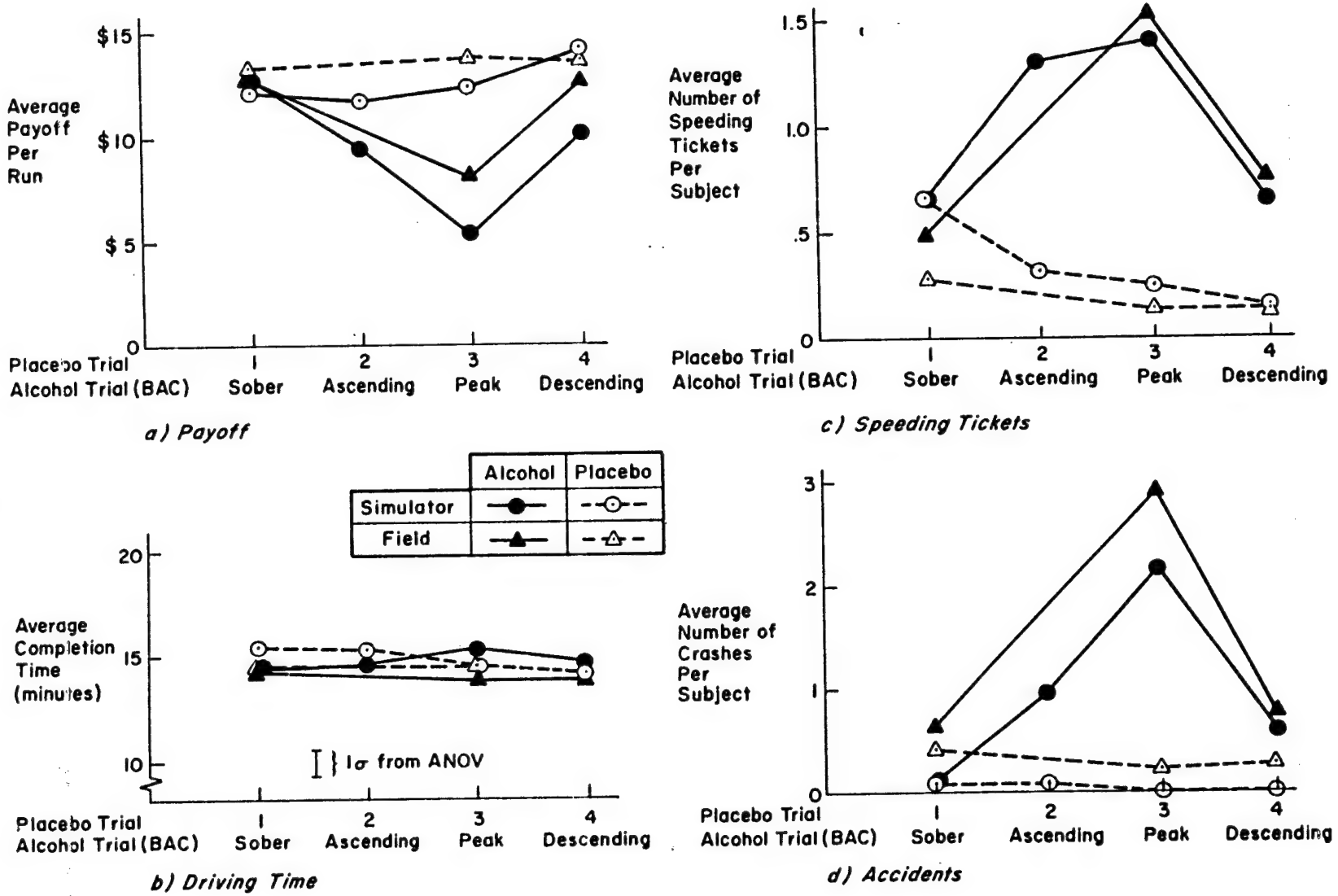

Figure 5. Overall Driving Scenario Performance Measures

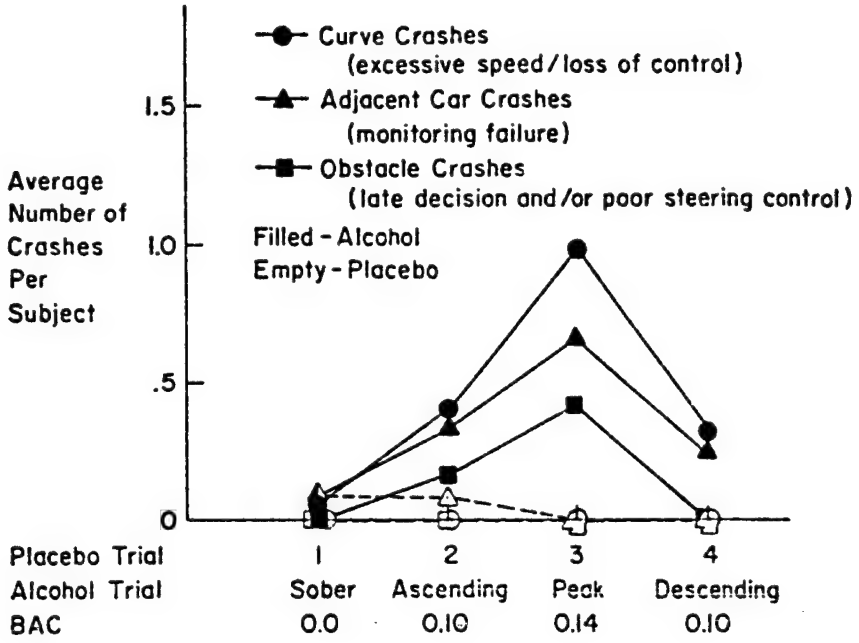

Figure 6. Simulator Curve, Adjacent Car and Obstacle Crash Results

The relative increase in experimental accident rate with BAC is compared with real-world data (Ref. 18) as shown in Fig. 7. Although there is some difference between the two experiments reported here (primarily due to different placebo accident rates), the data are still consistent with epidemiological statistics. The knee of the experimental data occurs in the region of 0.10 BAC and the data bracket the real-world rates. This data thus lend credibility to alcohol sensitivity of our simulated driving scenarios.

Signal Light Behavior

The probability of going on a given signal timing condition and the driver's estimate of failure (i.e., running the red light) are plotted in Fig. 8. There were 5 signal timings randomly distributed throughout the scenario, and the amber light timing was set to change the light when the driver was 3.4 seconds from the intersection (traveling at constant speed) in the simulator and 4.2 seconds in the field test for the data illustrated. The amber light interval was only 3 seconds long so the subjects would invariably run the red light under these conditions if they decided to go. There was some probability of going under this condition, however, which increased under alcohol.

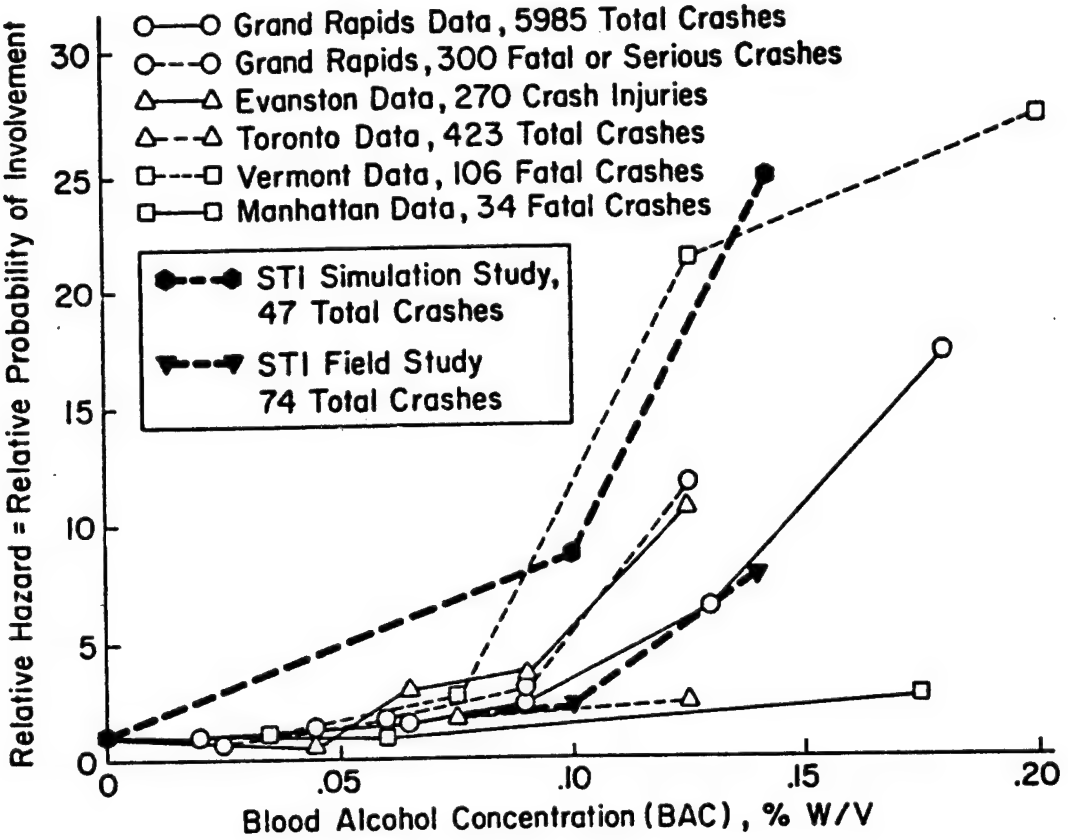

Figure 7. Comparison of Experimental Accidents With Real World Data (after Hurst, Ref. 18)

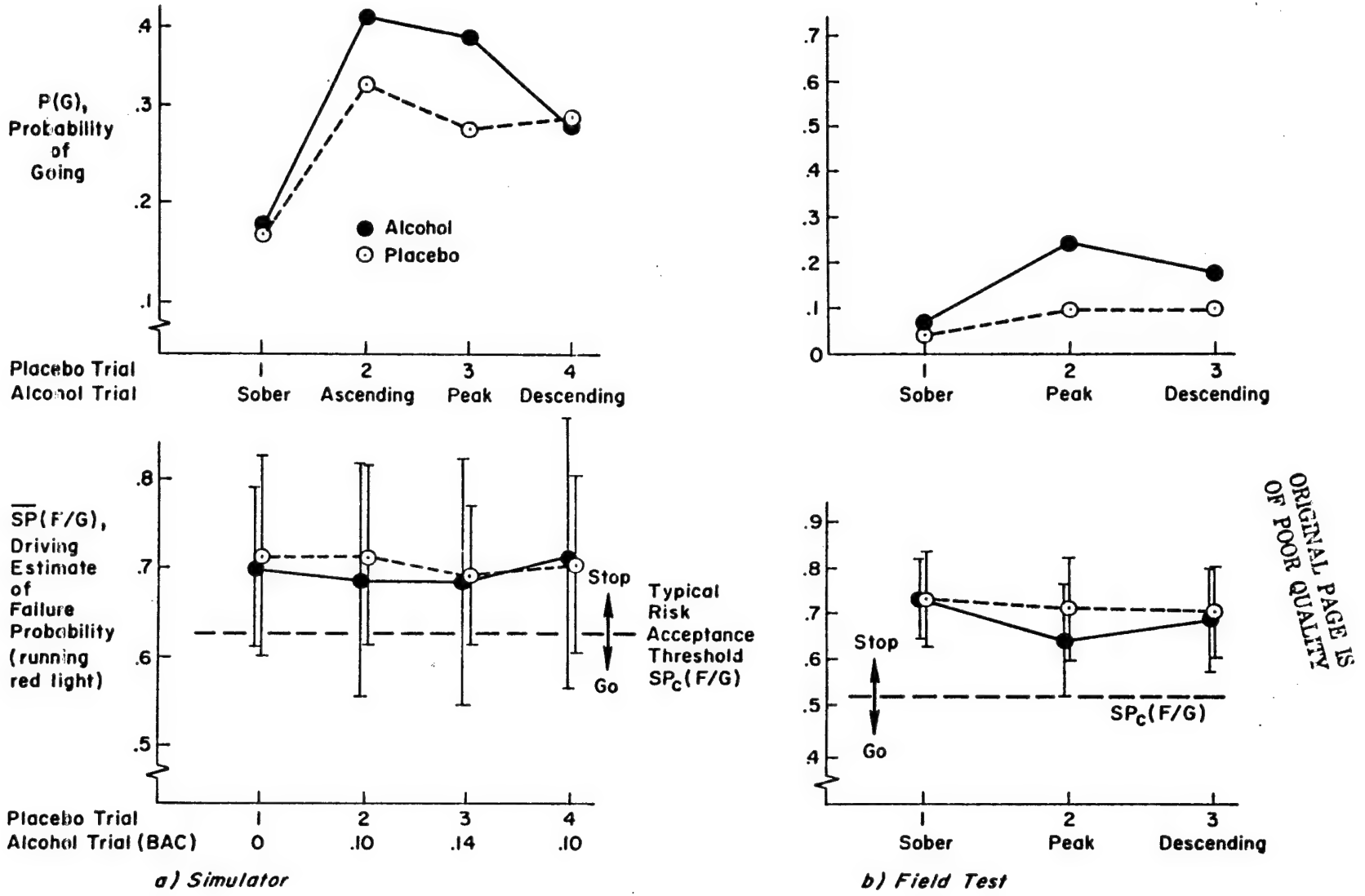

Figure 8. Signal Light Behavior Probability of Going and Driver Estimates of Failure (Running the Red Light) Given a Go

The drivers' subjective estimates of failure given that they decided to go, SP(F/G), are consistent with the probability of going. In the simulation experiment variability in the estimates increased with BAC. If we hypothesize a risk acceptance threshold for going, we see that the increased variability leads to an increased probability of going. In the field test a combination of increased variability and lower mean estimate of risk led to increased probability of going.

The subjects' failure probability estimates were obtained as soon as possible after passing through the intersection on randomly selected events where the subject did not receive a ticket (the police circuit was activated only 30 percent of the time). In order to check for performance biasing (probability estimates influenced by events after the decision point), a separate set of runs were conducted in the simulation where the whole roadway display and signal light were blanked at the end of the amber light interval. The estimates were no different under these circumstances than when the task was carried to completion. These results indicate that the failure estimates were a reflection of the drivers' perception or "Gestalt" of the time distance relationship existing at the appearance of the amber light and the decision point. These points and a complete decision theory analysis of the signal light behavior is given elsewhere (Ref. 15).

Brake response time on the signal light task was used as a measure of signal task psychomotor behavior. The results in Fig. 9 show no effect of alcohol on either the mean or variability in response time.

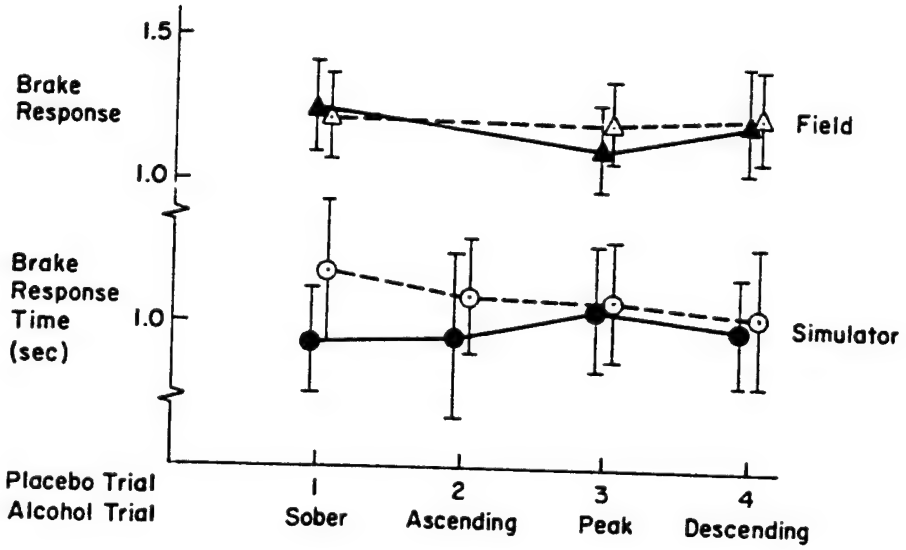

Figure 9. Alcohol Effects on Brake Response Time in the Signal Light Task

Curve Behavior

Drivers had to carefully control speed on the curves to avoid loss of control. As illustrated in Fig. 10, drivers did maintain safe speeds on the average with no significant effect due to BAC level. However, speed variability between curves (computed across several repeat curves/run/subject) did significantly increase under peak BAC. ANOV procedures showed this effect to be significant at the 0.05 level. By taking into account the speed mean and standard deviation values and assuming a normal distribution, we can compute the probability of exceeding the critical curve speed, which should equal the probability of crashing. In Fig. 11 computed and measured crashed probabilities for the simulator data are compared. The computed probabilities show an increase in the region of peak BAC, but are generally lower than the data by 30 percent. In the field test the mean and variability does not explain the increase in accident rate (field accidents were primarily due to g limit exceedences in the curves). However, experimenters noted that g exceedence often occurred with steering corrections. Steering actions by the driver can exceed the g limit at speeds below the critical speed. In the linear region of tire force characteristics, lateral acceleration for a neutral steer car can be expressed approximately as a function of the car's speed (U_o), wheelbase ($a + b$), and front wheel steer angle, δ_w:

$$a_y = \frac{U_o^2}{a + b} \delta_w < a_{y_{max}}$$

The driver could enter a curve and establish safe steady-state conditions (i.e., constant U_o and δ_w), then provide steering corrections which command lateral accelerations beyond the acceleration limit according to the above. As noted, the higher the speed (U_o), the less additional steering angle can be tolerated before the tires reach their acceleration limit. Errors in this mode might result from the driver not establishing a large enough steering angle at the beginning of the curve, then having to make a correction in midcourse which is beyond the acceleration limits of the tires.

Subjective estimates of risk or 'crash' probability were obtained in both studies at the end of selected curves. No effect of alcohol was noted on these estimates. Thus in spite of the increased accident rate under alcohol which was primarily due to loss of control on curves, drivers did not exhibit any perception of the elevated risk.

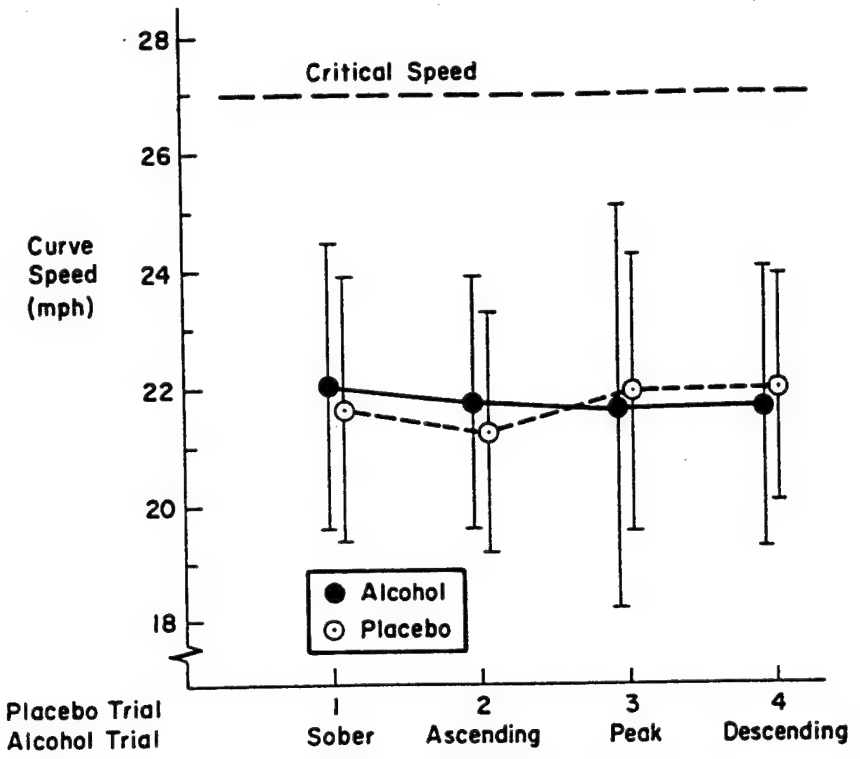

a) Simulation

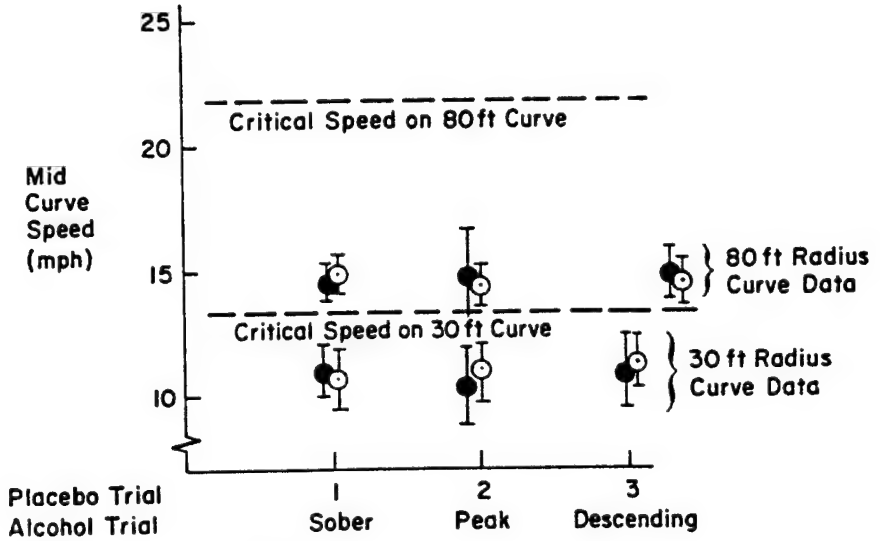

b) Field

Figure 10. Mean and Variability of Speed on Curves in the Simulator and Field Driving Scenarios

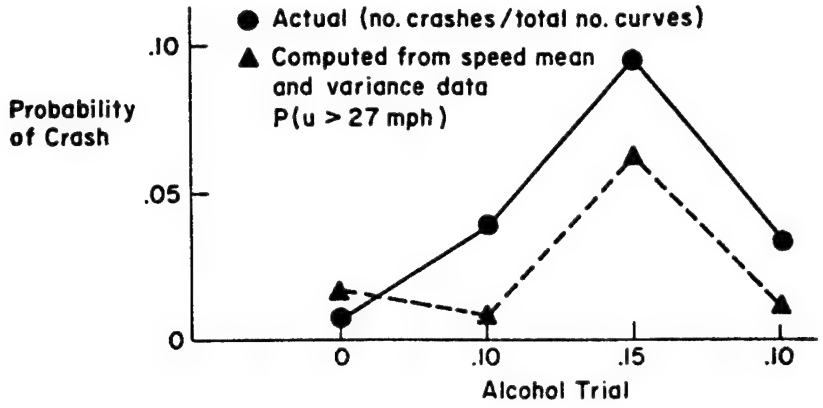

Figure 11. Comparison of Actual and Computed Curve Crash Probabilities for the Simulator Driving Scenario

SUMMARY AND CONCLUDING REMARKS

Overall performance on the driving scenario, as measured by accumulated payoff according to a reward/penalty structure, was appreciably degraded by BAC (blood alcohol concentration). Penalties due to accidents and speeding tickets increased with BAC and were primarily responsible for the decline in payoff.

Increased speed variability under alcohol was responsible for the increase in speeding tickets and curve accidents. On the average drivers did not perceive the increased hazard of the curve task with alcohol impairment as indicated by subjective estimates of risk; however, speed variability did increase, probably due to impaired perception of speed. Similarly, going behavior on the signal task increased under alcohol due to an increase in the variability of risk perception.

The above changes in speed variability and signal risk perception with increased BAC imply perceptual impairment unknown to the drivers. Alcohol increased perceptual variability which increased the driver's risk exposure. However, the mean level of subjective risk estimates was unchanged with alcohol in this experiment, which indicates the subjects were not aware of their increased risk exposure. The incidence of tickets and accidents under alcohol, although increased, was still a low probability event (roughly 1.5 and 1 incident per subject per run, respectively, at the peak BAC level) Although degraded psychomotor skill and perception combined to increase the changes of violations and accidents under alcohol, the subjects were not aware of these changes in risk.

REFERENCES

1. 1968 Alcohol and Highway Safety Report. Committee on Public Works, U.S. Congress, 90th, 2nd Session, Aug. 1968. (Available from Government Printing Office, Washington, D.C.)

2. Filkins, Lyle D.; Clark, Cheryl D.; Rosenblatt, Charles A.; et al.: Alcohol Abuse and Traffic Safety: A Study of Fatalities, DWI Offenders, Alcoholics, and Court-Related Treatment Approaches. Univ. of Michigan, Highway Safety Research Institute, 26 June 1970.

3. Study to Determine the Relationship between Vehicle Defects and Failures, and Vehicle Crashes, Volume I. DOT/HS-800 850, Univ. of Indiana, Inst. for Research in Public Safety, May 1973.

4. Allen, R. W.; Jex, H. R.; McRuer, D. T.; and DiMarco, R. J.: Alcohol Effects on Driving Behavior and Performance in a Car Simulator. IEEE Trans. on Systems, Man and Cybernetics, Vol. SMC-5, No. 5, Sept. 1975, pp. 498-505.

5. Cohen, John; Dearnaley, E. J.; and Hansel, C. E. M.: The Risk Taken in Driving Under the Influence of Alcohol. British Medical Journal, 21 June 1958, pp. 1438-1442.

6. Lewis, Everett M. Jr.; and Sarlanis, Kiriako: The Effects of Alcohol on Decision Making with Respect to Traffic Signals. ICRL-RR-68-4, Dept. of Health, Education and Welfare, 1969.

7. Ellingstad, V. S.; McFarling, L. H.; and Struckman, L. L.: Alcohol, Marijuana and Risk Taking. DOT-HS-801 028, Univ. of South Dakota, Human Factors Lab., Apr. 1973.

8. Snapper, Kurt; and Edwards, Ward: Effects of Alcohol on Psychomotor Skill and Decision-Making in a Driving Task. Paper presented at the SAE International Automotive Engineering Congress, Detroit, Mich., Jan. 1973.

9. Allen, R. W.; Hogge, J. R.; and Schwartz, S. H.: An Interactive Driving Simulation for Driver Control and Decision-Making Research. Proc. Eleventh Annual Conference on Manual Control. NASA TM X-62,464, May 1975, pp. 396-407.

10. Klein, Richard H.; Allen, R. Wade; and Peters, Richard A.: Driver Performance Measurement and Analysis System (DPMAS) Description and Operational Manual. TM-1039-1, Systems Technology, Inc., Jan. 1976.

11. Allen, R. W.; Schwartz, S. H.; and Jex, H. R.: Driver Decision-Making Research in a Laboratory Simulation. Paper presented at the NATO Symposium on Monitoring Behavior and Supervisory Control, Berchtesgaden, Federal Republic of Germany, Mar. 8-12, 1976.

12. Perchonok, K.: Accident Cause Analysis. DOT HS-800 716, National Highway Traffic Safety Administration, July 1972.

13. Moskowitz, H.: Alcohol Influences upon Sensory Motor Function, Visual Perception, and Attention. Alcohol, Drugs, and Driving, Perrine, M. W., Ed., DOT HS-801 096, National Highway Traffic Safety Admin., Mar. 1974, Chapter 3, pp. 49-69.

14. Stein, A. C.; Schwartz, S. H.; and Allen, R. W.: Use of Reward-Penalty Structures in Car-Driving Research. Proc. Fourteenth Annual Conference on Manual Control. USC, May 1978.

15. Allen, R. Wade; Schwartz, Stephen H.; and Jex, Henry R.: Driver Decision-Making Research in a Laboratory Simulation. Proc. Eleventh Annual Conference on Manual Control. NASA TM X-62,464, May 1975, p. 170.

16. Pelz, Donald C.: Hostility Questionnaire. Univ. of Michigan, Inst. for Social Research, Survey Research Center.

17. Hurst, P. M.; and Siegel, S.: Prediction of Decisions from a Higher Ordered Metric Scale of Utility. J. Exper. Psychology, Vol. 2, 1956, pp. 138-143.

18. Hurst, P. M.: Epidemiological Aspects of Alcohol in Driver Crashes and Citations. Alcohol, Drugs, and Driving, Perrine, M. W., Ed., DOT HS-801 096, National Highway Traffic Safety Admin., Mar. 1974, Chapter 6, pp. 131-171.

19. McRuer, D. T.: Simplified Automobile Steering Dynamics for Driver Control. Paper presented at the SAE Aerospace Control and Guidance Systems Committee Meeting No. 35, Palo Alto, CA, Mar. 19-21, 1975.

D42

N79-15630

A DECISION MODEL APPLIED TO ALCOHOL EFFECTS ON DRIVER SIGNAL LIGHT BEHAVIOR

Stephen H. Schwartz and R. Wade Allen

Systems Technology, Inc.
Hawthorne, California

ABSTRACT

A decision model including perceptual noise or inconsistency is developed from expected value theory to explain driver stop and go decisions at signaled intersections. The model is applied to behavior in a car simulation and instrumented vehicle. Objective and subjective changes in driver decision making were measured with changes in blood alcohol concentration (BAC). Treatment levels averaged 0.00, 0.10 and 0.14 BAC for a total of 26 male subjects. Data were taken for drivers approaching signal lights at three timing configurations. The correlation between model predictions and behavior was highly significant. In contrast to previous research, analysis indicates that increased BAC results in increased perceptual inconsistency, which is the primary cause of increased risk taking at low probability of success signal lights.

INTRODUCTION

One of the motivations for developing the driver decision model described here was to measure and analyze the behavior of alcohol-impaired drivers. We desired to separate risk taking into components of risk perception and acceptance. If a driver takes increased risks, is it because he perceived the risk and decided to accept it or because he does not perceive the increased risk? Expected value theory provides a simple construct for making this distinction and has been applied in the past to describe impaired driver behavior, (References 1, 2, and 5).

Here we apply a Subjective Expected Value (SEV) model to explain driver stopping and going behavior at signaled intersections. Perceptual noise is included to reflect one type of driver inconsistency in the decision-making process (Reference 3). The model is applied to data collected as part of an automobile simulator study involving a typical drive-home scenario. Although measures were taken throughout the scenario on several tasks, we concentrate here on signal light behavior. We briefly present the decision model, the experimental results, and our analysis and interpretation in view of previous studies.

630

DECISION-MAKING MODEL

The model was derived to guide experimental design and measurement. The expected value approach is not new; however, the inclusion of perceptual noise as applied to signal light behavior is original. The basic scenario is a signal light at an intersection which has changed from green to amber and will change to red in 3 seconds. Based on his perception of speed and distance the driver must then decide whether to stop or go. The kinematics for this task have been described previously, Reference 4. Here we briefly derive an appropriate decision model subject to several assunptions.

We begin by simplifying what is actually a complex decision task, Reference 11, in a simple two-alternative situation. Conceptually we are assuming this decision process takes place in parallel with the driver's continuous speed control behavior as illustrated in Figure 1. Perceptions of vehicle

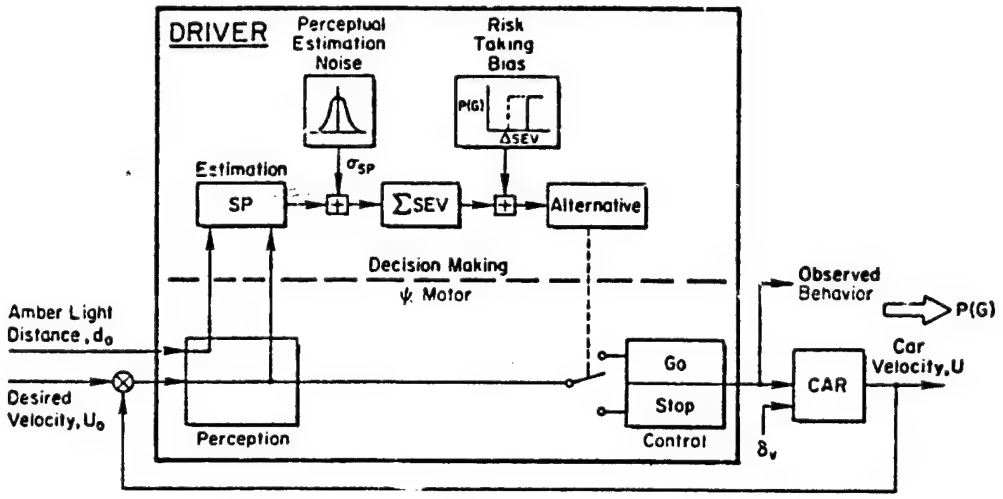

Figure 1. Signal Light Risk Acceptance Model

velocity and distance to the signal at the time the light changes to amber are used to form a subjective estimate of the probabilities of success and failure for the various alternatives. As indicated in the figure and discussed further below, these subjective probabilities are stochastic in nature. They are weighted with appropriate utilities or values and the driver selects the alternative with the highest expected value. We define Subjective Expected Values (SEVs) for the two alternatives, go or stop, respectively:

$$SEV(Stop) = SP(Pass/Stop)V(Pass/Stop) + SP(Fail/Stop)V(Fail/Stop) \quad (1)$$

$$SEV(Go) = SP(Pass/Go)V(Pass/Go) + SP(Fail/Go)V(Fail/Go) \quad (2)$$

where SP(·) and V(·) are conditional subjective probabilities and values, respectively. From these equations and the several other simplifying assumptions, we can express the probability that a driver will attempt to go through the signal light. Further simplifying notation so that F = Fail and G = Go, the probability of Going is:

$$P(G) = \iint_{\text{Region}} f[SP(F/G), SP(F/S)]\, dSP(F/G)\, dSP(F/S) \qquad (3)$$

where the region is defined by:

$$P(G) = P[SEV(G) \geq SEV(S)] \qquad (4)$$

With the assumptions listed in Table 1, it can be shown (see Reference 6 for derivation) that the P(G) is the Gaussian integral:

$$P(G) = \frac{1}{\sigma_{SP(F/G)}\sqrt{2\pi}} \int_{o}^{SP_c(F/G)} \exp\left\{\frac{-[SP(F/G) - \overline{SP}(F/G)]^2}{2\sigma^2_{SP(F/G)}}\right\} dSP(F/G) \qquad (5)$$

TABLE 1. SOME MODEL ASSUMPTIONS

1. Operator selects decision alternative with largest subjective expected value. Values reflect utilities and are constant.
2. Subjective probabilities are mutually exclusive and exhaustive.
3. Subjective probabilities are Gaussian random variables in the region of interest.
4. Increased SP(F/G) decreases P(G), i.e., the values discourage go-failures.
5. The verbal estimates of SP(F/G) linearly reflect subjective perception.
6. The threshold value of SP(F/G), below which the operator selects the go alternative is $SP_c(F/G)$:
   - $\triangleq \overline{SP}(F/G)$ where P(G) = 0.5
   - is a constant as compared with being a random variable
7. SP(F/S) = 0.

A typical example of these concepts is illustrated in Figure 2. Repeated observations for a given situation, e.g., signals with the same time to the intersection, result in a distribution of subjective estimates illustrated by the top probability density curve. Assuming a cutoff subjective probability, $SP_c(F/G)$, as illustrated, the area under the density curve and to the left of the criterion is P(G). This is illustrated in the bottom of Figure 2, where the relationship of P(G) as a function of the average subjective estimate, $\overline{SP}(F/G)$, is illustrated. The slope of this relationship is determined by the variability of the subjective estimates, σ_{SP}. Note that the effect of increasing the variance of the subjective estimates is to increase P(G) for the case illustrated. Also shown is the consequence of a change in the driver's risk acceptance, $SP_c(F/G)$.

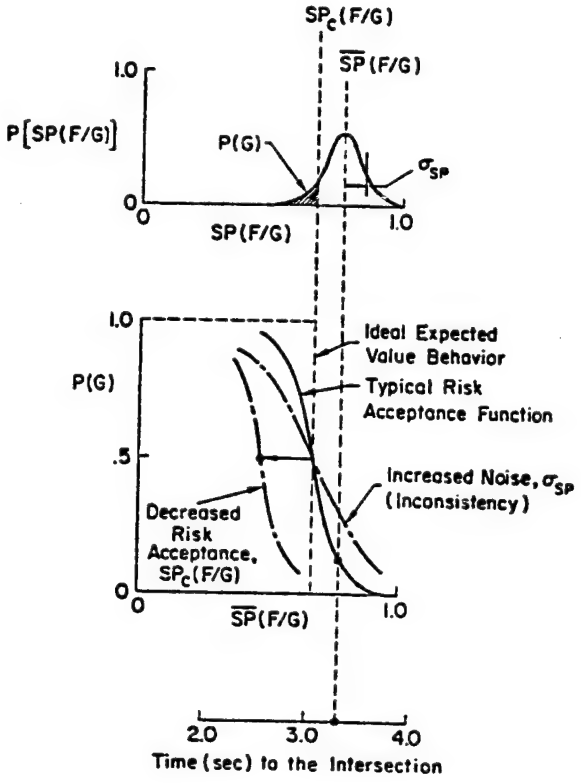

Figure 2. Typical Relationship Between Probability of Going, P(G), Subjective Probabilities of Fail Given a Go, SP(F/G), and Signal Timing

A useful empirical relationship is also apparent in Figure 2. Evaluation of Eq. 5 for the condition $SP_c(F/G) = \overline{SP}(F/G)$ results in $P(G) = 0.5$. Thus, the subjective cutoff $SP_c(F/G)$ can be determined empirically from objective behavior probabilities by selecting the value of $\overline{SP}(F/G)$ at $P(G) = 0.5$.

THE EXPERIMENTS

The signal light task was simulated in both a fixed-base simulator and instrumented vehicle on a closed course as described in the companion paper (see Reference 14). The signal light timing was controlled similarly in both simulation and field studies. When the vehicle approached the intersection, the signal light initially turned green. At a random-appearing time later, the signal turned amber. This time was controlled by a circuit which compensated for car speed such that the time interval to the intersection was the same for a given intersection type, regardless of the approach speed, if the driver maintained that speed. The amber light interval was fixed at 3 seconds, following which the light turned red. Thus, the probability for successfully making a light was controlled without placing an artificial speed restriction on the subject. Five signal timings were automaticlly commanded. One was set to require a sure stop (early yellow) and another a sure go (long green). The remaining three timings ranged from a probable stop to a probable go. The times to the intersection from the amber light typically ranged from 2.0 to 3.5 seconds. (The kinematics of stopping or going for these timings are discussed more fully in Reference 4.)

The subjects were instructed to behave as they normally would in a driving situation with a reasonable motivation for timely progress and a desire to avoid tickets and accidents. Also, a monetary incentive structure was provided as a tangible and quantifiable motivation for performance (see Reference 14).

Subjects were trained until objective performance and subjective estimates were consistent in the view of the experimenter. Subjective estimate training began with a short tutorial written exam used as a basis for discussion of the concepts of probabilities. Following this, each subject received two to three hours of practice driving in half-hour sessions spread over two days. Feedback on performance and subjective estimates was given throughout these training trials.

Subjects completed trials on each of two days. During an alcohol day, the trials corresponded to an across-subject average blood alcohol concentration (BAC) of 0.00 (baseline), 0.10 (ascending — when measured), 0.14 (peak), and 0.10 (descending). During the placebo day, the trials were given at approximately the same time of the day as for the above trials. The day order was counterbalanced among subjects.

Objective and subjective measures were taken, and the number of stop and go decisions was recorded. The number of failures and successes for each decision was detected automatically and recorded irrespective of whether or

not the driver received a ticket. Corresponding subjective estimates were recorded during the run. Subjects were asked to give their estimate of failure on a scale of 0 to 100 percent immediately following randomly selected intersections. Nominally, six of each type of intersection were selected. Intersections for which the driver received a ticket were ignored. (A tacit assumption in using subjective estimates received after the execution of the signal task is that the subjective probabilities were unbiased by performance outcomes as perceived by the subject. To test this assumption, a parallel simulation experiment used selected intersections where the visual scene was blanked out immediately following the driver's commitment to a decision and prior to going through the intersection. Thus the driver received no feedback on his performance for these selected intersections. These results were similar to the "after the fact" estimates.)

RESULTS

The data were examined for each intersection independently over the eight trial conditions (four trials per session for placebo and alcohol sessions). Both objective and subjective data were analyzed to differentiate between changes in risk acceptance vs. risk perception.

In Figure 3 the objective probabilities of going, P(G), and failing given a go, P(F/G), for both the simulation and field test are compared to determine driver risk-taking behavior. The probabilities were computed by dividing the total number of outcomes by the total number of opportunities (e.g., P(F/G) = Number of go failures/Number of go's). For example, Intersection 2 in the simulation resulted in the subjects always going, P(G) = 1, and the timing was such as to preclude go failures, P(F/G) = 0. The timing was also adequate on Intersection 3 to allow safe go's; however, in this case the drivers did not always go, i.e., P(G) $\doteq$ 0.75. This behavior was not sensitive to alcohol, and the subjects appear to have been behaving conservatively on Intersection 3. Subjects did not go very frequently on Intersection 4 and had a high failure rate when they did. There is an indication of increased go behavior under alcohol for Intersection 4. This is also apparent for all the intersections in the field test.

Part of the reason for this increased going behavior on some intersection timing in spite of increased failures is illustrated in Figure 4. Here we note that the variability of the subjective risk perception, σ_{SP}, increases although the average perception of risk, $\overline{SP}(F/G)$, remains relatively constant. Considering a typical switching criterion, as shown in Figure 4, we see that the increased variability of risk perception with increased alcohol leads to a greater percentage of subjective estimates below this criterion. The justification for this interpretation was validated via statistical analysis of parameters for the proposed model.

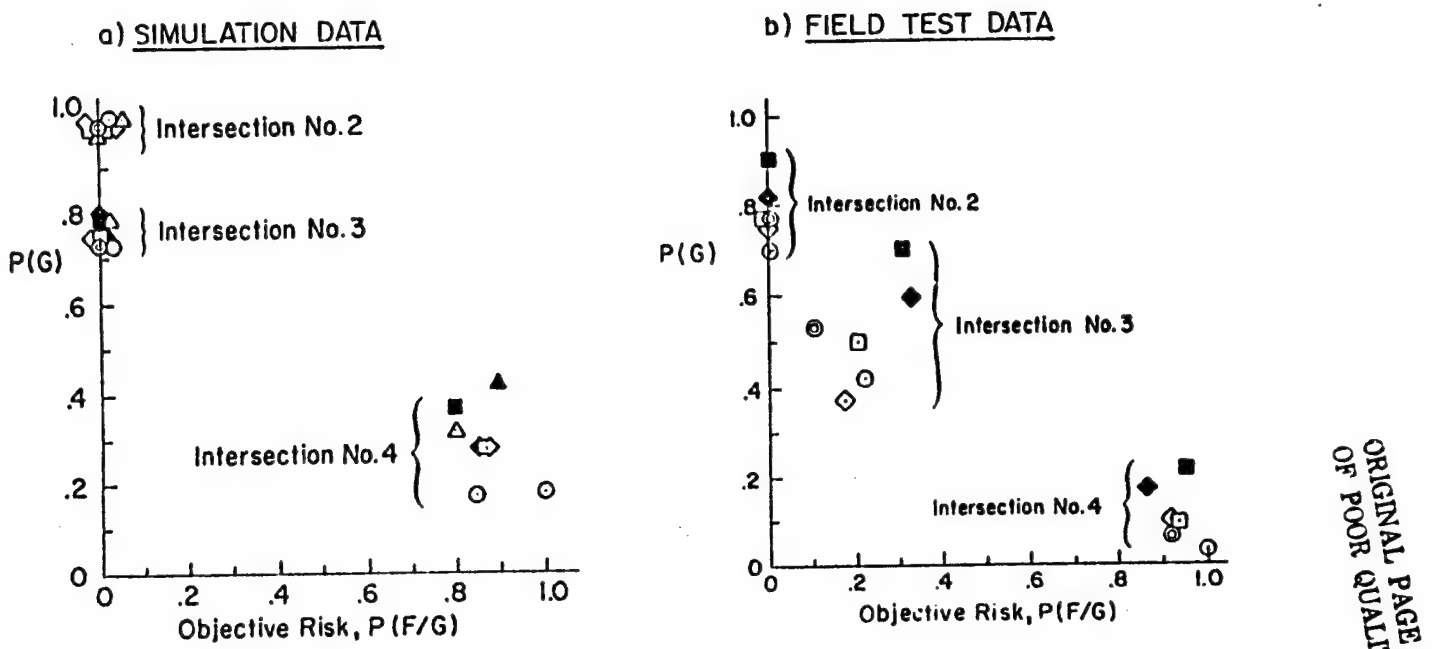

Figure 3. Alcohol Effects on Signal Light Risk-Taking Behavior

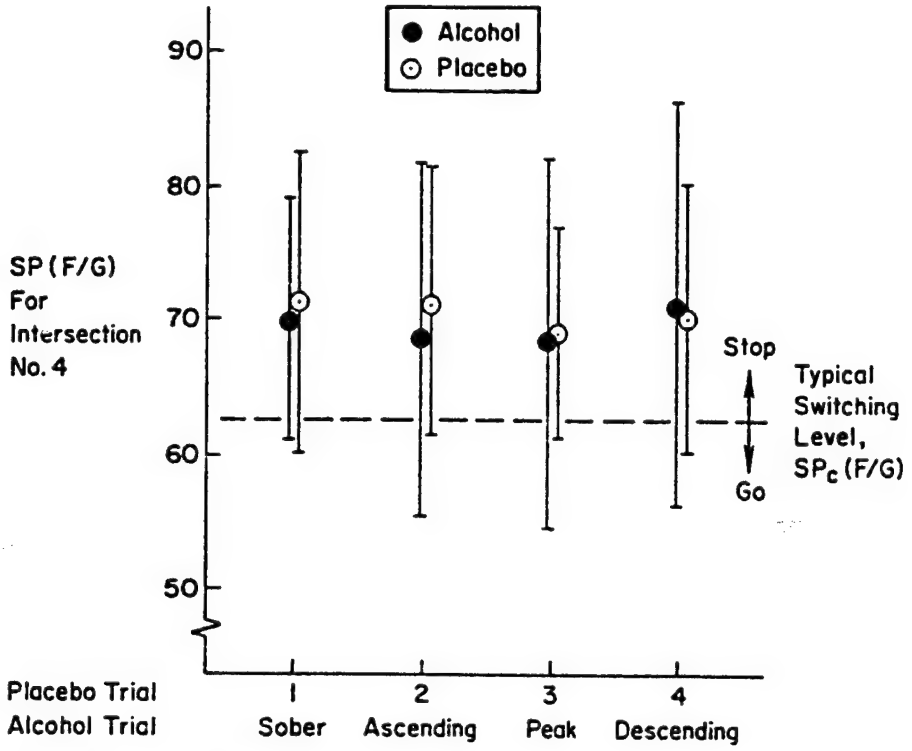

Figure 4. Changes in Subjective Estimates of the Probability of Failure Given a Go Attempt, SP(F/G) with BAC Condition

MODEL EVALUATION

The decision-making model discussed above was used to analyze driver risk acceptance behavior. This was accomplished in three steps. First, driver risk acceptance thresholds, $SP_c(F/G)$, were computed for each experimental treatment. Then the threshold data were analyzed to investigate changes under intoxication. Finally, the various risk perception data were combined according to Eq. 5 and resulting computed or estimated values of the probability of going, $\hat{P}(G)$, were compared with actual P(G) data to establish model validity.

Risk acceptance thresholds were computed for each subject and each run by curve fitting a risk acceptance function (Figure 5) to P(G) and $\widetilde{SP}(F/G)$ data for the three intersection timing conditions. A trigonometric function was used to describe the risk acceptance function:

$$P(G) = \frac{1}{2}\left[1 + \sin\left(\widetilde{SP}(F/G) - SP_c(F/G)\right)\right] \qquad (6)$$

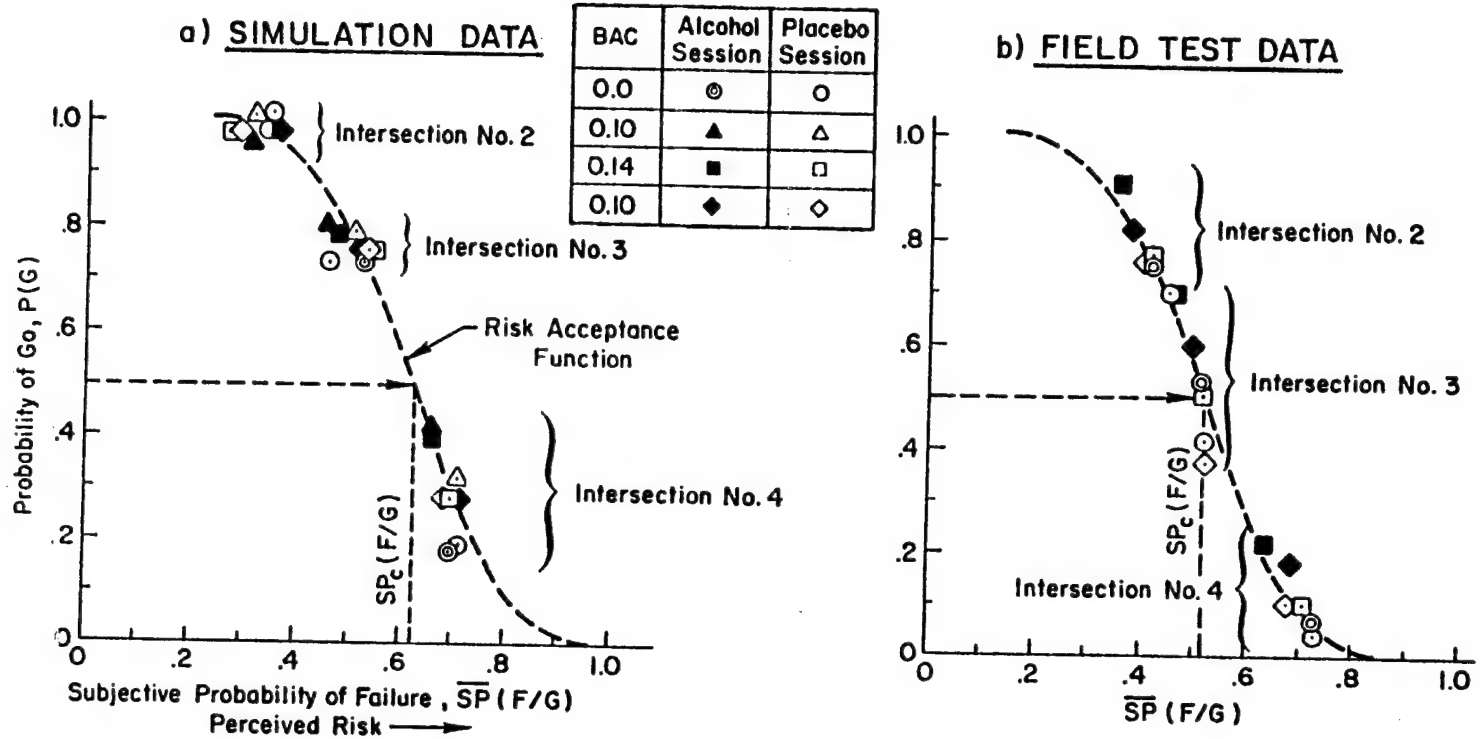

Figure 5. Alcohol Effects on Signal Light Decision Making Behavior

By rearranging this formula we obtain a relationship which can be used for a linear regression fit:

$$a\overline{SP}_i(F/G) - aSP_c(F/G) = \sin^{-1}[2P_i(G) - 1] \qquad (7)$$

The data input for this regression fit is the mean subjective probability of failure and probability of going for each intersection. The derived values are then a and the risk acceptance threshold $SP_c(F/G)$. The parameter a describes the slope at the midpoint of the risk acceptance and is inversely proportional to the risk perception variability σ_{SP}.

The $SP_c(F/G)$ were computed and analyzed with no indication of alcohol effects on driver risk acceptance. The SP_c and $SP(F/G)$ data were then used to compute probability of go estimates, $\hat{P}(G)$, according to Eq. 5. These compare favorably as shown in Figure 6. Analysis of covariance procedures were employed to compare the actual and estimated values of P(G). The F ratios indicated that P(G) was highly correlated with the computed estimate $\hat{P}(G)$, Reference 6.

These results suggest that the alcohol effects on the drivers' subjective risk perception, both $\overline{SP}(F/G)$ and σ_{SP}, are responsible for drivers increased going behavior while intoxicated. They also validate the usefulness of the model in analyzing that behavior.

There are other possible interpretations of these results. An intuitive one is that the variations in subjective estimates are due to variations in the time of the decision and not to variations in perception for a given time and distance relation. However, a preliminary analysis of the time histories for several of the subjects indicated that the response times did not change significantly under alcohol, Reference 7. In addition, there are other models which could be applied to the observed signal light behavior. A potentially fruitful approach is the signal detection model as developed by Green and Swets, Reference 8, expanded for application to man/vehicle problems by Curry, et al., Reference 9, and applied to the lane change maneuver by Cohen and Ferrell, Reference 10. Other types of criteria suggested in this work, such as likelihood ratio threshold and Newman-Pearson strategy, may be applicable. However, it is apparent from Figure 6 that the additional refining assumptions used in these models may not be necessary for interpreting the major effects of alcohol on decision behavior.

PREVIOUS RESEARCH

While increasing frequency of driving decision errors with increased BAC has been found by other researchers, the interpretation of which behavior component is primarily responsible for this increase has been inconsistent. Comparison between studies is confounded because of differences in tasks, reward and penalty conditions, alcohol treatment methods, and analytical approaches. However, the results can be interpreted and compared as follows.

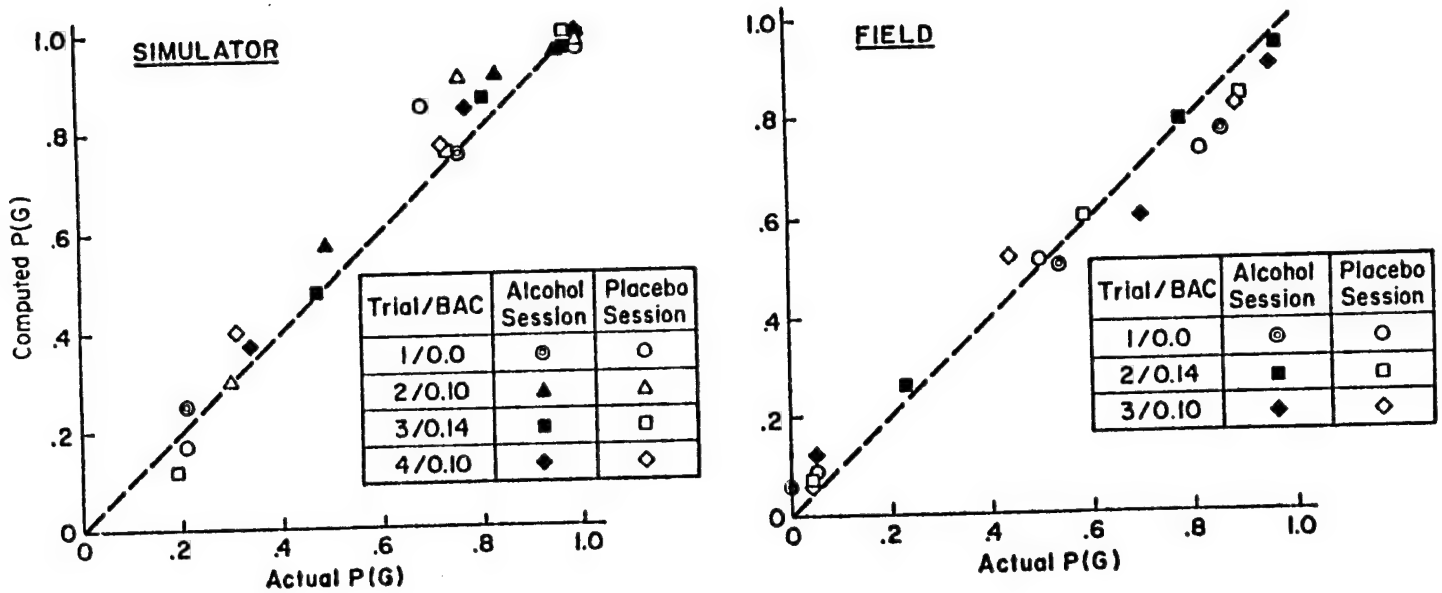

Figure 6. Comparison of Measured Versus Computed Probability of Going. $\hat{P}(G)$ Estimates Computed Using Measured Values of $SP(F/G)$, σ_{SP}, and $SP_c(F/G)$

In agreement with our results, four of the five other studies commented on here found increased risk taking with increased alcohol intake. Cohen, Dearnaley, and Hansel, Reference 1, in evaluating bus drivers' willingness to drive through a cone-delineated gap found the number of attempts increased with alcohol intake. Lewis and Sarlanis, Reference 11, using a simulated traffic signal, found the number of go responses significantly increased under alcohol. Light and Keiper, Reference 12, also found an increased number of attempted passes in a simulated overtaking and passing task. Finally, Ellingstad, McFarling, and Struckman, Reference 13, in evaluating performance on laboratory analogs of automotive passing tasks with multiple discriminant analysis, found the discriminant "riskiness/indecisiveness" increased with alcohol. This discriminant included a positive loading on passing attempts. The only exception to this trend was presented by Snapper and Edwards, Reference 2, who found no significant change with BAC in the number of attempted lane changes through a given gap size on their closed course.

The interpretation of these data as resulting from changes in psychomotor skill, perceptual ability, or cognitive risk acceptance varies between authors. Re-analysis is difficult because only two of these studies took sufficient measures to delineate changes in decision strategies. Cohen, et al., Reference 1, asked the bus drivers to indicate levels of confidence expressed as the number of times out of five the driver thought he could succeed in driving through the different size gaps. The estimates did not change significantly on the average for the narrowest accepted gap; however, the accepted gap size decreased with increased alcohol intake. Therefore, he assumed "If the difficulty of the task remained unchanged, they became more optimistic and attached a higher subjective probability to the task." The variances in the estimates were not reported. Cohen concluded that the primary effects of alcohol were to decrease psychomotor skill and deteriorate "judgment," where we interpret judgment to include mean perception. Snapper and Edwards, on the other hand, asked their subjects for subjective probabilities and found no significant change in the mean for a given gap size. As they found no change in the mean subjective estimates and no increased risk taking, but with increased failures in execution, they concluded that the primary effect of increasing BAC was degraded psychomotor skill. Again, no data on the effects of BAC on the consistency or variability of the subjective probabilities were presented.

By comparison, our findings agree with most of these results but not with the authors' interpretations. As in most of these studies, we found increased risk taking and no change in risk acceptance, i.e., no change in the mean subjective estimate for a given intersection. However, our data suggest that increased risk taking is primarily due to increased variance or inconsistency in perceptual estimates. This interpretation could also explain the results found by the first four authors mentioned above if data on mean and variances of subjective estimates were available. The disparity between this conclusion and Snapper and Edwards' conclusion may be due to at least two factors. Their lane change task placed more emphasis on psychomotor execution than does the current signal light task; hence their results may have been more sensitive to this type of degradation. In fact, we found considerable degradation in the consistency of psychomotor performance in the other tasks in our driving scenario (Reference 7). In addition, a fundamental difference between our

simulated driving tasks and those of both of the previous studies using subjective estimates is addition of temporal pressure. Our subjects were required to form their estimates in "real time" as opposed to the "stop action" type of judgments and driving scenarios used in previous studies.

Thus, the behavior skills required for the decision-making tasks of the other researchers are somewhat different from those studied here. Allowing for these differences, the other studies may have had the same cause for the increased risk taking as measured here, namely, distorted perception, but they did not present sufficient data to determine it.

In summary of previous decision-making studies, those aspects of our results which are directly comparable with previous research largely agree with those findings. Risk taking generally increased with increasing BAC. Interpretation of previous work beyond this point is difficult because of insufficient measures. However, that work does not disagree with the current conclusion that there is no change in risk acceptance. Our interpretation of these results, that perceptual distortion is a primary cause of alcohol-induced increased risk taking observed for simple tasks, is new.

CONCLUSIONS

An expected value model accounted for the effects of perceptual noise on decisions for drivers in a simulated signal light task. With this model, analysis of the significant changes in behavior for increasing BAC indicated no changes in risk acceptance; that is, subjects did not change their subjective criterion level. The primary cause of the increased risk taking found for intersections timed with a low probability of success was increased inconsistency or variance in their subjective perceptual estimates.

These results have ramifications both for researchers in this field and those attempting to apply the results. In future human decision-making work, measures of inconsistency in perception should be given as much attention as measures of central tendency. Also suggested by these results is that one method of reducing drinking driver errors may be to improve the driver's perceptual environment to decrease his inconsistency. We could expect these results to generalize the effects of alcohol on other such real-time decision tasks as aircraft and spacecraft control. In addition, the analytical framework used here may be useful in evaluating the effects of other drugs and stressors on human decision behavior.

ACKNOWLEDGMENT

This work was supported by the Department of Transportation, National Highway Traffic Safety Administration, under Contract No. DOT-HS-4-00999. The views expressed in this paper are those of the authors and do not necessarily represent those of the National Highway Traffic Safety Administration.

REFERENCES

1. Cohen, J.; Dearnaley, E. J.; and Hansel, C. E. M. The Risk Taken in Driving Under the Influence on Alcohol. Brit. Med. J., 21 June 1958, pp. 1438-1442.

2. Snapper, K.; and Edwards, W. Effects of Alcohol on Psychomotor Skill and Decision-Making in a Driving Task. Univ. of Michigan, Department of Psychology, NIAAA Grant No. MN22063-01, 1973.

3. Hurst, P. M. Consistency in Driver Risk Taking. Behavioral Res. in Driving Safety, combined issues, vol. 2, nos. 1-2, Spring-Fall 1971, pp. 73-82.

4. Allen, R. W.; Schwartz, S. H.; and Jex, H. R. Driver Decision-Making Research in a Laboratory Simulation. NATO Symposium on Monitoring Behavior and Supervisory Control, Berchtesgaden, 8-12 Mar. 1976.

5. Rapoport, A.; and Wallsten, T. S. Individual Decision Behavior. Ann. Review of Psych., vol. 23, 1972, pp. 131-176.

6. Allen, R. W.; Schwartz, S. H.; Hogge, J. R.; and Stein, A. C. The Effects of Alcohol on the Driver's Decision-Making Behavior. Systems Technology, Inc., TR-1053-1, Feb. 1978.

7. Allen, R. W.; Schwartz, S. H.; Stein, A. C.; and Hogge, J. R. The Effects of Alcohol on Driver Performance in a Decision-Making Situation. Presented at the 14th Annual Conference on Manual Control; published in this volume.

8. Green, D. M.; and Swets, J. A. Signal Detection Theory and Psychophysics. New York: Wiley, 1966.

9. Curry, R. E.; Gai, E. G.; and Nagel, D. C. Decision Behavior with Changing Signal Strength. In Proc. 10th Annual Conf. on Manual Control, Wright-Patterson AFB, OH, 9-11 Apr. 1974.

10. Cohen, H. S.; and Ferrell, W. R. Human Operator Decision-Making in Manual Control. IEEE Trans., vol. MMS-10, no. 2, June 1969, pp. 41-47.

11. Lewis, E. M., Jr.; and Sarlanis, K. The Effects of Alcohol on Decision Making with Respect to Traffic Signals. Dept. of Health, Education, and Welfare, Rept. No. ICRL-RR-68-4, 1969.

12. Light, W. O.; and Keiper, C. G. Effects of Moderate Blood Alcohol Levels on Automobile Passing Behavior. Dept. of Health, Education, and Welfare Report No. ICRL-RR-69-4, 1971.

13. Ellingstad, V. S.; McFarling, L. H.; and Struckman, L. L. Alcohol, Marijuana and Risk Taking. Dept. of Transportation, Rept. DOT HS-801 028, Apr. 1973.

14. Stein, A. C.; Schwartz, S. H.; and Allen, R. W. Use of Reward-Penalty Structures in Human Experimentation, published elsewhere this volume.

COMBINED MONITORING, DECISION AND CONTROL MODEL FOR THE HUMAN OPERATOR IN A COMMAND AND CONTROL TASK

by

Ramal Muralidharan, Sheldon Baron
Bolt Beranek and Newman Inc., Cambridge, MA

SUMMARY

This paper reports on the ongoing efforts to model the human operator in the context of the task during the enroute/return phases in the ground based control of multiple flights of remotely piloted vehicles (RPV). This is a part of our research aimed at investigating human performance models and at modeling command and control systems.*

The approach employed here uses models that have their analytical bases in control theory and in statistical estimation and decision theory. In particular, it draws heavily on the models and the concepts of the optimal control model (OCM) of the human operator. We are in the process of extending the OCM into a combined monitoring, decision, and control model (DEMON) of the human operator by infusing Decision theoretic notions that make it suitable for application to problems in which human control actions are infrequent and in which monitoring and decision-making are the operator's main activities. Some results obtained with a specialized version of DEMON for the RPV control problem are included.

1. INTRODUCTION

1.1 Modeling Goals

We are involved in a program of research aimed at investigating human performance models and approaches to modeling command and control systems (see reference 1). A part of our research effort concerns the study of the feasibility of modeling the human operators in command and control systems via control and decision theoretic models. This paper describes the salient aspects of this part of our ongoing research effort.

1.2 Modeling Approach

The approach employed here uses models that have their analytical bases in control theory and in statistical estimation and decision theory. In particular, it draws heavily on the models and concepts of the OCM (references 2-6). The modeling approach is normative, in that one determines what the human operator ought to do, given the system objectives and the operator's

* The research reported in this paper was supported by the Air Force Office of Scientific Research under contract F44620-76-C-0029.

limitations, and this serves as a prediction of what well-trained, motivated operators will do.

In the basic OCM concern is more with the operator's continuous interaction with the system, as demanded by closed loop analysis, than with his response to discrete events. The development of the basic OCM and its model structure has been dictated by the principal areas of its previous application, viz., vehicle control. We shall extend the OCM by incorporating structures and notions that make it suitable for application to problems in which human control actions are infrequent and in which monitoring and decision-making are the operator's main activities.* The expected end product is a combined monitoring, decision, and control model for the human operator in a command and control task.

1.3 Task definition

In this paper we shall discuss our modeling effort as it relates to the task facing the human operator during the enroute/return phases in the ground based control of multiple flights of remotely piloted vehicles (RPV).

The enroute/return phases together with a terminal control phase constitute an "RPV mission". An RPV-mission consists of coordinated flights of several RPV-triads. Each triad has a strike vehicle (S), an electronics countermeasures vehicle (E) and a low- reconnaisance vehicle (L). Each RPV is automatically controlled along a pre-programmed flight plan assumed optimal with respect to terrain and defenses. The RPVs deviate from their flight plan due to navigation system errors, position reporting errors, communication jamming by the enemy, equipment malfunctions etc. These deviations are kept in check by external monitoring and control from the ground station. This supervision is provided by human enroute controllers, who are equipped with CRT displays for monitoring flight path and vehicle status and with keyboards and light pens for introducing changes in RPV flight parameters. The ultimate objective of the enroute controllers is to ensure that the S and E RPVs fly on schedule over the target 15 seconds apart followed by the L RPV two minutes later to assess damage. This time-phasing at the target is accomplished by time-phased handoffs at designated hand-off coordinates on the flight plan. The S RPV's are handed off to the terminal controller (pilot) equipped with a televised view from the nose of the RPV and with standard aircraft controls and displays in order to direct each vehicle to a specific designated target, release its payload, and hand it back to one of the enroute controllers.

Terminal phase control is achieved only if the S RPV is within a 1500' corridor around its flight plan. It is the responsibility of the enroute operator to command "patches" to alter the flight plan as necessary to achieve terminal phase control. These patches are acceptable ("GO") only if they satisfy constraints such as turning radius, available fuel, command link status etc.

---

* This type of extension is feasible because of the basic information processing structure of the OCM. Indeed, there have already been applications of OCM to account for visual scanning(references 7,8) and decision making(references 9,10).

In summary, the enroute operator's task is to monitor the trajectories and ETAs of N vehicles, to decide if the lateral deviation or ETA error of any of these exceeds some threshold, and to correct the paths of those that deviate excessively by issuing acceptable patches.

2. THE CLOSED LOOP MODEL

A block diagram modeling the flow of information and the control and decisions encountered by the human operator (enroute operator) is shown in Figure 1.

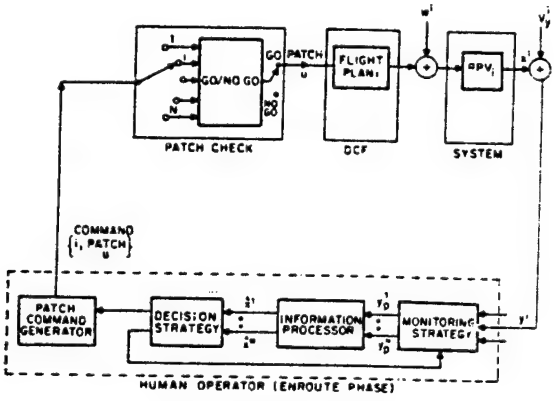

Figure 1. Block Diagram for RPV Monitoring/Control Decision Problem

DCF: The DCF (Drone control facility) contains the stored flight plans that drive the N subsystems RPV_i, i=1,2,...,N. They are usually "optimal" with respect to current terrain and other information. We will assume they can be computed using state-variable equations.

System: The N RPVs undergoing monitoring/control constitute the system. A simple non-linear representation of their dynamic behavior will be assumed for this analysis. Linearization will be carried out if necessary for implementation of the model. The true status x^i of the i-th RPV may be different from the stored flight plans due to "disturbances" w^i. The reported status y^i will be different from the true status x^i due to reporting error v_y^i. The observed status y_p^i will depend on the reported status y^i and on the "monitoring strategy" (to be discussed later on).The disturbances w^i and reporting error v_y^i will be modeled by suitable random processes. The y^i are the displayed variables corresponding to RPV_i.

Monitoring Strategy: Since the human must decide which RPV or which display to look at, he needs to develop a monitoring strategy. This is important because his estimates of the true status of each RPV (and hence his patch decision strategy) will depend upon his monitoring strategy. To account for the interaction of the patch decision strategy with the monitoring strategy we formulate and solve a combined monitoring and patching decision problem (Appendix B has the details).

Monitoring strategies may be distinguished by whether they predict temporal (time histories of) monitoring behaviour or average monitoring behaviour over some chosen time horizon. Most of the earlier work in the literature, including that with the OCM, falls in the latter category. The monitoring strategy we derive will predict temporal behaviour which can be simulated . Some of the monitoring strategies derived in the literature which we expect to investigate in the DEMON setup are:

(i) A simple strategy involving cyclical processing of the various RPVs(reference 11).

(ii) A strategy generalizing the Queueing Theory Sampling Model (reference 12), which would minimize the total cost of not looking at a particular RPV at a given time. This strategy is mainly useful for maintaining lateral deviations within allowable limits. The costs for errors and for the different RPVs would be functions of the time-to-go and, possibly, RPV type.

(iii) A strategy of sampling when the probability that the signal exceeds some prescribed limit is greater than a subjective probability threshold(references 13,14).

(iv) A strategy aimed at minimizing total estimation error(reference 7). This strategy would be consistent with monitoring for the purpose of minimizing lateral deviation errors.

Information Processor: This block models the processing that goes on in the human operator to produce the current estimate of the true RPV status from past observed status. This block is the well known control- theoretic model consisting of a Kalman filter-predictor which produces the maximum-likelihood, least-squares estimate $\hat{x} = (\hat{x}^1, \hat{x}^2, \ldots, \hat{x}^N)$ of the true status x of all the RPVs. It also produces the variance of the error in that estimate.(Note that an estimate of the state of each RPV is maintained synchronously at all times. Observation of a particular RPV improves the accuracy of the estimate of the status of that RPV while uncertainty about the status of the remaining, unobserved vehicles increases.) Given the assumptions generally made for this kind of analysis, the information processor can thus generate the conditional density of x based on the past observations y.

Decision Strategy: This block models the process of deciding which, if any, RPV to patch. We consider the decision process to be discrete (it takes 5 sec to get a new display). The cost of making a patch would reflect the lost opportunity to monitor and/or patch other RPVs as well as breaking radio-silence; the gain (negative cost) is the presumed reduction in error for the "patched" vehicle. The decision strategy attempts to minimize the (expected) cost. This block translates the best estimate $\hat{x}$ into a decision to (i) command a patch to one of the RPVs and/or (ii) modify the future monitoring strategy.

Patch Command Generator: This block generates the commanded patch. We shall investigate a strategy based on minimizing a weighted sum of the time to return to the desired path and the total mean-square tracking error. The allowable paths would be constrained by the RPV turning radius limits. Random execution errors would be added to the commanded patch to represent human errors.

Patch Check: This consists of a GO/NO GO check on the patch using conditions on turning radius, command link status, etc.

3. MATHEMATICAL DETAILS OF THE MODEL

3.1 System

The system under study consists of the N-RPV subsystems and may be described by the state equations:*

$$\dot{x} = Ax + dBu + Ew + Fz \qquad , x(t_0) = x_0 \tag{1}$$

where the state vector x includes the states x^i of the N-RPV subsystems. Here d is a vector of decision variables (to be explained below) and z is a non-random input vector which will be used to model non-zero means of the random inputs w as well as any predetermined command inputs. In the present RPV context z will be used to generate the flight plan for the RPVs. The vector u denotes the patch control input to the RPVs. In partitioned form equation (1) appears as follows:

$$\begin{bmatrix} \dot{x}^1 \\ \dot{x}^2 \\ \vdots \\ \dot{x}^N \end{bmatrix} = \begin{bmatrix} A^{11} & A^{12} & \cdots & A^{1N} \\ A^{21} & A^{22} & \cdots & A^{2N} \\ \vdots & & \ddots & \\ A^{N1} & A^{N2} & \cdots & A^{NN} \end{bmatrix} \begin{bmatrix} x^1 \\ x^2 \\ \vdots \\ x^N \end{bmatrix} + \begin{bmatrix} d_1 I & & & \\ & d_2 I & & \\ & & \ddots & \\ & & & d_N I \end{bmatrix} \begin{bmatrix} B^1 \\ B^2 \\ \vdots \\ B^N \end{bmatrix} u +$$
$$\begin{bmatrix} E^{11} & E^{12} & \cdots & E^{1N} \\ E^{21} & E^{22} & \cdots & E^{2N} \\ \vdots & & \ddots & \\ E^{N1} & E^{N2} & \cdots & E^{NN} \end{bmatrix} \begin{bmatrix} w^1 \\ w^2 \\ \vdots \\ w^N \end{bmatrix} + \begin{bmatrix} F^{11} & F^{12} & \cdots & F^{1N} \\ F^{21} & F^{22} & \cdots & F^{2N} \\ \vdots & & \ddots & \\ F^{N1} & F^{N2} & \cdots & F^{NN} \end{bmatrix} \begin{bmatrix} z^1 \\ z^2 \\ \vdots \\ z^N \end{bmatrix} \tag{2}$$

For the system under study, the following observations hold:

A1: Only one of the N-RPV subsystems may be controlled by the patch-control u at any given time. A decision to control the i-th RPV subsystem then implies the following conditions on the decision variables:

$$d_i = 1 \quad , d_j = 0 \quad , j \neq i \tag{3}$$

A2: The N-RPV subsystems are decoupled (except for the interdependence of the decision variables via (3)), that is,

---

* For the purpose of discussion, a linear model is assumed. In actual implementation, we may use a simple non-linear model in which case (1) would represent a linear perturbation equation for the system about some nominal trajectory.

$$A^{ij} = 0,\ E^{ij} = 0\ ,\ F^{ij} = 0,\ i \neq j \tag{4}$$

The N-RPV subsystems may thus be described by

$$\dot{x}^i = A^{ii}\, x^i + d_i B^i u + E^{ii} w^i + F^{ii} z^i,\ x^i(t_0) = x_0^i \tag{5a}$$

$$d_i = 0 \text{ or } 1 \tag{5b}$$

$$\sum d_i = 1 \text{ or } 0 \tag{5c}$$

3.2 Flight Plan (DCF)

When there is no disturbance w^i and no (patch) control u then the N-RPV subsystems follow the flight plan $\bar{x}^i$

$$\dot{\bar{x}}^i = A^{ii}\, \bar{x}^i + F^{ii} z^i,\ \bar{x}^i(t_0) = \bar{x}_0^i \tag{6}$$

Flight plans made up of straight lines are easily generated using a piecewise constant time function for z^i and $\bar{x}_0^i$ as the launch point.

3.3 Patching

Any disturbance w^i causes the i-th RPV to deviate from its flight plan. Denoting these deviations by $e^i = x^i - \bar{x}^i$ it follows from (5) and (6) that

$$\dot{e}^i = A^{ii}\, e^i + d_i B^i u + E^{ii} w^i\ ,\ e^i(t_0) = x_0^i - \bar{x}_0^i \tag{7a}$$

$$d_i = 0 \text{ or } 1 \tag{7b}$$

$$\sum d_i = 1 \text{ or } 0 \tag{7c}$$

It is the purpose of the (patch) control u to correct any such deviation. Since w^i is an unknown random disturbance and d^i is nonzero for at most a single RPV subsystem, it is not possible to maintain $e^i = 0$ for all i. The operator thus faces the patching problem which consists of the following three sub-problems:

(i) Monitoring decision - which RPV to monitor?
(ii) Patching decision - whether to patch the monitored RPV?
(iii) Patch computation - what patch command to issue?

3.3.1 Monitoring Decision

As mentioned before, the monitoring decision is intimately connected with the patching decision because it restricts the available patching options. For example, in the present RPV context only a monitored RPV can be patched. The combined monitoring and patching decision problem is analyzed in appendix B.

3.3.2 Patching Decision

A patching decision consists of deciding if the monitored RPV subsystem is to be patched. At most one of the RPVs may be patched at a given time. One idea of patching is to reduce deviations from the flight plan to below some threshold values. Some facts to note are:

(i) Cross-track error of less than 250' is desired for type-S RPVs

(ii) Terminal-phase control not possible if cross track error exceeds 1500'

We assume a normative model, in which the operator attempts to optimize some (subjective) measure of performance via a patching decision. This performance measure would depend on his understanding of the mission objectives. Some of the objectives of the RPV mission are: Don't lose an RPV, maintain ETA, maintain lateral position, maintain radio silence. We consider two alternative cost functions to help in arriving at a patching decision:

Piecewise constant cost function

$C(e^i) = \bar{C}^i$ if $e^i \in e_T^i$, a threshold set

$C(e^i) = C^i$ if $e^i \notin e_T^i$

Quadratic Cost function

$C(e^i) = e^{i'} K e^i$

The choice of e_T^i and K will be made based on facts of the type (i) and (ii) noted above. The costs C^i, $\bar{C}^i$, $C(e^i)$ will be chosen to be functions of mission time to reflect the importance of ETA. As mission time gets closer to ETA for RPV-i, C^i will be made larger and/or e_T^i will be shrunk to reflect "urgency". The optimal patch decision will be chosen to minimize the expected cost using subjective probabilities computed with the help of the information processor. The details are in Appendix B.

3.3.3 Patch Control Computation and Generation

Once a decision is made to patch a particular RPV-subsystem, it is necessary to compute and execute the patch control. The purpose of a patch control is to guide the aircraft from its initial location and heading to intercept and fly along the planned flight path. Various criteria may be considered to compute the optimal patch control, for example, a strategy that minimizes the time to return to the planned flight path (see appendix A and also reference 15).

4. IMPLEMENTATION OF THE MODEL

DEMON, the combined monitoring, decision, and control model of the human operator is being implemented in FORTRAN. The program has a modular structure to facilitate ease of adding further modules to include alternative monitoring, control, and decision strategies that may appear promising at a future date.

To accomodate the random aspects of the problem, the program will basically have a Monte-Carlo simulation character. The specialized version of DEMON for

the RPV problem will produce as outputs the "true" time-histories of the RPV flights, the sequence of monitoring and patching decisions made, and the resulting performance.

The important aspects of the simulation program implementing Demon are

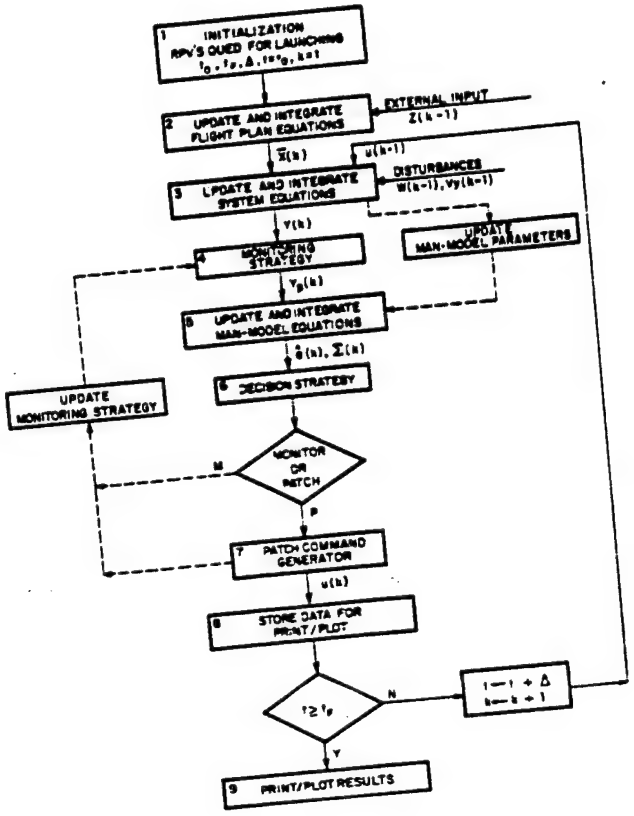

Figure 2. Flow Diagram for the simulation program implementing DEMON

shown in the flow diagram in Figure 2. There are, as indicated, nine major modules in the program. Modules 4, 6 and 7 are of special interest because they do not arise in the usual manual control models. The theory behind these modules is developed in Appendices A and B. As indicated in Appendix A, the patch command generator could involve a non-linear control law.

5. EXAMPLE

In order to test some of the modeling concepts and to debug the DEMON program we consider a simple example which captures the essence of the RPV mission while discarding the nitty gritty details. The lateral motion of the RPVs about their flight plan is represented by random walk processes over the assumed mission duration of 600 frames (the display frame update rate is every 5

seconds). Each RPV is observed via a single lateral deviation display and controlled via a constant velocity comand. The permissible patch back to the flight plan is constrained by the maximum allowable speed which represents the turning radius constraint. The patch control strategy is to use maximum allowable speed adjusted by a "safety factor" which depends on the "NO GO" patches issued previously by the operator for that RPV.

Some preliminary results have been obtained using DEMON on the above simplified RPV mission. The flavour of the results we obtained is indicated in Figure 3 which shows the combined effect of ETA dependent (shrinking) threshold and different RPV priority on the simulated simple RPV mission. As mission time increases RPV monitoring frequency increases . But there comes a time when monitoring resources are not adequate to satisfy the increasing needs of each of

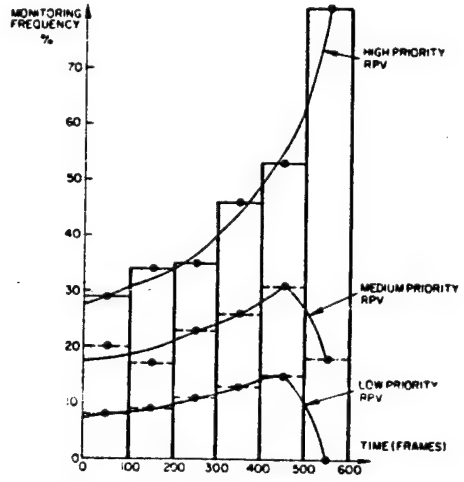

Figure 3. Effect of Shrinking Threshold and RPV Priority

the RPVs and then the highest priority RPV demands most of the attention it can get while the lowest priority RPV gets no attention from the operator.

6. CONCLUSION

We have developed DEMON, a combined monitoring, decision and control model for the human operator in the context of the enroute phase of an RPV mission. Since the monitoring strategy derived from DEMON is temporal it has obvious application to developing instrument scanning strategy for flight control and management. We have structured the model to have wider applicability (than the problems addressed by the basic OCM or the RPV control problem) and expect it to be useful to model human operators whose control actions may be infrequent but whose monitoring and decison making may be the primary activities. We anticipate testing and refining the DEMON model furthur using an existing data base for the RPV control problem(reference 16).

7. APPENDIX A: PATCH CONTROL STRATEGY

7.1 System Dynamics and Patch Computation

In Section 3, the N-RPV system dynamics were considered in general terms. Here, we shall use a simple model for the RPV-subsystem dynamics and derive a specific patch control strategy. Considering only the projected motion in the horizontal plane we shall re-write the normalized equations of motion derived in

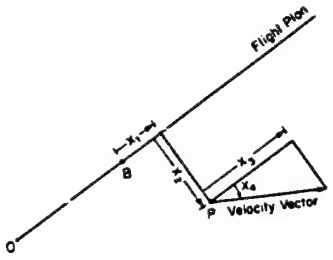

Figure 4. Choice of Co-ordinates for System Equation

reference 15, using the state variables(see Figure 4) x_1 = ground-speed error, x_2 = cross-track error, x_3 = velocity component along track, x_4 = heading relative to track:

$$\dot{x}_1 = \cos x_4 - 1 \quad , x_1(0) \text{ given}, x_1(T) \text{ free}$$

$$\dot{x}_2 = \sin x_4 \quad , x_2(0) \text{ given}, x_2(T) = 0$$

$$\dot{x}_3 = u \sin x_4 \quad , x_3(0) \text{ given}, x_3(T) = 1$$

$$\dot{x}_4 = -u \quad , x_4(0) \text{ given}, x_4(T) = 0$$

$$T \text{ free}$$

$$x_3^2 + x_4^2 = 1$$

Once a decision is made to patch a particular RPV-subsystem, it is necessary to compute and execute the patch control. The purpose of a patch control is to guide the aircraft from its initial location and heading to intercept and fly along the planned flight path. Various criteria may be considered to compute the optimal patch control. Many criteria may be written in the form,

$$J = 1/2K_1x_1^2(T) + 1/2K_2 \int_0^T x_2^2 \, dt + K_3 \int_0^T dt$$

which is a weighted sum of the square of the ground speed error, integral square of the cross-track deviation, and time to return to the planned flight path.We shall only solve the special problem of minimum time to return to the flight path by choosing the weights to be $K_1=0=K_2$ and $K_3=1$.

7.2 Minimum Time Patch Strategy

Using the necesssary conditions for minimum time it is easy to see that the optimal control is Bang-Bang except for possible singular arcs. It can furthur be shown that the singular control is identically zero.

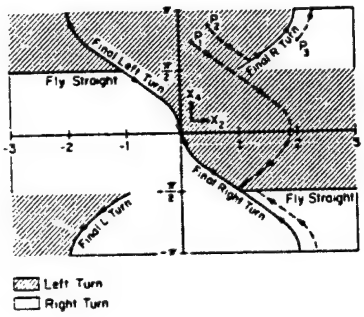

Figure 5. Minimum Time Patch Control Strategy

The computed minimum-time patching strategy is indicated in Figure 5. For example, all points in state space that can be brought to the planned flight path using a single left turn u=1 are characterized by the equation $x_2(0) = \cos x_4(0) - 1$.

The minimum time required for the patch will be checked against the scheduled hand-off times for the given RPV to determine if the computed patch should be executed. Velocity patches to correct for ETA errors with due regard to fuel constraints may be included by a simple extension of the above problem (for example, append to the minimum time patch a velocity patch to minimize ETA errors).

The operator does not observe the states x directly, and will base his control actions instead on the best estimates of these states available to him based on all his observations. This disjoining of estimation and control is justified by the "separation principle" (see reference 17).

8. APPENDIX B: PATCH DECISION STRATEGY

8.1 Introduction

In this appendix we shall formulate and solve the combined monitoring and patching decison problem encountered by the enroute operator in the RPV mission. As stated in section 3, the information processor produces the current estimate $\hat{x}$ of the true status x of all the RPVs at any time. It also produces the variance of the error in that estimate. The information available for making monitoring and patching decisions may be summarized in terms of the posterior distribution of x^i conditioned on all observations based on past monitoring and patching decisions and control. Under the usual assumptions, this posterior distribution for x^i is $N(\hat{x}^i, X^{ii})$.

Let x_T^i denote a threshold set associated with the i-th RPV, that is, $x^i \in x_T^i$ is a desirable condition. Let H^i denote the hypothesis that $x^i \in x_T^i$ and P^i be the probability that H^i is true. P^i is easily calculated using the available information on the posterior distribution of x^i:

$$P^i = 1 - \int_{x_T^i} N(\hat{x}^i , X^{ii})\, dx^i$$

Monitoring the i-th RPV results in a tighter distribution for x^i around its mean $\hat{x}^i$ because it reduces the uncertainty X^{ii} associated with $\hat{x}^i$. Patching the i-th RPV requires monitoring as well. The effects of patching are: first, to correct the error e^i which might have 'wandered off' from zero due to disturbances, by assuring that $\hat{x}^i \in x_T^i$; and second, to provide a tighter distribution of x^i around its mean $\hat{x}^i$.

To formulate and solve the combined monitoring and patching decision problem, we shall assume that C_i is the cost if H^i is true. Recall that H^i has a (subjective) probability P^i of being true. Just as H_i, P^i, C_i were defined in relation to the set x_T^i, let $\bar{H}_i$, $\bar{P}^i$, $\bar{C}_i$ be defined in relation to the set $\bar{x}_T^i$, the complement of x_T^i. We shall use minimum expected cost EC(d*) as the criterion for selecting the best monitoring and patching decision d*.

Let d_{ij} denote a decision to monitor RPV-i and patch RPV-j in the combined monitoring and patching decision problem. Since a patch can be done only on a monitored RPV, there are only 2N+1 available decisions. They are:

(i) Do nothing decision d_{00}, that is, monitor no RPV and patch no RPV.*

(ii) N pure monitoring (no patching) decisions d_{j0}, j=1,2,..,N.
(iii) N patching (and monitoring) decisions d_{jj}, j=1,2,...,N.

Let P_{ijk} denote the probability that the hypothesis H^i is true when the decision is d_{jk}. Because the RPV subsystems are non-interactive, it follows that the probabilities associated with RPV-i when some other RPV is monitored and/or patched is same as that associated with RPV-i when no RPV is monitored. That is,

$$P_{i00} = P_{ijk} \quad \text{any } j \neq i,\ i=1,2,\ldots,N;\ k=j \text{ or } 0$$

Thus, there are only 3N distinct probabilities to be computed
(i) N probabilities P_{i00} associated with do-nothing decision d_{00}
(ii) N probabilities P_{ii0} associated with pure monitoring decision d_{i0}
(iii) N probabilities P_{iii} associated with patching decision d_{ii}

Let $(PP)_i$ denote the probability that the patch decision d_{ii} "takes", that is, results in $x^i \in x_T^i$, and let T_{ij} denote the cost of implementing decision d_{ij}. The costs T_{ij} will be chosen to be functions of mission time to reflect the importance of ETA. As mission time gets closer to ETA for RPV-i, T_{ij} will be made larger and/or x_T^i will be shrunk to reflect "urgency".

---

* This could correspond to performing some other task such as communication.

The combined monitoring and patching decision problem is described in terms of a decision-tree diagram in Figure 5.* The actual cost of a particular

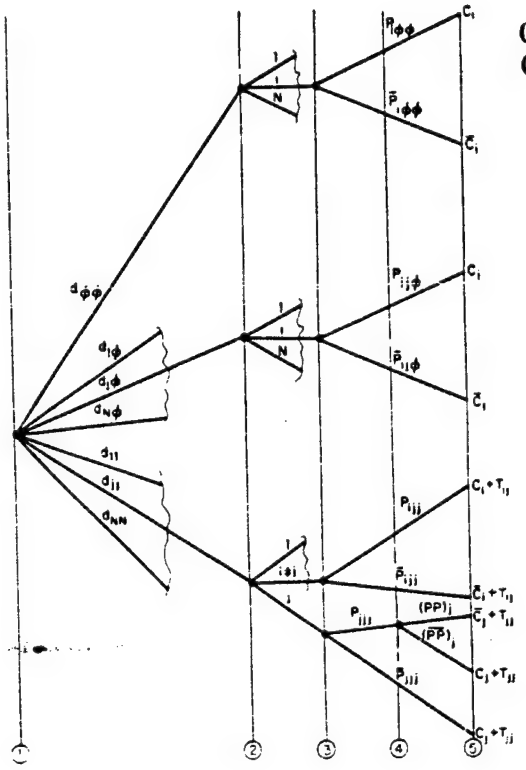

ORIGINAL PAGE IS
OF POOR QUALITY

Figure 6. Decision Tree Diagram for Combined Monitoring and Patching

decision depends on the path chosen to traverse the tree from level 1 to level 5. The exact path from level 1 to level 5 for the N-RPVs are determined both by the decision maker (the human operator) and by Nature (the random elements in the problem) . Since a decision has to be made at level 1 before Nature has

* For reasons similar to the one we stated for combining the monitoring and patching decision problem, one might argue that the decision problem over the rest of the mission duration must be considered by the operator at any decision instant during the mission. We shall not do this because: first, the analysis for this case is no different from the one we present here - only the expressions are messier; and second, the actual computations of the decisions would become infeasible .

taken its course at the monitoring level 3 and at the patching level 4 , the decision maker can only evaluate his 2N+1 alternative decisions in terms of their expected costs. This he can do as follows: The expected cost of the do-nothing decision d_{00} is

$$EC(d_{00}) = \sum_1^N (C_i P_{i00} + \bar{C}_i \bar{P}_{i00})$$

Expected cost of pure monitoring decision d_{j0} is

$$EC(d_{j0}) = EC(d_{00}) - (C_j P_{j00} + \bar{C}_j \bar{P}_{j00}) + C_j P_{jj0} + \bar{C}_j \bar{P}_{jj0}) + T_{j0}$$

Expected cost of a patching decision d_{jj} is,

$$EC(d_{j0}) = EC(d_{00}) - (C_j P_{j00} + \bar{C}_j \bar{P}_{j00}) + (C_j P_{jjj} + \bar{C}_j \bar{P}_{jjj}) - (PP\ P \qquad T_{jj})$$

The optimal decision d^* is the one which results in maximum opportunity gain, that is,*

$$d^* = \arg\min (EC(d_{00}, EC(d_{m0}), EC(d_{kk}))$$

where

$$m = \arg\max_j ((C_j P_{j00} + \bar{C}_j \bar{P}_{j00}) - (C_j P_{jj0} + \bar{C}_j \bar{P}_{jj0}) - T_{j0})$$

$$k = \arg\max_j ((C_j P_{j00} + \bar{C}_j \bar{P}_{j00}) + (C_j P_{jjj} + \bar{C}_j \bar{P}_{jjj}) - (PP_j P_{jjj} (C_j - \bar{C}_j) - T_{jj}))$$

Consider a specialization of the above decision problem where the probabilities P_{ijk} are assumed to be independent of the decisions d_{jk} (that is, $P_{ijk} = P_i$) , the costs $\bar{C}_i$ and T_{ij} are all zero, and the patch success probabilities $(PP)_i = 1$ for each subsystem RPV. Then the optimal decision is

$$d^* = d_{jj}$$

where

$$j = \arg\max_i (P_i C_i)$$

This is the result obtained by Carbonell(reference 12).

An implicit assumption made in the computation of expected cost in the combined monitoring and patching decision problem is that the costs are constant over the entire sets $\vec{x}_T$ and x_T^i. This assumption is easily dropped when non-constant cost functions are desired, e.g.,

$$C(e^i) = e^{i'} M e^i$$

In such a case, $P_{ijk} C_i$ in the above analysis will be replaced by an appropriate integral which would yield $P_{ijk} C_i$ as a function of $\hat{x}^i$ and X^{ii} and appears amenable for computations.

---

* The notation arg. min. implies $d^* = d_{00}$ or d_{m0} or d_{kk} depending on which of the three values $EC(d_{00})$, $EC(d_{m0})$, $EC(d_{kk})$ is the smallest. Here d_{m0} is the best monitoring decision and d_{kk} is the best patching decision.

We close this appendix, with an example of a piecewise-constant cost function that appears meaningful for the N-RPV system under study. Recall from appendix A that the first two components of x^i are:

x_1^i = ground speed error (along track)

x_2^i = cross-track error

One choice for the piecewise-constant cost function is:

$$C(e^i) = 1 \text{ if } |x_2^i| > x_{2T}^i = 250$$
$$= 0 \text{ if } |x_2^i| \leq 250$$

REFERENCES

1. Miller, D., Feehrer, C., Muralidharan, R., Pew, R. and Baron, S., "Development of Human Performance models for Man-Machine System Simulation", BBN Report No. 3739, December 1977.

2. Baron, S., "A Model for Human Control and Monitoring Based on Modern Control Theory," **Journal of Cybernetics and Information Sciences**, Vol. 4, No. 1, Spring 1976.

3. Baron, S. and W. Levison, "An Optimal Control Methodology for Analyzing the Effects of Display Parameters on Performance and Workload in Manual Flight Control, "**IEEE Trans. on Systems Man and Cybernetics**, Vol. SMC-5, No. 4, July 1975.

4. Baron, S., D. L. Kleinman, et al., "Application of Optimal Control Theory to the Prediction of Human Performance in a Complex Task," Wright Patterson Air Force Base, Ohio, AFFDL-TR-69-81, March 1970

5. Kleinman, D. L. and S. Baron, "A Control Theoretic Model for Piloted Approach to Landing," **Automatica**, Vol. 9, 1973, pp. 339-347

6. Kleinman, D. L., S. Baron and W. H. Levison, "An Optimal-Control Model of Human Response, Part 1: Theory and Validation," **Automatica**, Vol. 6, 1970, pp. 357-369

7. Baron, S. and D. L. Kleinman, "The Human as an Optimal Controller and Information Processor," **IEEE Trans. on Man Machine Systems**, MMS-10, No. 1, March 1969

8. Kleinman, D. and R. Curry, "Some New Control Theoretic Models for Human Operator Display Monitoring", **IEEE Trans. on Systems , Man and Cybernetics**", Vol. SMC-7, No.11, November 1977, pp. 778-784

9. Levison, W. and R. Tanner, "A Control Theoretic Model for Human Decision-Making", NASA CR-1953, December 1971

10. Gai, E. and R. Curry,"A Model of the Human Observer in Failure Detection Tasks", **IEEE Trans. System , Man and Cybernetics**, Vol. SMC-6, No. 2, February 1976

11. Senders, J., "The Human Observer as a Monitor and Controller of Multidegree of Freedom Systems", **IEEE Trans. Hum. Factors Electron.**, Vol. HFE-5, No. 1, September 1964

12. Carbonell, J. R.,"A Queueing Model of Many-Instrument Visual Sampling," **IEEE Transactions on Human Factors in Electronics**, Vol. HFE-7, No. 4, December 1966, pp. 157-164

13. Senders, J.,J. Elkind, M. Grignetti and R. Smallwood, "An Investigation of the Visual Sampling Behaviour of Human Observers", NASA CR-434, April 1966

14. Gai, E. and R. Curry, "Failure Detection by Pilots During Automatic Landing: Models and Experiments", **J. Aircraft**, February 1977

15. Erzberger, H. and H. Q. Lee, "Optimum Horizontal Guidance Techniques for Aircraft," **J. Aircraft**, Vol. 8, No. 2, February 1971, pp. 95-101

16. Mills, R.,R. Bachert and N. Aume, "Supplementary Report of the RPV System Simulation Study II : Evaluation of RPV Position Report Smoothing and Automatic Heading Correction", AMRL-TR 75-87, September 1975.

17. Bryson, A. E. and Y. C. Ho, "**Applied Optimal Control**", Hemisphere, newyork, 1969

D4

N79-15632

A MODEL OF HUMAN EVENT DETECTION IN MULTIPLE PROCESS MONITORING SITUATIONS*

Joel S. Greenstein and William B. Rouse

Department of Mechanical and Industrial Engineering
Coordinated Science Laboratory
University of Illinois
Urbana, Illinois 61801

SUMMARY

It is proposed that human decision making in many multi-task situations might be modeled in terms of the manner in which the human detects events related to his tasks and the manner in which he allocates his attention among his tasks once he feels events have occurred. A model of human event detection performance in such a situation is presented. An assumption of the model is that, in attempting to detect events, the human generates the probabilities that events have occurred. Discriminant analysis is used to model the human's generation of these probabilities. An experimental study of human event detection performance in a multiple process monitoring situation is described and the application of the event detection model to this situation is addressed. The experimental study employed a situation in which subjects simultaneously monitored several dynamic processes for the occurrence of events and made yes/no decisions on the presence of events in each process. Input to the event detection model of the information displayed to the experimental subjects allows comparison of the model's performance with the performance of the subjects.

INTRODUCTION

In many systems, the human operator spends much of his time monitoring subsystems for events which call for action on his part. Aircraft, power stations, and process control plants are examples of such systems. As the complexity of these systems increases, the operator becomes responsible for more subsystems of greater variety. There is consequently a greater probability that the operator will encounter situations in which there are more tasks than he can acceptably perform.

One means of maintaining the operator's workload at a satisfactory level is the introduction of automation capable of performing some of the operator's tasks. Models of the operator's task performance would be of use

*This research was supported by the National Aeronautics and Space Administration under NASA-Ames Grant NSG-2119.

in predicting the performance gains to be expected from the introduction of such aids. Further, in systems in which the responsibilities for some tasks are shared by the operator and an automated decision maker, these models might also be used within the system to coordinate the actions of the two decision makers.

Senders [1] and Smallwood [2] have modeled human decision making in multiple process monitoring tasks. Senders postulated that the human monitor samples his displays in a manner which allows reconstruction of the displayed signals. An information theory approach is employed to determine how often and for what duration the human must sample each display. Smallwood proposed that the human operator forms an internal model of the processes he is monitoring and of the environment relevant to his task as a result of his past perceptions of them. A situation is considered in which the operator seeks to detect excursions of instruments beyond threshold values. The operator is modeled as directing his attention to the instrument whose current probability of exceeding threshold (based on the operator's internal model) is greatest. It might be noted, in passing, that the internal model concept discussed by Smallwood is perhaps as appropriate to the design of automated decision makers as it is to modeling the human decision maker. If the automated decision maker is to interact appropriately with the human, it would seem that its internal model of the relevant environment should include a model of the human.

Carbonell [3,4] and Senders and Posner [5] have proposed queueing theory approaches to the modeling of human decision making in multiple process monitoring tasks. Carbonell uses a priority queueing discipline. He assumes that the human operator attempts to minimize the risk involved in not observing other instruments when he chooses to monitor a particular instrument. Senders and Posner employ a first come first served service discipline. They suggest two models which might be used to estimate the inter-observation intervals for an instrument (i.e., the time between arrivals of the instrument to the queue of instruments awaiting observation by the human monitor). The first model involves the degree of the observer's uncertainty about the value of the variable displayed on the instrument. The second model involves the probability that the displayed variable will exceed an acceptable limit.

The models cited above emphasize the monitoring of displays, rather than the decisions or actions that result from the human operator's perception of the displayed values. The operator's motivation for monitoring the displays is the possibility that an event which requires his action will occur. The multi-task decision making problem addressed in this paper concerns the event detection and action selection decisions the operator makes on the basis of the information he gains through monitoring.

Human decision making in such multi-task situations, then, might be modeled in terms of the manner in which the human detects events related to his tasks and the manner in which he allocates his attention among his tasks once he feels events have occurred. Gai and Curry [6] have developed a model of the human monitor in a failure detection task. The model has two stages, the first being a Kalman filter which estimates the states and observations

of the monitored process and the second a decision mechanism which operates on the Kalman filter residuals using sequential analysis concepts. The model can be used to describe the human monitor's detection of additive failures in stationary random processes.

Sheridan and Tulga [7] have modeled the manner in which the human operator allocates his attention among various tasks. They address a situation in which events present themselves unequivocally and use a dynamic programming approach to determine the action sequence which maximizes the operator's earnings. This action sequence is begun, but can be superceded by a new sequence calculated in response to the appearance of additional tasks.

Rouse [8] has investigated the issue of allocation of decision making responsibility between a human operator and an automated decision maker. He presents a mathematical formulation of the multi-task decision making situation appropriate to the modeling of either decision maker. Based on displayed information, the decision maker is assumed to generate probabilities that events have occurred in his tasks. He also generates density functions which characterize his perceptions of what might occur in his tasks while his attention is diverted to a particular task and how long his attention will be diverted should he decide to take a given action. Combining estimates of the probabilities events have occurred with the density functions of time between events in the tasks and action times with respect to the tasks, the decision maker chooses his actions to minimize an appropriate cost criterion. In this paper, we present a model of the human's event detection performance consistent with this mathematical formulation, describe an experimental study of event detection performance in a multiple process monitoring situation, and address the application of the model to the process monitoring situation.

THE EVENT DETECTION MODEL

The event detection model assumes that, in attempting to detect events, the human generates the probabilities that events have occurred. A discriminant analysis approach [9,10] is used to model the human's generation of these probabilities. Our use of discriminant analysis to model the human's generation of event probabilities is motivated by the fact that this approach does not require explicit models of the systems the human is monitoring. An understanding of the systems is certainly helpful in determining the features to extract from the observations. But explicit models of the systems' structures are not required.

For each task i, various features x_{ij}, $j=1,2, \ldots,m_i$, are extracted from the human's task related observations $\underline{z}_i$. These features are properties of the observations that characterize (or are believed to characterize) the presence or absence of events related to the task. Following the extraction of a set of features, the value of a linear discriminant function

$$Y_i = v_{i1}x_{i1} + \cdots + v_{im_i}x_{im_i} \quad (1)$$

is calculated. Based on previous experience with the task, estimates are made of the discriminant function coefficients v_{ij}, $j=1,2, \ldots,m_i$, with which to combine the feature values x_{ij} to obtain the discriminant function score Y_i that best differentiates observations of events from the rest of the task related observations. Estimates of the mean and variance of the discriminant function over observations of events and over the rest of the observations are also formed. The a posteriori probability that an event has occurred is generated using the value of the discriminant function score, the estimates of the means and variances of this score over events and "non-events", and an estimate of the a priori probability of the event.

If the human operator is forced to make a yes/no response on the presence of an event, we might assume that he chooses the response which maximizes his expected reward. We can then express his decision in a signal detection manner and state that he should respond "yes, an event related to task i has occurred" if the following inequality holds:

$$\frac{P(e_i/Y_i)}{1 - P(e_i/Y_i)} > \frac{V_{CR_i} + C_{FA_i}}{V_{H_i} + C_{M_i}} \quad (2)$$

$P(e_i/Y_i)$ is the a posteriori probability that an event related to task i has occurred. The value of this probability is generated by the event detection model. V_{CR} is the value of correctly responding "no event" (a correct rejection), C_{FA} is the cost of incorrectly responding "event" (a false alarm), V_H is the value of correctly responding "event" (a hit), and C_M is the cost of incorrectly responding "no event" (a miss).

It is predicted, then, that if the operator is forced to make a yes/no decision on the presence of a task related event, he calculates the likelihood ratio of the event (the left hand side of Eq. (2)). He compares the magnitude of the likelihood ratio with a threshold determined by the values of correct responses and the costs of incorrect responses (the right hand side of Eq. (2)). He responds "event" if the likelihood ratio exceeds the threshold.

THE EVENT DETECTION EXPERIMENT

An experiment has been run employing a situation in which subjects simultaneously monitor several dynamic processes for the occurrence of events and make yes/no decisions on the presence of events in each process. Figure 1 illustrates the display observed by the subjects in the experiment. The static display was generated on a Tektronix 4010 by a time-shared DEC-System 10 and depicts the measured values of the outputs of nine processes over 100 sampling intervals (i.e., 101 points). The processes had identical second order system dynamics with a natural frequency of 0.75 rad/sec and a damping

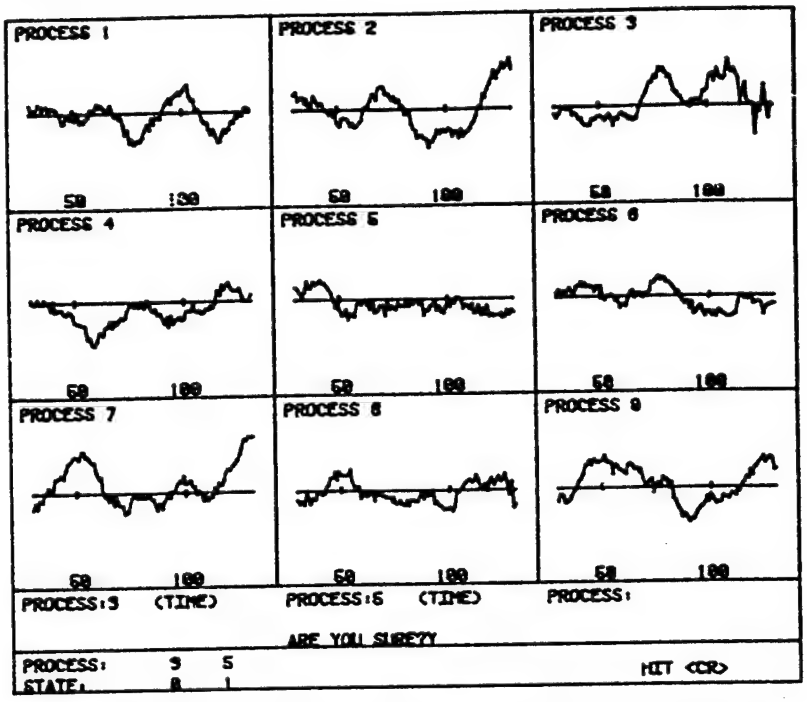

Figure 1. The Multiple Process Monitoring Situation

ratio of 0.5. Samples were taken at 0.2 second intervals. The inputs to the processes were zero-mean Gaussian white noise sequences of identical variance. The displayed measurements were obtained by corrupting the process outputs with additive zero-mean Gaussian white noise sequences which normally had identical variance. The measurement noise variance was normally selected to yield measurements with signal-to-noise ratios of 25.0. An abnormal event in a process was defined by an increase in the measurement noise variance such that the signal-to-noise ratio following an event occurrence was decreased to 95% of the signal-to-noise ratio of the preceding measurement. Thus, abnormal events became more pronounced with each measurement following their occurrence.

After scanning the nine process histories, the subject was given an opportunity to key in the numbers of processes in which he had decided an abnormal event had occurred. He was then given feedback regarding the actual states of the processes he had keyed in ("1" indicating the normal state, "0" indicating the abnormal state). An iteration in a trial was completed by erasing the display, scoring the subject's performance, and returning all abnormal processes detected by the subject to the normal state. Another iteration was then begun by generating a new display depicting the process histories advanced 10 sampling intervals in time as illustrated by Figure 2. (The dashed vertical lines indicated to the subject the point at which he last responded to each process.)

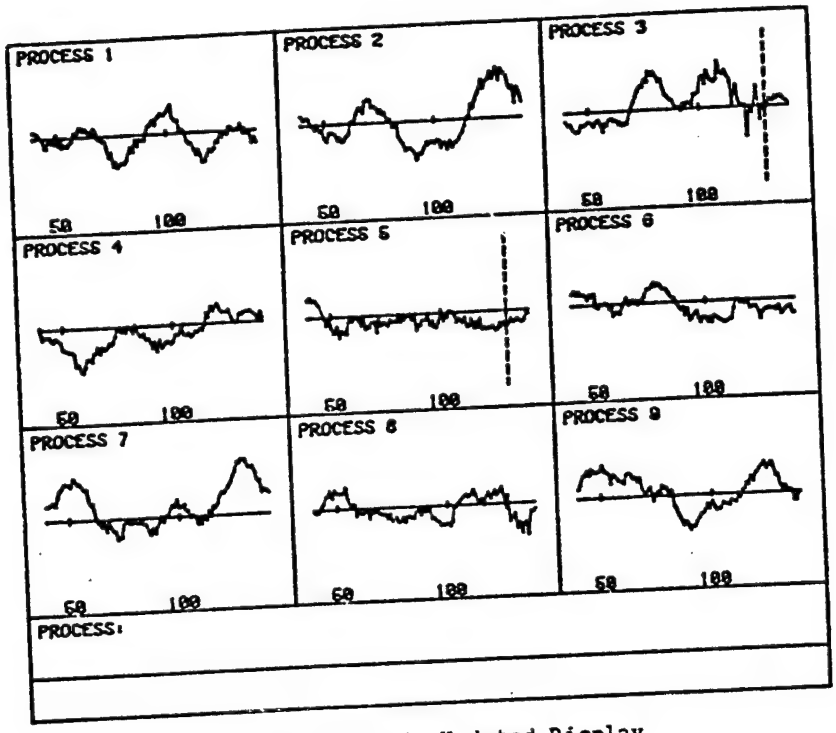

Figure 2. An Updated Display

The subject was allowed to respond to as many events as he thought had occurred. He was awarded points for his hits, receiving high scores for responding to events soon after their occurrence and lower scores for tardier responses. A fixed number of points was deducted for each false alarm. The subject was allowed to study the displays as long as he wished, but any time taken beyond the first minute on each iteration reduced the score awarded for hits made on that iteration.

Eight subjects were given three trials spaced over several days. Each trial was 20 iterations long. The first and third trials given half the subjects were identical, with one event scheduled to occur per iteration. Their second trial scheduled the same events as the first and third trials, but also scheduled an additional event occurrence each iteration. The rest of the subjects were given the same trials in different order so that two events were scheduled to occur per iteration in the first and third trials while one occurrence per iteration was scheduled in the second trial. (Not all scheduled events actually occurred. If an event was scheduled to occur in a process in which a previous event had not yet been detected by the subject, the scheduled event was deleted from the trial.) Events were scheduled to occur uniformly over the nine processes and over the 10 new points displayed for each process on each iteration (the last 10 points on the first iteration, in which all 101 points were new) within the constraint that no two events could occur in a process within 30 sampling intervals of

each other.

Before each trial, the subject was told the average number of new events he could expect to occur per iteration. He was not given any information regarding the dynamics of the processes, but was told that he could expect the processes to exhibit similar characteristics when operating normally. He was also not told what parameter changes defined events, but was told that all events would generally exhibit similar characteristics, and all would become more pronounced as time passed. The subject was given several iterations of training before each trial during which solid vertical lines were included on the process histories to mark exactly when and where events had occurred.

During each trial, the subject was asked to keep a log in which he described his strategies for event detection and noted characteristics of the process measurements he used in his attempts to detect events. After each trial, he was asked to order these characteristics in terms of their usefulness in event detection.

APPLICATION OF THE MODEL TO THE EXPERIMENTAL SITUATION

The event detection model suggests that the human operator in the experimental situation just described extracts various features from his observations of the process measurements. He attempts to select features which characterize the presence or absence of task related events. Through his experience with the processes, the operator has formed estimates of the discriminant function coefficients with which to combine the features to obtain a discriminant function score. He has also formed estimates of the means and variances of this score over observations of events and over the rest of his observations. The operator generates the likelihood ratio that an event has occurred based on the value of the discriminant function score. his estimates of the means and variances of the score, and his estimate of the a priori probability of an event occurrence. He compares the likelihood ratio with a threshold that is based solely on the values of correct responses and the costs of incorrect responses and responds "event" if the likelihood ratio exceeds the threshold.

Four features of the process measurements were selected for use with the event detection model. Selection of these features was guided by the comments of the experimental subjects regarding the characteristics of the process measurements they found useful in event detection. The first feature involves the magnitude changes between successive measurements in a sequence of the most recent measurements. The second feature involves the presence of reversals in direction in this sequence (changes from positive slope to negative, or vice versa, of the line segments connecting the measurements of the sequence). The third feature tests for the simultaneous occurence of large magnitude changes and reversals. The fourth feature, like the first, is a measure of magnitude changes, but it is much more local in that it

involves only the four most recent measurements of the process output.

In extracting these features from the process measurements, the values of the features over recent measurements are weighted more heavily than the values over earlier measurements. The weight decreases exponentially with the age of the measurement and the rate of this decrease is a free parameter. The value of the first feature, for example, a measure of the magnitude changes between successive measurements in a sequence of the n most recent measurements of a process' output, is given by

$$x_1 = \{ \sum_{k=1}^{n-1} |z(k+1)-z(k)| \cdot \exp[-\beta(n-1-k)] \} / \sum_{k=1}^{n-1} \exp[-\beta(n-1-k)] \qquad (3)$$

where z(k) is the k th measurement in the sequence, z(n) is the most recent measurement, and β is the free parameter governing the relative weighting of the feature's value over recent and earlier measurements in the sequence.

In the generation of the likelihood ratio of an event in a process at a given iteration of an experimental trial, the sequence of process measurements over which the features are calculated ends with the last measurement displayed for the process on that iteration. The cutoff length used in extracting the features from the process is a free parameter. Values of the features over process measurements taken earlier than the cutoff are not calculated (or, effectively, are assigned zero weight). If the subject responded "event" to the process at some point following the cutoff, then features are calculated over only those measurements occurring after this response. The information on the state of the process that the subject gains when he responds to the process motivates this constraint. If the process is in the normal state, then on succeeding iterations the subject knows that if an event has occurred, it must have occurred following his last response. If the process is in the abnormal state, then the process is reset to normal when the subject keys in his response. On succeeding iterations the subject knows that if another event has occurred in the process, it must have occurred following his last response. In either case, the subject (and the model) should calculate features only over measurements occurring after the subject's last response.

The estimation of discriminant function coefficients requires a representation of normal and abnormal process measurements. This representation was formed using the process histories displayed to the subject on his third experimental trial. The process histories are separated into two groups of sequences - normal and abnormal. Sequences of measurements beginning when a process was returned to the normal state and ending when an event occurred are defined to be normal. Sequences of measurements beginning when an event occurred and ending when the process was returned to the normal state are defined to be abnormal. The values of the four features were calculated over the entire length of each of the sequences in the two groups. A discriminant analysis was then performed on the resulting two groups of feature values to determine the discriminant function coefficients v_j, j=1,2,...,m, with which to combine the features to best differentiate between the two groups. The mean value and the variance of the

resulting discriminant function scores for the sequences in each of the two groups was also calculated.

The final requirements for application of the event detection model to the experimental situation are estimates of the a priori probabilities of event occurrences and the selection of a threshold against which likelihood ratios of events can be compared. For experimental trials in which one event was scheduled to occur per update of the display over the nine processes monitored by the subject the a priori probability of an event occurrence in each process was fixed at 1/9. For trials in which two events were scheduled to occur per display update, the a priori probability was fixed at 2/9. The threshold against which the likelihood ratios of events are compared is assumed to remain constant through an experimental trial. The magnitude of this constant is a free parameter.

RESULTS

Figure 3 compares the event detection performance of the model with the actual performance of each of the eight subjects in the third trial of the experiment. In this trial, 20 events were scheduled to occur in the trials given subjects A,B,C. and D, while 40 events were scheduled to occur in the trials given subjects E,F.G, and H. In applying the model to each of these trials, the number of measurements over which features were extracted (cutoff

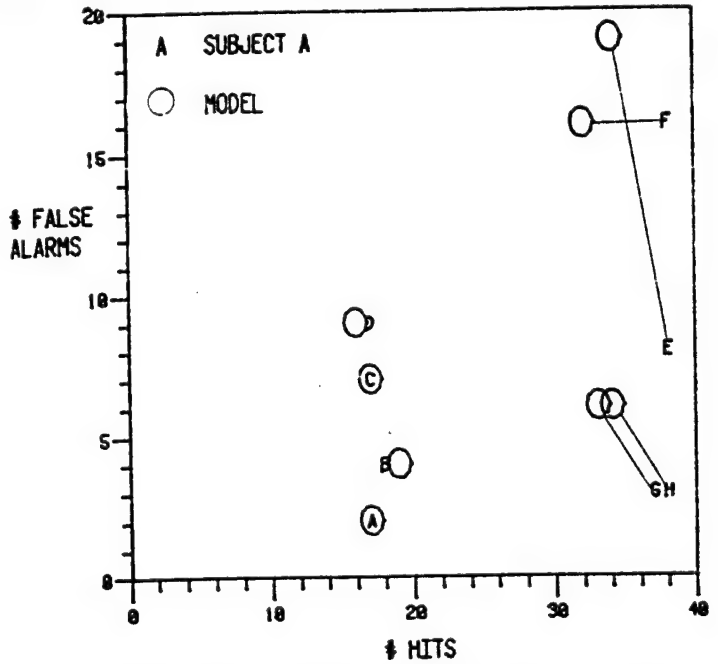

Figure 3. Comparison of Model with Subjects on Third Trial

length) and the relative weighting of recent and older points (β) were adjusted to improve the fit of the model's performance to each subject's performance. The value of the threshold against which likelihood ratios of events were compared was also adjusted to improve the fit. Figure 3 reveals a high degree of correspondence between the model's performance and the performance of most subjects.

Figure 4 compares the event detection performance of the model with the actual performance of the eight subjects in the second trial of the experiment. In this trial, 40 events were scheduled to occur in the trials given subjects A,B,C, and D, while 20 events were scheduled to occur in the trials given subjects E,F,G, and H. In applying the model to each of these trials, none of the parameters of the model were changed from the settings used to obtain the results presented in Figure 3. Despite the fact that the numbers of events scheduled in these trials differ from those in the trials used to assign the values of the parameters, the correspondence between the model's performance and the performance of most subjects is reasonable.

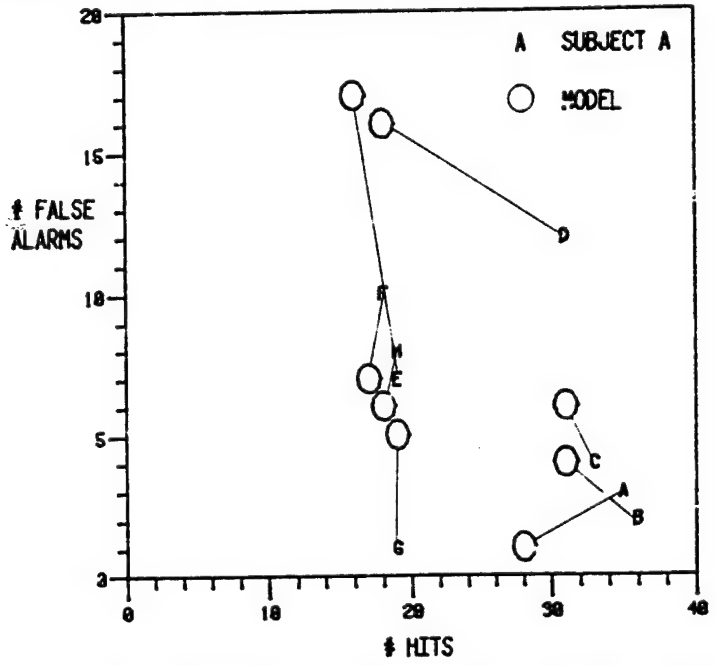

Figure 4. Comparison of Model with Subjects on Second Trial

Table 1 compares the mean detection times (in terms of the number of sampling intervals which elapsed from the occurrence of an event to the time of its detection) for hits common to both subject and model in the trials presented in Figures 3 and 4. It should be noted that the fact that the mean detection times of the model are consistently smaller than those of the subjects is an artifact of the manner in which the model's performance was investigated. The model was tested on the process histories displayed to a subject in his experimental trial. In these trials, a process was returned to the normal state at the point at which the subject detected an event in

the process. Thus, in going over the process histories the model can never respond to an event later than the subject responded to it. If the model fails to respond to an event by the time of the subject's response, the model is scored as having missed that event.

Table 1. - Comparison of Mean Detection Times

	Trial 1		Trial 2	
Subject Code	Subject	Model	Subject	Model
A	24	19	24	20
B	26	21	25	19
C	28	17	28	17
D	32	21	30	16
E	18	13	22	17
F	17	14	27	16
G	20	17	27	20
H	20	17	22	18

We plan to evaluate the model in the near future using a somewhat different approach. Rather than running the model over the process histories displayed to a subject on an earlier experimental trial (and constraining the timing of the model's responses by the timing of the subject's responses in that trial), we will use the model in place of the subject in the event detection experiment. Processes in which events occur will then remain in the abnormal state until the model responds to the process. The only constraint on the model's detection times will be the end of the experimental trial. Because the model's detection time for each event need no longer be less than or equal to the subject's detection time for that event, we expect that, for a given number of hits, the model's threshold can be raised to achieve the longer mean detection times and smaller numbers of false alarms characteristic of the subjects in the experiment.

CONCLUDING REMARKS

In applying the event detection model to the experimental situation described in this paper, we studied a situation in which the subject was forced to respond yes or no to the possibility of an event related to each of nine processes. In general, the human operator is not forced to make such yes/no decisions with respect to each of his tasks. Instead he uses his estimates of the probabilities of task-related events (which the event detection model generates) in deciding how to allocate his attention among his tasks. We plan to run an experiment investigating the human's attention allocation performance in a multiple process monitoring situation similar to

the one employed in the event detection experiment discussed here. Data from this experiment will be used to develop and validate a model of attention allocation performance in multi-task situations. (The modeling of human attention allocation performance in multi-task situations is considered in [11].) This model might be used in conjunction with the event detection model as a part of the design process for, and the implementation of, automated decision making systems.

REFERENCES

1. Senders, J. W.: "The Human Operator as a Monitor and Controller of Multidegree of Freedom Systems," IEEE Trans. Human Factors in Electronics, vol. HFE-5, no.1 pp.2-5, Sept. 1964.

2. Smallwood, R. D.: "Internal Models and the Human Instrument Monitor," IEEE Trans. Human Factors in Electronics, vol. HFE-8, no.3, pp. 181-187, Sept. 1967.

3. Carbonell, J. R : "A Queueing Model of Many-Instrument Visual Sampling," IEEE Trans. Human Factors in Electronics, vol. HFE-7. no.4, pp. 157-164. Dec. 1966.

4. Carbonell, J. R.; Ward, J L.; and Senders, J. W : "A Queueing Model of Visual Sampling: Experimental Validation," IEEE Trans. Man-Machine Systems. vol. MMS-9, no.3, pp.82-87, Sept. 1968.

5. Senders, J. W ; and Posner M. J. M.: "A Queueing Model of Monitoring and Supervisory Behavior," in T. B. Sheridan and G. Johannsen, Eds., Monitoring Behavior and Supervisory Control, New York: Plenum 1976, pp.245-259.

6. Gai E. G.; and Curry, R. E.: " A Model of the Human Observer in Failure Detection Tasks," IEEE Trans. Systems, Man. and Cybernetics, vol. SMC-6, no.2, pp.85-94, Feb. 1976.

7. Sheridan, T. B.; and Tulga, M. K.: "A Model for Dynamic Allocation of Human Attention Among Multiple Tasks," Proceedings of the Fourteenth Annual Conference on Manual Control, University of Southern California, April 1978.

8. Rouse, W. B.: "Human-Computer Interaction in Multitask Situations," IEEE Trans. Systems, Man, and Cybernetics, vol. SMC-7, no.5, pp. 384-392, May 1977.

9. Tatsuoka, M. M.: Multivariate Analysis. New York: Wiley, 1971.

10. Afifi, A. A.; and Azen, S. P.: Statistical Analysis. New York: Academic Press, 1972.

11. Rouse, W. B.; and Greenstein, J. S.: "A Model of Human Decision Making in Multi-Task Situations: Implications for Computer Aiding," Proceedings of the 1976 International Conference on Cybernetics and Society, Washington, Nov. 1976.

D45

N79-15633

PILOT DECISION MAKING IN A COMPUTER-AIDED FLIGHT MANAGEMENT SITUATION*

Yee-yeen Chu and William B. Rouse

Department of Mechanical and Industrial Engineering
Coordinated Science Laboratory
University of Illinois
Urbana, Illinois 61801

SUMMARY

An experimental representation of a computer-aided multi-task flight management situation has been developed. A computer aiding program was implemented to serve as a back-up decision maker. An experiment was conducted with a balanced design of several subject runs for different workload levels. This was achieved using three levels of subsystem event arrival rates, three levels of control task involvement, and three levels of availability of computer aiding. Experimental results compared quite favorably with those from a computer simulation which employed a $(M/E_k/2):(PRP/K/K)$ queueing model. It was shown that the aiding had enhanced system performance as well as subjective ratings, and that the adaptive aiding policy further reduced subsystem delay.

INTRODUCTION

As aircraft become more complicated and greater demands and better performance are being required of pilot, the development of automated airborne systems to share the tasks of piloting an airplane becomes increasing attractive. Advances in electronics and computer technology have made this approach both feasible and promising. Progress in sophisticated cockpit design and growth in avionic computer systems reflect the trend.

Equiped with autopilot and airborne computers performing automatic navigation, guidance, energy calculations, flight planning, information management, etc., the next-generation of aircraft are quite likely to be capable of carrying out all phase of flight automatically. However, the human pilot is likely to reamin a part of the system to cope with unpredicted or failure situations for which automation may be economically or politically infeasible. The pilot's roll then is changing from one of controller to one of supervisor and manager, responsible for monitoring, planning and decision making.

* This research was supported by the National Aeronautics and Space Administration under NASA-Ames Grant NSG-2119.

676

The pilot as the airborne system manager has responsibility to monitor the aircraft subsystems such as navigation, guidance, etc. as well as the autopilot and to detect possible hardware failures and potential hazards. He must constantly respond to action-evoking events such as: to communicate information, to change aircraft configuration and to reduce 4-D accuracy errors. He is also required to respond to unexpected events such as a change in flight plan, to establish the backup mode, and to declare emergencies, etc. [1]. The pilot is in a multi-task situation.

If the pilot perceives an irregularity in one of the subsystems, he may seek more detailed information through either the on-board information system or actual sensor readings. Or, if he considers the irregularity to be minor, he may decide to continue his monitoring for higher priority events. There may also be autopilot malfunctions or sudden changes requiring the pilot to take charge of flight control. A proper representation of information through a flight map display indicating the continuous functioning of automatic control may help to ensure his remaining alert and responding quickly.

As described above, the automated system can normally take charge of the whole system except during critical situations such as when the system is suffering from a malfunction. Or a high-workload situation may develop when the aircraft is close to the ground when a high level of pilot activity is required. In all of these situations, the pilot is more than usually busy and further assistance of a computer would be most useful.

The recent development of fast and intelligent computer systems presents the potential for providing sound, well-evaluated airborne decisions which could reduce system risk, pilot workload and errors. While the computer as a decision maker is basically an implemented set of algorithms, adaptation and learning is possible. It is reasonable to expect that this evolving "intelligent" computer may be employed as the supervisor to the subsystem computers, taking charge of the tasks within its decision capability. The pilot and the computer thus have comparable abilities and overlapping responsibilities in performing these tasks. The problem that arises is how to allocate responsibility between the pilot and the computer for a subset of all tasks.

We have proposed that responsibilities not be strictly assigned to each decision maker. Instead, allocation should adapt to the state of the aircraft and the state of the pilot [2]. Further, to retain a coherent role, the pilot should be given overall responsibility for the whole aircraft while the computer would enable the pilot to avoid having to continually exercise all of these responsibilities. On one hand, it may not be appropriate for the computer to make the vital, final judgement where losses may extend beyond the point of recovery. On the other hand, there may be vigilance problems and the pilot's performance may degrade. This leads to the idea of utilizing the computer as a backup for the pilot. The allocation problem becomes one of deciding when the computer should request and relinquish responsibility.

Given these descriptions, we will explore several issues concerned with pilot decision making in computer-aided flight management situations. Is system performance enhanced by computer aiding? How effective are different aiding policies? How does the pilot feel about aiding? Is his role or performance affected? To investigate the feasibility of the approach, and to predict the effects of numerous system variables and aiding policies, a queueing formulation of multi-task decision making was developed and will be discussed in the next section.

APPROACH

The pilot in the automated flight management system described earlier has a variety of tasks to perform. As the number and variety of tasks increases, the workload of the pilot is increased. It is essential to appropriately allocate his attention and effort among the tasks. He may be in a situation that he wants both to monitor the tasks often enough to reduce growing uncertainty and risk, and to perform a task quickly and accurately to lessen the cost involved in the delay of action. This issue is being investigated by Greenstein and Rouse [3]. To simplify the issue, the pilot is assumed to employ a quasi-optimal decision making strategy for scanning displays and allocating attention. This is based on the assumptions that the tasks are independent and that events unequivocally present themselves. The pilot scans the task display in order of decreasing priority at a given rate. He then performs the first task for which he perceives some action-evoking events. The computer is assumed to adapt the same strategy either by being hard-wired or learning from the pilot. Now we may look at the multi-task decision making as a queueing system with two servers (the pilot and the computer) and K+1 classes of customers (K subsystem events plus control events represented by displayed 4-D errors in manual control mode).

In the queueing model, each server is characterized by his observation of system state, his perceptions of event occurrences, of event arrival rates and of event service rates. Combining the above information and the system cost criteion allows the model to predict system performance measures such as event delay statistics and server occupancy which is fraction of time the server is busy.

A convenient cost criterion, in terms of a stationary expected cost structure, includes waiting cost, service cost, and switching cost. When the computer service cost and switching cost may be negligible, the optimal policy is to have the computer on all the time. However, it is more likely that the human will be better at performing the task but not have sufficient time to do all the tasks. Also evidence of vigilance and warm-up decrements suggests that there is an acceptable workload range that sustains performance on long tasks. Thus we may want to seek a policy for computer aiding such that a minimum waiting cost is achieved while maintaining a specified workload level.

Based on results from literature [4], we will advocate the use of the stationary expected cost policy, subject to minimizing deviation from acceptable pilot workload, for computer on-off of the following form: turn

the computer on at arrival epochs when $N = c_1n_1 + c_2n_2 + \ldots + c_Kn_K > M$, and turn it off when $N < m$, where $c_1, c_2, \ldots, c_K$ are cost rates assessed according to relative priorities and n_k is the number of events waiting in the subsystem k. This policy (i.e., M and m) should vary as the system variables vary. Specific values of M and m have to be determined for various levels of traffic demand (i.e., event arrival rates), server performance and task complexity (i.e., service rates and probabilities of errors). An appropriate approach to implement the adaptive policy is to set up a table of stationary control policies beforehand and to employ a table look-up along with on-borad estimation of system variables.

To obtain the optimal stationary policy, i.e., to determine the values of M and m, a computer simulation was performed. Poison arrivals and Erlang service time distributions for subsystem were assumed. The K subsystem tasks were preempted by the control task whenever it occurred. The system was represented as a preemptive resume priority queueing system: $(M/E_k/2):(PRP/K/K)$ with implemented threshold control.

A simple case was considered in which the model parameters were determined in the following manner. 1) Subsystem arrival rates, service rates, and waiting cost rates were all uniform among the subsystems. 2) Two levels of arrival rates were assumed, i.e., low arrival (at 0.0167 events per second) and high arrival (at 0.0333 events per second). 3) Pilot performance in terms of service rates, service errors and control services were obtained from the experiment discussed in the next section. 4) The computer aiding employed the same service rates as the pilot and automatically went off when no event needed service (i.e., m=0). The results based on the computer simulation of 10,000 events for K=6 and server occupancy for pilot of = 0.7 showed that, without control task, M=7 for low arrival and 3 for high arrival; with control task, M=3 for low and 1 for high arrival. If workload is the primary consideration, these are threshold values which the computer should employ to adapt to both the subsystem arrival rate and the control task involvement.

Prediction of system performance by the model was also obtained through the computer simulation. The results will be discussed in the later section.

THE EXPERIMENT

Two experiments are to be discussed here. A brief review is given of an experiment previously reported by Walden and Rouse [5] investigating pilot decision making in an unaided situation. The second experiment, considering the computer aiding and autopilot malfunction situations, employs basically an outgrowth of the experimental representation used in the previous experiment.

The experimental situation developed earlier [6] used a PDP-11 driven CRT graphic system to represent a cockpit-like display to an experimental subject. The display shown in Figure 1 included standard aircraft instruments such as artificial horizon, altimeter, heading and airspeed indicators. Also displayed was a flight map which indicated the airplane's

position relative to the course to be followed. A small circle moved along the mapped course indicating the position the aircraft should have for it to be on schedule.

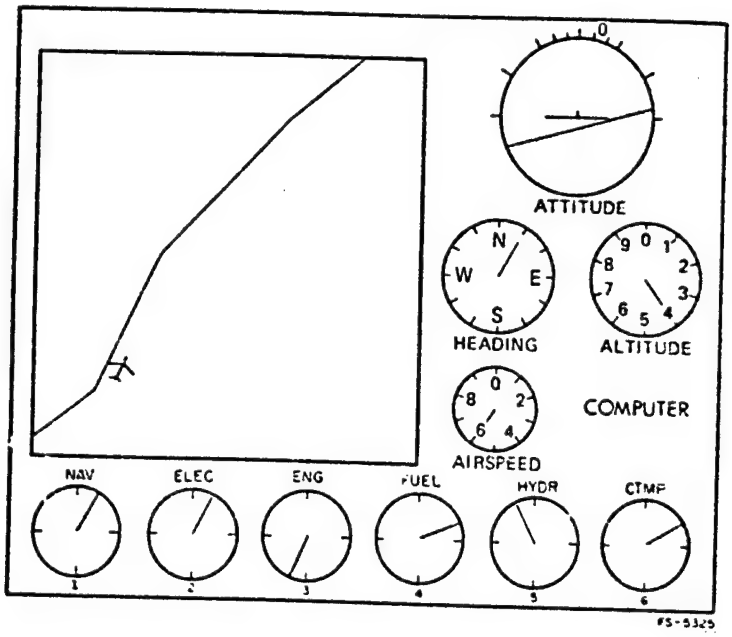

Figure 1. The Flight Management Situation.

In the manual control mode, the pilot controlled the pitch and roll of Boeing 707 aircraft dynamics with a joystick. Another control stick controlled the airspeed. The pilot's control task was to fly the airplane along the mapped route while maintaining a fixed altitude and stable pitch and roll attitude.

Below the map were the subsystem dials that represented the numerous aircraft subsystems which the pilot monitored for possible action-evoking events. Upon detecting an event (represented by the pointer pointing downward as shown for the engine subsystem in Figure 1) to which he wished to respond, the subject selected that subsystem via a 4x3 keyboard. The display shown in Figure 2 then appeared. This represented the first level of a check list-like tree associated with the subsystem of interest. He then searched for a branch labeled with a zero and seleted the branch with his keyboard. After completing the last level of the tree, the action was completed and the display shown in Figure 1 returned, with the subsystem information or diagnostic check complete.

Using the experimental situation, an experiment was performed by Walden [5] to study unaided pilot decision making strategies and the resulting performance. The two independent variables in the experiment were the inter-arrival time of subsystem events and the difficulty of the flight path.

The results showed that, while average waiting time increased with subsystem event arrival rate, the average service time appeared to be independent of subsystem arrival rate. The waiting time was also shown to increase as the control task was added. This effect was only a function of the mere presence of the control task, rather than the control task difficulty. Incorrect actions in servicing subsystems tended to increase with subsystem arrival rate, but showed no consistent variation with control task difficulty. False alarms, however, tended to occur more frequently with the easier control task and lower subsystem arrival rate. This presented evidence of performance degradation under low workload situations.

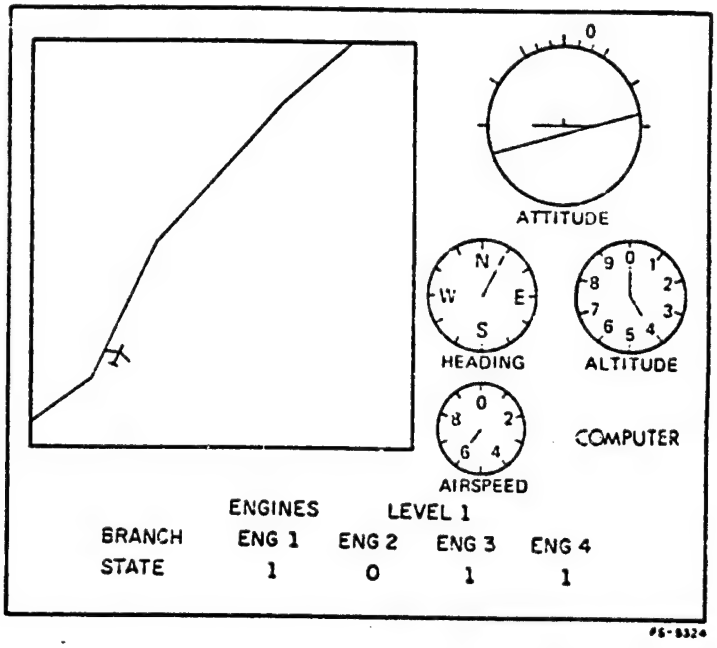

Figure 2. Display When Pilot Had Reacted To an Event in Engine Subsystem.

The data collected was used in the queueing model of pilot decision making in an unaided monitoring and control situation. The model gave a reasonable prediction of pilot performance in performing subsystem tasks, suggesting that it was an adequate description of pilot decision making in the given situation and that a similar model would be useful in the adaptive aiding system.

Based on the experimental representation discussed above, a new experimental situation for adaptive aiding was developed with the aiding program (i.e., the computer decision maker) and the coordinator program (i.e., the on-off algorithm) added to the original system. Issues concerning the capability of the computer to perform the subsystem tasks, the communication linkage between the pilot and the computer, and the activities of the coordinator deserve further discussion.

The computer is assumed to be able to perform monitoring and diagnostic check procedures using information from channels linked with subsystem computers and from the data links. It makes no errors such as false alarms, missed events, or incorrect actions after it gains confidence in performing the task. The detection and service times are assumed constant. As for the service discipline among the subsystems, the computer employs the same priority rule as that used by the pilot. To be consistent in its back-up role, the computer probably adapts itself to the pilot and avoids interference with him. To this end, the pilot is allowed to override any decision the computer has made.

Without knowing what each other is doing, the pilot and the computer may compete for the same task or resource. The prospect of conflict between the two is highly undesirable, since, it simply causes confusion, results in higher workload and degraded performance. The question as to how to design effective communication links without increasing the pilot's workload becomes important.

To inform the pilot of the computer's action, a succinctly displayed computer status indicator on or near the subsystem displays would seem to be satisfactory. Relevant information, if needed by the pilot for further details, may be structured into a hierarchical check-list procedure. In the experimental situation shown in Figure 3, The 'NAV' symbol over the navigation dial flashed, if the computer decided that an event had occurred and was waiting to be serviced in the navigation system. This was to tell the pilot that he could take charge of the navigation system and the computer would take some other responsibility to avoid interference; otherwise, the symbol would continue to flash for a total period of four seconds until the computer started interacting with the navigation system, resulting in a dim indicator showing in the navigation dial. If the pilot was in the middle of performing some other subsystem check procedure, say, within the engine system, he would not see the flashing 'NAV' symbol over the navigation dial. The status of the computer was then shown on the lower right hand corner of the CRT by an 'AIDING NAV' symbol (flashing during the interval of possible pilot preemption), if the computer was awaiting preemption or interacting with the navigation subsystem. This computer status area was blank if the computer was not actively involved in the subsystems.

Airborne pilot-to-computer communication is, in general, more complicated. Problems involved include estimating and processing signals as well as matching or recognizing system status. For the purpose of the experiment reported here, however, the communication channel from the pilot to sybsystems was predefined. For our experimental situation, these included the keyboard input and stick response sampling (through an A/D converter). These channels provided the monitoring computer a way of determining if the pilot was interacting with any portion of the system. If a number had been received through keyboard, and the checklist was being processed then the pilot had to be performing a subsystem task. The deviation of stick from normal position revealed that the pilot was performing the control task.

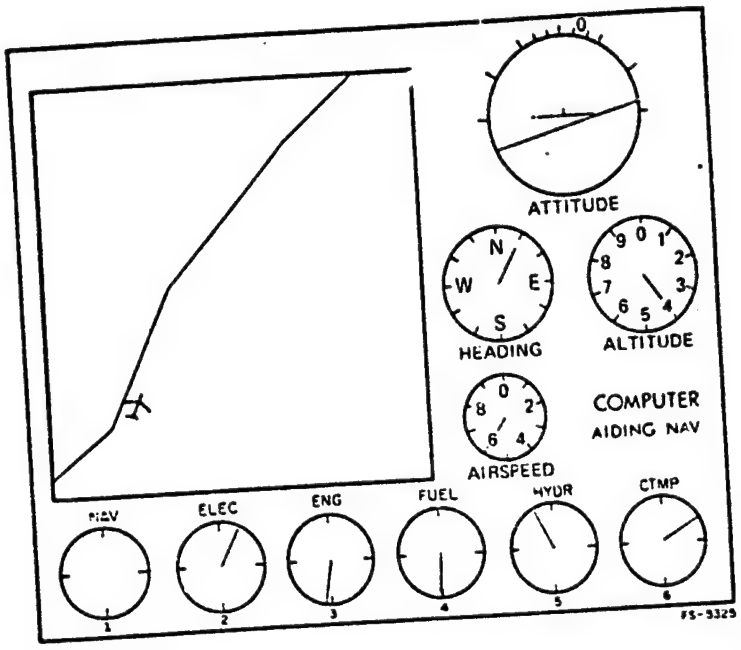

Figure 3. Display When the Computer Is Servicing Navigation System.

While the computer had to constantly check the pilot's action to avoid a conflict, the coordinator had to synchronously check the subsystem states to determine if there was any system change. The decision epoch was when an event arrival or departure occurred. Then the coordinator calculated both the weighted sum of events and the threshold. The criterion discussed earlier was used to determine if the computer was to be turned on at the arrival epoch or to be turned off at completion epoch.

Data, sampled synchronously (twice per second), included subsystem status and states, autopilot status, aircraft dynamic variables, stick and keyboard responses, computer status and the threshold values.

An experiment based on the experimental representation described above was conducted. Eight trained subjects, all of them male students in engineering, participated in a balanced sequence of sixteen experimental runs (see Table 1) with different workload levels. This was achieved by combining three levels of control task involvement (perfect autopilot, manual control, autopilot with possible malfunctions), three levels of subsystem event arrival rates (no arrival, low arrival, high arrival), and three levels of availability of computer aiding (no aiding, aiding with fixed switching policy, and aiding with adaptive policy). For each experimental run, the subject was first told the specific tasks to perform, then a 14-minute trial was given, and a questionare was filled out by the subject.

Table 1. Design of Experiment.

	Subject 1	Subject 2	Subject 3	Subject 4
Autopilot without Malfunction	(training)	(training)	(training)	(training)
	low arrival with aiding	low arrival without aiding	high arrival with aiding	high arrival without aiding
	low arrival without aiding	low arrival with aiding	high arrival without aiding	high arrival with aiding
	high arrival with aiding	high arrival without aiding	low arrival with aiding	low arrival without aiding
	high arrival without aiding	high arrival with aiding	low arrival without aiding	low arrival with aiding
Manual Control	(training)	(training)	(training)	(training)
	no arrival	no arrival	no arrival	no arrival
	low arrival with aiding	low arrival without aiding	high arrival with aiding	high arrival without aiding
	low arrival without aiding	low arrival with aiding	high arrival without aiding	high arrival with aiding
	high arrival with aiding	high arrival without aiding	low arrival with aiding	low arrival without aiding
	high arrival without aiding	high arrival with aiding	low arrival without aiding	low arrival with aiding
Autopilot with Malfunction	(training)	(training)	(training)	(training)
	no arrival	no arrival	no arrival	no arrival
	low arrival with aiding	low arrival without aiding	high arrival with aiding	high arrival without aiding
	low arrival without aiding	low arrival with aiding	high arrival without aiding	high arrival with aiding
	high arrival with aiding	high arrival without aiding	low arrival with aiding	low arrival without aiding
	high arrival without aiding	high arrival with aiding	low arrival without aiding	low arrival with aiding
	low arrival adaptive aid	low arrival adaptive aid	high arrival adaptive aid	high arrival adaptive aid
	high arrival adaptive aid	high arrival adaptive aid	low arrival adaptive aid	low arrival adaptive aid

For the experiment runs with perfect autopilot, only the subsystem task was considered. An "autopilot" kept the aircraft on course and on schedule. These runs served as baseline performance for the subsystem task. In the manual control runs, the subject had to perform both subsystem and control task. He was told that the control task was more important than the subsystem task. For the runs where autopilot maufunctions were posible, the autopilot was available during most of the experiment such that the subject was not required to fly the airplane except to occasionally check autopilot performance. As soon as he detected an autopilot malfunction, which was characterized by the airplane deviating from the mapped course at a rate of one degree per second, he was required to take over the flight control task, and fly the airplane back to the mapped course. In this case, the airplane would lock on the desired course as soon as it flew within the 800-feet oval of the on-schedule circle, and the autopilot mode was restored. The autopilot malfunction happened relatively infrequently, based on a Poison distribution with mean inter-arrival time of 160 seconds.

After the pilot detected the autopilot malfunction, he would have to devote a major portion of his attention to the control task, leaving subsystem tasks less attended, while risk and uncertainties grew as subsystem event detection and service were further delayed. This is one of many situations in which airborne computer aiding is more valuable. Also, in this period, the pilot's workload suddenly increased. To adapt to this type of change, a lower threshold value can be used to reduce subsystem service delay and pilot workload.

Based on this idea, two experiment runs with adaptive computer aiding were included in the set of runs with autopilot malfunctions possible. Instead of using M=3 all the time as in the fixed threshold policy, the adaptive policy used M=1 whenever the pilot was in manual mode. In total, there were seven experimental runs with autopilot malfunction: one run with no subsystem arrival (serving as a baseline performance for malfunction), two runs with no aiding, two with fixed-threshold aiding, and two with adaptive aiding. This arrangement allowed for the evaluation for the effectiveness of computer aiding and further the benefit of the adaptive policy beyond that of fixed aiding.

Three or more, depending on the task situation, of the following performance measures were evaluated in every experimental run:

1) average delay in response and service for subsystem events,
2) subsystem service errors (e.g., false alarms, incorrect actions, etc.),
3) 3-D RMS and average flight course errors,
4) flight control inputs including aileron, elevator, speed, etc.,
5) detection and service times for autopilot malfunctions,
6) server occupancy in terms of the fraction of time the subject was performing either subsystem or control tasks,
7) subjective ratings of level of effort required for the tasks and the desirability of computer aiding.

All these measures were obtained by analyzing the sampled data. The subsystem event response time was measured from the time of event occurrence to the time at which an action was initiated. The service time was measured from the time of last action initiation to the time of action completion for the event. The waiting time was measured from the time of event occurrence to the time of action completion for the event. Waiting time is equal to the sum of response time and service time only when the event is serviced by one server and no incorrect action is incurred. The results based on the analyses of variance are discussed in the next section.

RESULTS

The subsystem event waiting times averaged across subjects for the various task situations are shown in Figure 4. An analysis of variance conducted showed that among the statistically significant factors (at the .05 level) are the three experiment variables, i.e., the control mode, the subsystem arrival rates, and the computer aiding. As expected, the subsystem waiting time increased as the subsystem arrival rate increased, as the control involvement increased, and when no computer aiding was provided. A

separate test showed that the adaptive policy was also significant, i.e., the adaptive aiding further reduced the subsystem waiting time beyond the fixed-threshold aiding, even though the adaptive policy was only effective during a small portion of time in the experiment.

The subjective ratings of the level of effort across subjects are shown in Figure 5. Factors of significance include all three experiment variables. As expected, the perceived level of effort increased as control involvement increased, as subsystem arrival increased, and as computer aiding was removed. However, a separate test showed that the effect of the adaptive policy was not significant, probably because the adaptive policy was employed rather infrequently, and when it was being used, the subjects usually were too involved with restoring the autopilot to notice the fact that the computer was helping more often then usual.

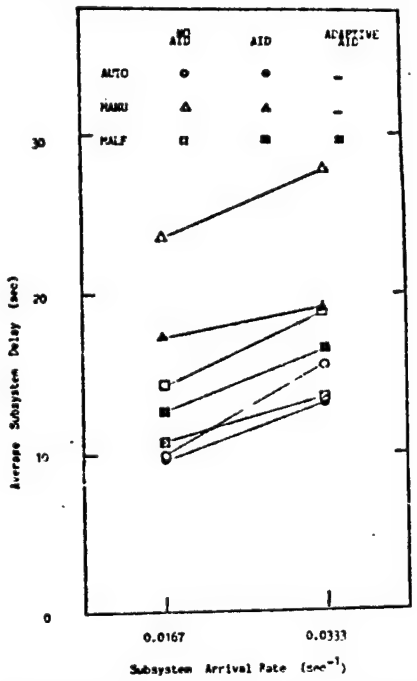

Figure 4 Average Subsystem Delay.

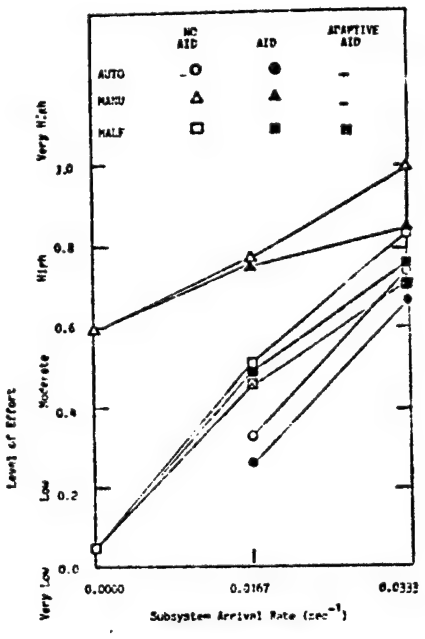

Figure 5 Subjective Ratings of Effort.

The RMS course error across subjects is shown in Figure 6. The analysis of variance showed that only control mode had an effect on the control error. No consistent variation in the course error was shown as subsystem arrival rate or aiding situation varied. The lower course RMS error for the autopilot malfunction mode probably resulted from subject's more intense attention to the control task in the case of malfunction.

The RMS roll angle across subjects is shown in Figure 7. Also, only control mode had a significant effect on the control input. The subjects were found to use more extreme control actions and more attention to fulfill

the malfunction task requirements. Sumarizing the above, systems that are designed to relax control requirements, such as the autopilot, seem to improve both control and subsystem performance, while systems that are designed to relax subsystem requirement, such as computer aiding or highly reliable subsystems, seem to improve only subsystem performance. The possible reason for this is that the control task perempts subsystem tasks, and thus, the control task inefficiency is likely to affect the performance of subsystem tasks; the reverse is not true.

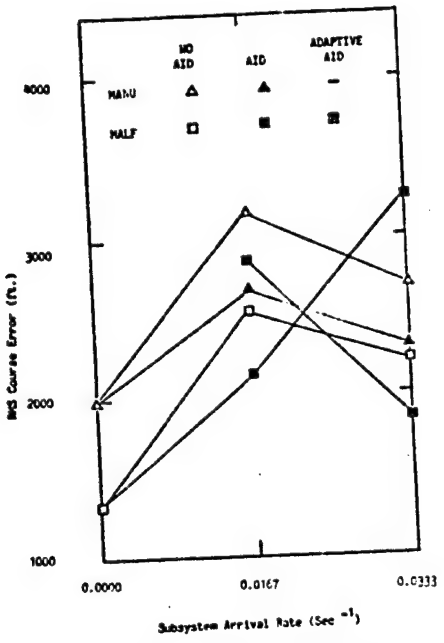

Figure 6. RMS Course Error.

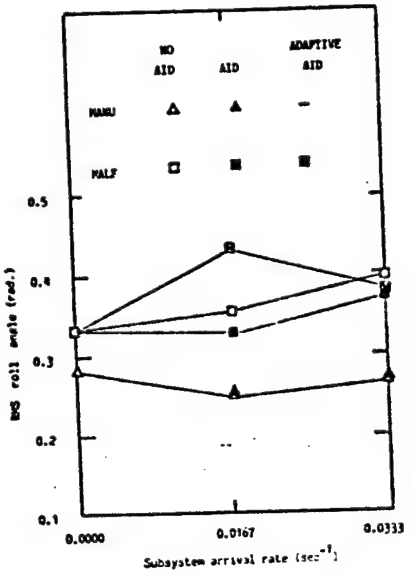

Figure 7. RMS Roll Angle.

Subjective ratings of three aspects of computer aiding were also determined: effectiveness, desirability of the aiding, and ease of interaction with the aiding. The results indicate that the aiding was considered easy to interact with and desirable by the subjects. Its effect on performance improvement was perceived to be from moderate to large. The subjects perceive the aiding to be relatively more effective and more desirable with a high subsystem arrival rate or a high control involvement situation. They, however, did not feel that it was more difficult to interact with the aiding in those situations. In fact, all the subjects were quite in favor of both the aiding scheme used in the experimental situation and the general computer aiding idea. More analyses of performance measures are discussed by Chu in his thesis [7].

The empirical data were compared with simulation results from the queueing model of pilot decision making in computer aided situation discussed earlier. This allowed an evaluation of the model's ability to represent the

given situation. The comparison of subsystem waiting statistics is shown in Table 2.

Table 2. Comparison of Waiting Time.

Arrival Rate	Aiding Type	Mean		Standard Deviation	
		Model	Data	Model	Data
Autopilot Mode					
Low	No Aiding	9.73	9.71	5.39	6.04
Low	Aiding	9.34	9.82	4.30	5.13
High	No Aiding	14.71	15.79	13.46	14.21
High	Aiding	13.79	13.16	12.00	7.43
Manual Mode					
Low	No Aiding	20.13	23.62	16.24	23.53
Low	Aiding	17.56	17.17	10.26	11.31
High	No Aiding	32.87	27.81	45.51	28.64
High	Aiding	19.58	19.19	11.85	12.17
Autopilot Malfunction Mode					
Low	No Aiding	12.00	14.25	8.85	13.81
Low	Aiding	11.13	12.84	6.79	10.52
Low	Adaptive Aiding	10.25	10.68	4.91	5.52
High	No Aiding	17.47	19.03	18.96	21.16
High	Aiding	13.66	15.52	8.52	11.55
High	Adaptive Aiding	12.32	13.25	7.10	8.33

In the model, a Poison distribution of control event arrivals and an Erlang distribution of control service times with shape parameter $k=2$, were assumed. To generate the results in Table 2, the values of 0.1 sec^{-1} (in manual mode) and 0.16 (in malfunction mode) were used as mean control arrival rates, and 0.47 and 0.34 as mean control service rates. These values were obtained by analyzing subject's aileron control input and, serve as a first approximation.

The results compare reasonably well. All parameters in the model were empirically measured and no adjustments were made. The model predicts performance in autopilot mode very well. A better estimate of control task parameters will surely improve the model accuracy in manual control and autopilot malfunction modes.

CONCLUSION

The experimental results show that all the experimental variables, i.e., the subsystem arrival rates, the control task involvement, and the availability of computer aiding, were statistically significant in terms of affecting the performance measures of interest, mainly, the subsystem delays, and subjective effort ratings. It was shown that the aiding enhanced system

performance in terms of subsystem average delays and subjective effort ratings. The adaptive aiding policy was shown to further reduce subsystem waiting time.

The queueing model fits the experiment result reasonably well. Further exploration of control task preemption is needed to improve model accuracy. The model also provides the capability to predict the server occupancy for different task situations. Included in the future work will be a test of the correlation between this server occupancy measure and the subjective effort ratings to determine if this measure may effectively serve as a workload indicator.

Finally, the computer-aided flight management situation will next be implemented in an aircraft simulator where regular pilots will be used as subjects.

REFERENCES

1. Wempe, T.E., "Flight Management - Pilot Procedures and System Interfaces for the 1980 - 1990's", AIAA Paper No. 74-1297, AIAA Life Science and System Conference, November 1974.

2. Chu, Y. and Rouse, W.B., "Optimal Adaptive Allocation of Decision Making Responsibility between Human and Computer in Multi-task Situations", Proceedings of the International Conference on Cybernetics and Society, pp. 168-175, September 1977.

3. Greenstein, J.S. and Rouse, W.B., "A Model of Event Detection in Multiple Process Monitoring Situations", Proceedings of the Fourteenth Annual Conference on Manual Control, April 1978.

4. Bell, C.E., "Optimal Operation of an M/G/1 Priority Queue with Removable Server", Operations Research, 21-6, 1973, pp. 1281-1290.

5. Walden, R. S. and Rouse, W.B., "A Queueing Model of Pilot Decision Making in a Multi-task Flight Management Situation", Proceedings of the Thirteenth Annual Conference on Manual Control, pp. 222-236, June 1977.

6. Rouse, W.B., Chu, Y., and Walden, R.S., "An Experimental Situation for Study of Pilot Interaction with Automated Airborne Decision Making Systems", Proceedings of the Twelfth Annual Conference on Manual Control, May 1976, NASA TM X-73, 170, pp. 39-44.

7. Chu, Y., Adaptive Allocation of Decision Making Responsibility between Human and Computer in the Multi-task Situations", Ph.D. Thesis in progress, University of Illinois, Urbana, Illinois.

SESSION L: WORKLOAD

Chairman: T. Sheridan

TIME ESTIMATION AS A SECONDARY TASK TO MEASURE WORKLOAD:

SUMMARY OF RESEARCH

Sandra G. Hart*
University of Utah
Salt Lake City, Utah

Duncan McPherson**
University of California
Berkeley, California

Leslie L. Loomis**
San Jose State University
San Jose, California

Abstract

This paper outlines the results of a series of experiments designed to evaluate the utility of time estimation as a secondary measure of piloting workload. Actively produced intervals of time were found to increase in length and variability, whereas retrospectively produced intervals decreased in length although they also increased in variability with the addition of a variety of flight-related tasks. If pilots counted aloud while making a production, however, the impact of concurrent activity was minimized, at least for the moderately demanding primary tasks that were selected. The effects of feedback on estimation accuracy and consistency were greatly enhanced if a counting or tapping production technique was used. This compares with the minimal effect that feedback had when no overt timekeeping technique was used.

Actively made verbal estimates of sessions filled with different activities decreased in length as the amount and complexity of activities performed during the interval were increased. Retrospectively made verbal estimates, however, increased in length as the amount and complexity of activities performed during the interval were increased. These results support the suggestion that time estimation provides a useful index of the workload involved in performing concurrent tasks.

* Supported by NASA Grant NGR-45-003-108 to the University of Utah.

** Supported by NASA Grant NSG 2269 to the San Jose State University Foundation.

INTRODUCTION

The workload involved in performing different manual control and decision making tasks is often difficult to measure within a single task or to compare between different tasks. It is difficult to infer an operator's workload from his measurable performance because: 1) individuals may compensate for additional task load by working harder, resulting in little measurable variation in performance and 2) the total workload is composed of a variety of subtasks such that performance on any one may or may not reflect varying degrees of task load in the others. In addition, different measurement techniques may be required to determine subtask-specific variation in workload.

The purpose of this research program was to develop a battery of primary task indices and unobtrusive secondary tasks that would specifically measure the load imposed by different subtasks that make up the total piloting task in order to measure the overall workload in real and simulated flight. Performance on secondary tasks is often used as an index of primary task workload. Secondary tasks that are commonly used often load the operator to determine his remaining capacity to perform additional tasks while performing the primary task. However, it was decided that tasks selected for inclusion in the workload assessment battery should be unobtrusive and measure primary task load with minimal interference. The tasks also should be similar to tasks that are normally performed in flight, easily learned, implemented and scored.

The results of this research have suggested time estimation as one such secondary measure of the cognitive demands of piloting because it has been shown that an individual's ability to estimate intervals of time varies as a function of concurrent task load. Time estimation is a task that is normally performed in flight. It is unobtrusive, easily learned, implemented and scored and is not altered by repeated presentations unless knowledge of results is given.

Intra- and Inter-Subject Variability

Although individuals tend to be consistent in the length of their time estimates, there are large differences among different individuals. For this reason, each subject should be used as his own control: estimates obtained under different conditions of primary task load can be most easily and unambiguously analyzed by comparison with estimates obtained from the same subject in the absence of concurrent task demands. Individual estimation accuracy seems to be a less important measure than are the direction of change in the length of estimates and the increase in variability of estimates with the addition of a primary task.

Estimation Measurement Method

Four methods have been used extensively to measure an individual's ability to estimate or produce specified intervals of clock time. The verbal estimation method requires that individuals vocalize or record their judgement of the duration of an operationally presented interval. The production method requires that subjects physically generate an interval whose duration is specified by the experimenter. The reproduction method, which combines elements of verbal estimation and production, requires the operational production of an interval whose duration was presented operationally. The method of comparison involves a relative judgement between the durations of two or more operationally presented intervals.

Estimation Mode

Rather than being perceived directly, the temporal aspects of experiences are inferred or deduced from the events that occur in time. Man has adopted objective standards and labels to allow quantification of and communication about temporal experiences because of the difficulties involved in dealing with time in the abstract. Individuals represent durations subjectively by correlating personally

Figure 1.

BASELINE ESTIMATES COMPARED TO THOSE PRODUCED DURING COMPENSATORY TRACKING

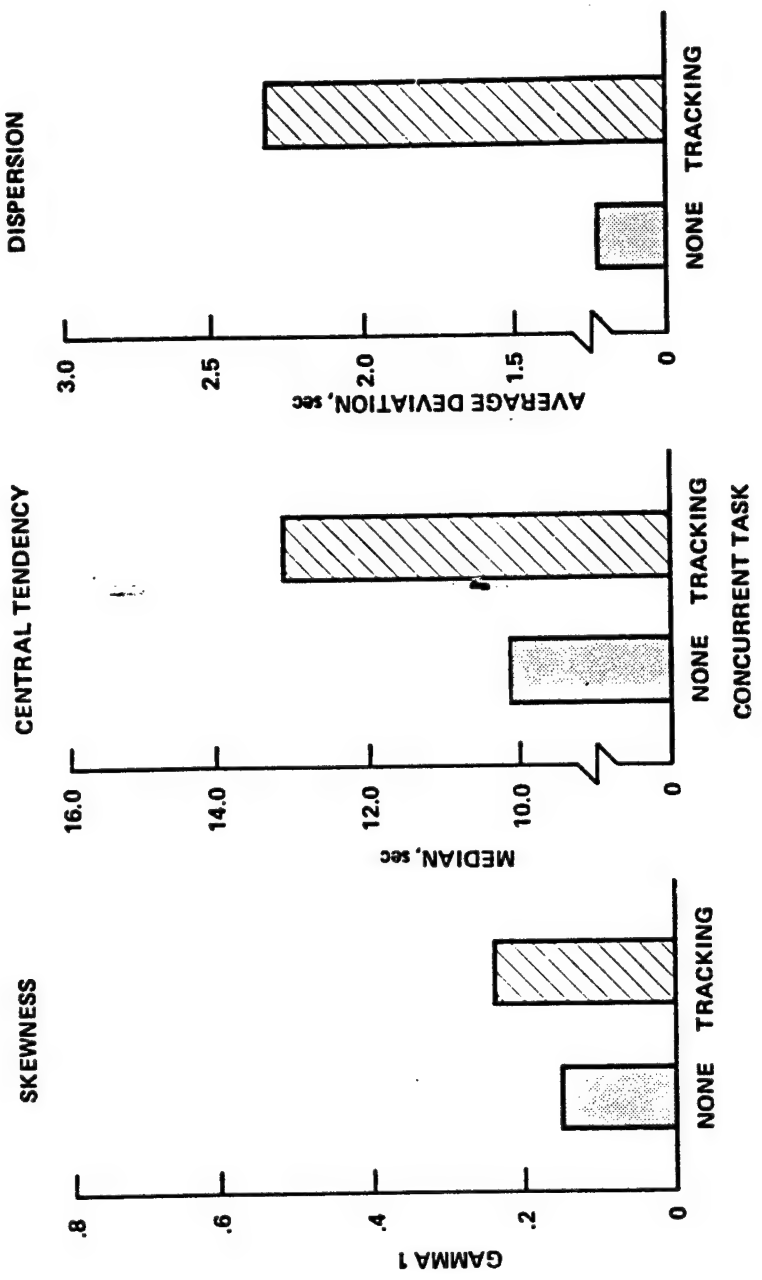

experienced events with objective temporal standards or rules, such as clocks.

Active Mode

When individuals must produce a specific duration or verbally estimate the length of a presented interval unaided by an objective timing device, they may rely on impressions of past events or mentally or physically replay or generate a sequence of events that is believed to last a specific interval of time in order to make the temporal dimension of the interval concrete. This mode of estimation has been referred to as active estimation (ref. 1).

Retrospective mode

Individuals may also make temporal estimates without attending to time as it passes. They may estimate the duration of an interval at its conclusion by comparing the number and complexity of events that occurred during the interval with remembered durations of intervals similarly filled (ref. 2). This mode of estimation has been referred to as retrospective estimation (ref. 1).

Influence of Concurrent Activity on Active Estimation

The attention demanded by concurrent activity tends to interfere with active estimation. Whenever attention is diverted from active estimation, time passes unnoticed so that individuals may wait too long to terminate a production or verbally underestimate the length of the interval.

Active productions

Hart and McPherson (ref. 3) and Hart and Simpson (ref. 4) have shown that subjects do indeed wait too long to terminate their productions when distracted from active time estimation by competing simple compensatory tracking tasks (fig. 1) or speech recognition. A series of stylized representations of the mean length of 10 sec

Figure 2.

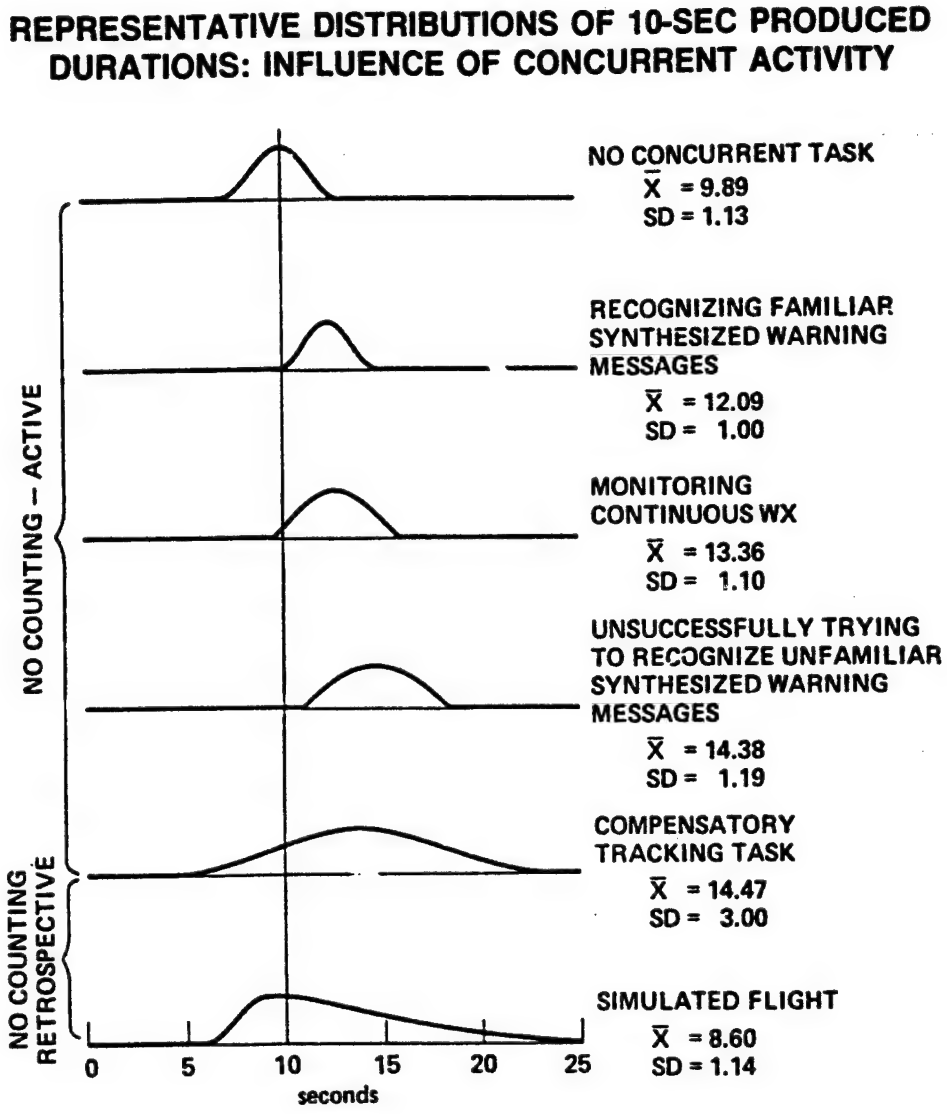
REPRESENTATIVE DISTRIBUTIONS OF 10-SEC PRODUCED DURATIONS: INFLUENCE OF CONCURRENT ACTIVITY
NO CONCURRENT TASK
X̄ = 9.89
SD = 1.13
RECOGNIZING FAMILIAR SYNTHESIZED WARNING MESSAGES
X̄ = 12.09
SD = 1.00
MONITORING CONTINUOUS WX
X̄ = 13.36
SD = 1.10
UNSUCCESSFULLY TRYING TO RECOGNIZE UNFAMILIAR SYNTHESIZED WARNING MESSAGES
X̄ = 14.38
SD = 1.19
COMPENSATORY TRACKING TASK
X̄ = 14.47
SD = 3.00
SIMULATED FLIGHT
X̄ = 8.60
SD = 1.14
NO COUNTING -- ACTIVE
NO COUNTING RETROSPECTIVE
0
5
10
15
20
25
seconds

Figure 3.

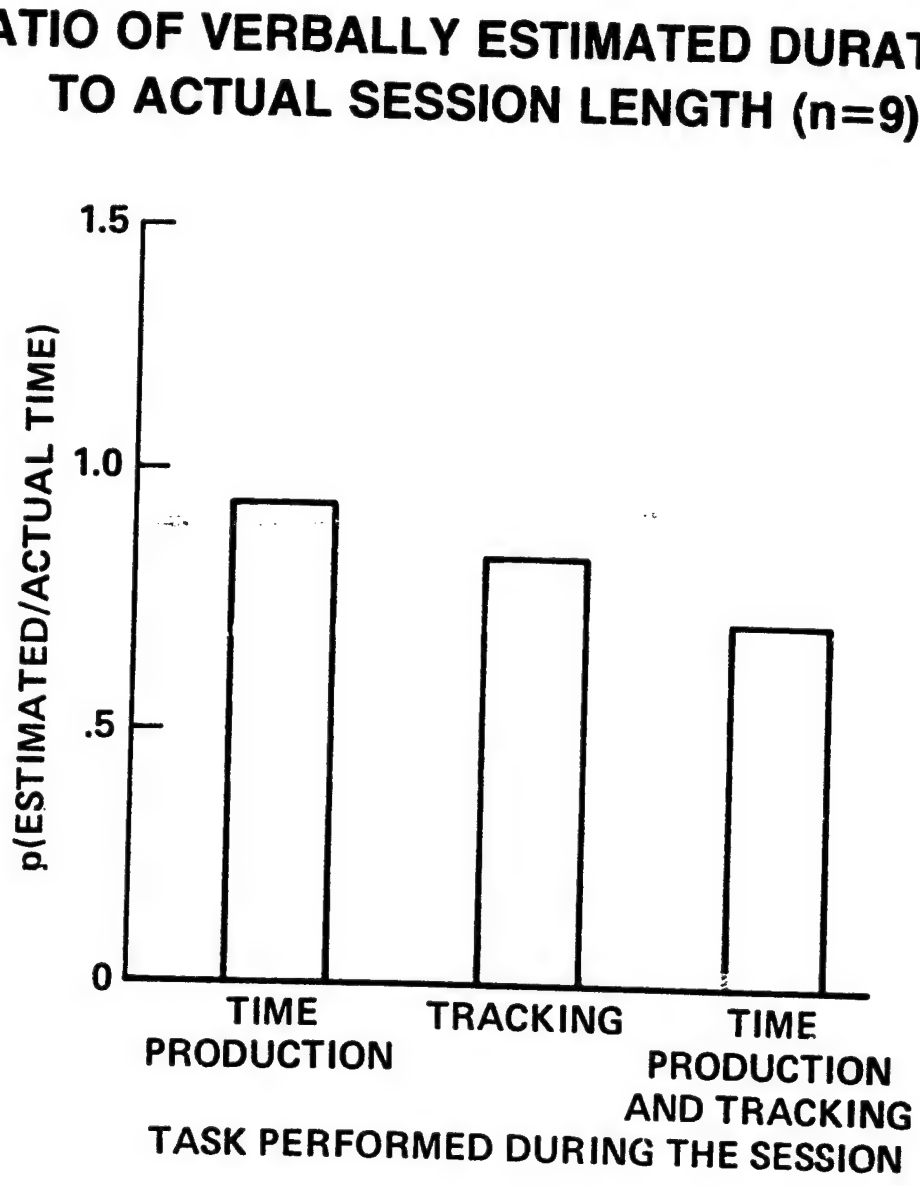
RATIO OF VERBALLY ESTIMATED DURATION TO ACTUAL SESSION LENGTH (n=9)
p(ESTIMATED/ACTUAL TIME)
1.5
1.0
.5
0
TIME PRODUCTION
TRACKING
TIME PRODUCTION AND TRACKING
TASK PERFORMED DURING THE SESSION

productions obtained under different experimental conditions is given in figure 2. Each distribution's shape approximates that of actual data obtained and was drawn to include three standard deviations about the obtained mean. As the demands of the concurrent tracking and recognition tasks were increased, the length of produced durations increased by 4 sec or more and their variability more than doubled. Other, less demanding concurrent tasks, such as monitoring continuous aviation weather broadcasts, were also associated with an increase in the central tendency and variability of estimate distributions, but to a lesser degree, as one would expect from their less demanding nature.

Active verbal estimates

Hart (ref. 5) and Hart, McPherson, Kreifeldt, and Wempe (ref. 6) found that actively made verbal estimates decreased in length with the addition of either a simple compensatory tracking task (fig. 3) or a complex multi-manned flight simulation (fig. 4b). The more difficult levels of each task were associated with the shortest active verbal estimates. This is consistent with the finding that active verbal estimation and active production are reciprocally related, and the observed directions of change in estimated and produced durations are both the consequence of underestimation of the passage of time.

Influence of Concurrent Activity on Retrospective Estimation

As the attention demands of a primary task increase, there is less and less attention available for time estimation. When active estimation becomes impossible the retrospective mode of estimation becomes necessary. Here, one presumably remembers the events that occurred during the interval, compares them to other experiences with known duration, and then verbally estimates the duration of the interval or decides whether or not it is time to terminate a production. As the number and complexity of events

Figure 4

A. PROPORTION OF VERBAL ESTIMATES OF THE DURATION OF FINAL APPROACHES THAT PILOTS REPORTED MAKING ACTIVELY AND RETROSPECTIVELY (n = 9)

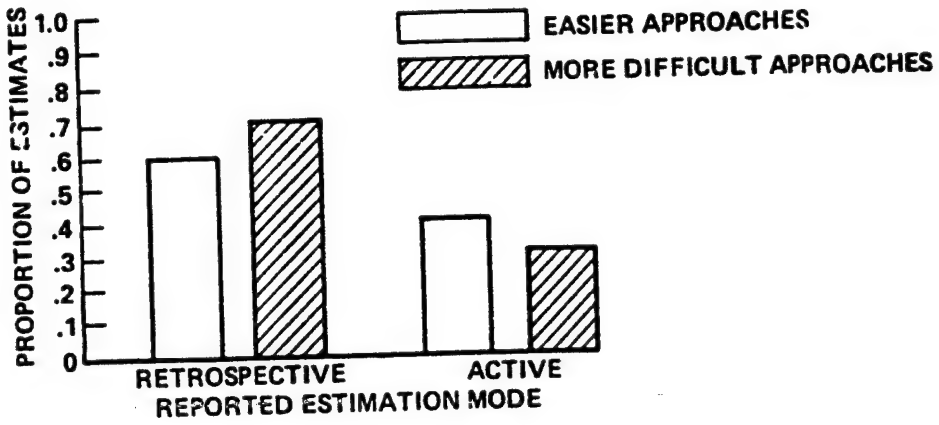

B. AVERAGE RATIO OF ESTIMATED DURATION TO ACTUAL DURATION FOR ACTIVE AND RETROSPECTIVE ESTIMATES

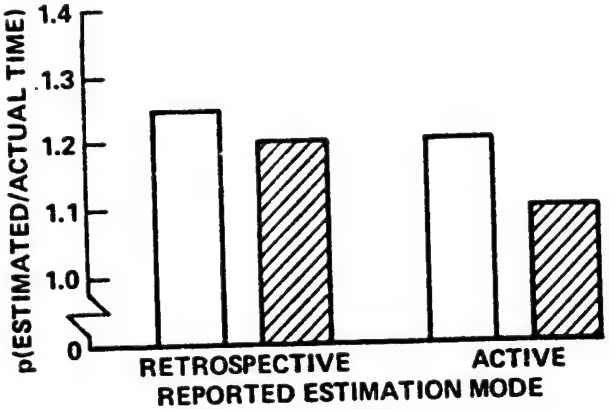

that fill the interval are increased, there is a tendency toward overestimation of the amount of time that has passed resulting in the termination of produced durations too soon or the verbal overestimation of elapsed time. Note that the directions of change in retrospectively verbally estimated and produced durations are the opposite of those obtained with active estimation and production and again the length of verbal estimates and productions are reciprocally related.

Retrospective productions

Hart and McPherson (ref. 3) have shown that the central tendency of 10 sec productions, obtained from pilots during simulated flight, decreased in length, as predicted, and the variability of the produced durations increased in comparison to estimates obtained with no competing activity. (fig. 5) Pilots reported that active estimation was difficult, resulting in their use of the retrospective mode. The distributions of retrospectively made productions were also positively skewed due to a few very long estimates which resulted from the estimation task occasionally being forgotten under conditions of high concurrent task load.

Retrospective verbal estimates

Following a complex multi-manned simulation flight, (ref. 6) pilot indicated that 66% of their estimates of the length of time taken to fly the final two miles of an approach were made retrospectively and that the proportion of retrospectively made estimates increased as the difficulty of the approach increased. (fig. 4a) Retrospectively made estimates were consistently longer than were estimates that pilots reported that they had made actively as predicted. (fig. 4b)

Interaction of Estimation Technique and Concurrent Task

Within the active mode of estimation there are many timekeeping techniques available. A standardized, rhythmic temporal metric (such as

Figure 5.

BASELINE ESTIMATES COMPARED TO THOSE PRODUCED DURING SIMULATED FLIGHT

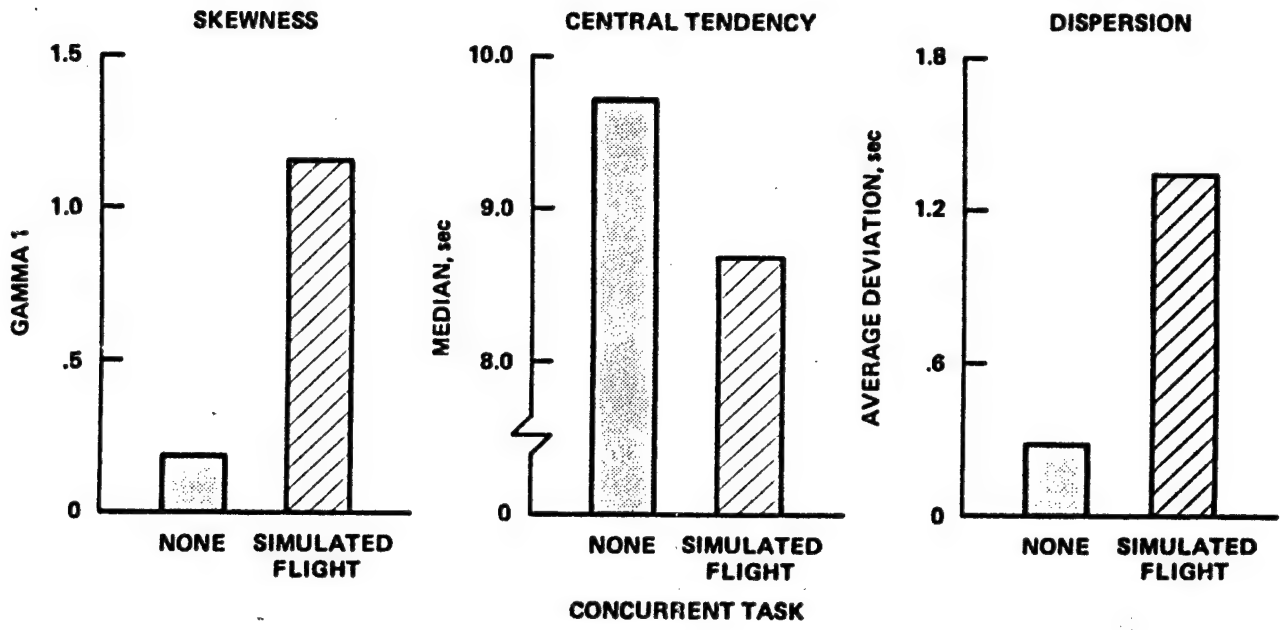

tapping) not only fixes an individual's attention on the time estimation task, which is otherwise difficult to do for a task as abstract and stimulus-deficient as time estimation, but also provides a concrete, repeatable way to keep track of time. Timekeeping techniques that are not externalized, however, are more easily disrupted by additional, more compelling activities and are less stable across time. Some of the estimation techniques that subjects have reported using to keep track of time include counting, tapping, mentally replaying a phrase of music estimated to have the appropriate duration, mentally rehearsing the pre-flight checklist for a helicopter, counting heart beats or breaths, picturing the dial of a clock with a second hand moving around it, or "just waiting" for 10 sec. Of these techniques, those that are externalized, such as counting, provide standard, repeatable units with which to mark off intervals of time resulting in improved estimation stability. Mental rehearsal of remembered experiences judged to have the appropriate duration resulted in less stable productions, because the interval that was repeated may or may not have lasted the appropriate duration. Further, it is difficult to control the rate at which one's mind steps through a memory.

Hart, Loomis and Wempe (ref. 7) found that when attention was focused on a time production task by requiring subjects to rhythmically count aloud 1-sec intervals, production accuracy and consistency were not affected by the addition of a concurrent task. (fig. 6 and fig. 7) With no overt counting, however, the length and variability of produced durations increased significantly with the addition of a tracking task, replicating earlier results (ref. 3). Because performance on the tracking task was the same with both productions techniques, it appears that the shift in attention away from time production found with the no-counting technique was not because subjects could not innately perform both tasks but merely that they in fact did not. When attention was focused on the time production task by the counting technique, production accuracy was not degraded and there was no concomitant degredation of tracking task performance.

Figure 6.

REPRESENTATIVE DISTRIBUTIONS OF PRODUCED DURATIONS: INTERACTION BETWEEN ESTIMATION TECHNIQUE AND INFLUENCE OF CONCURRENT ACTIVITY

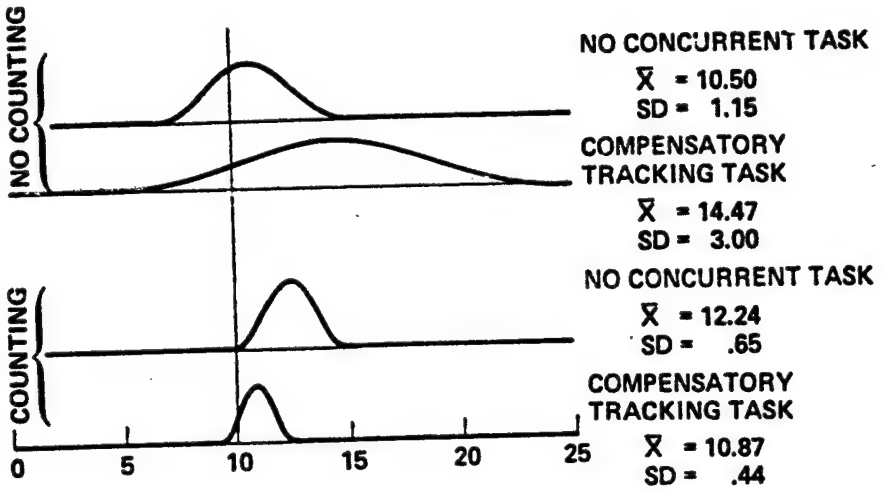

Figure 7.

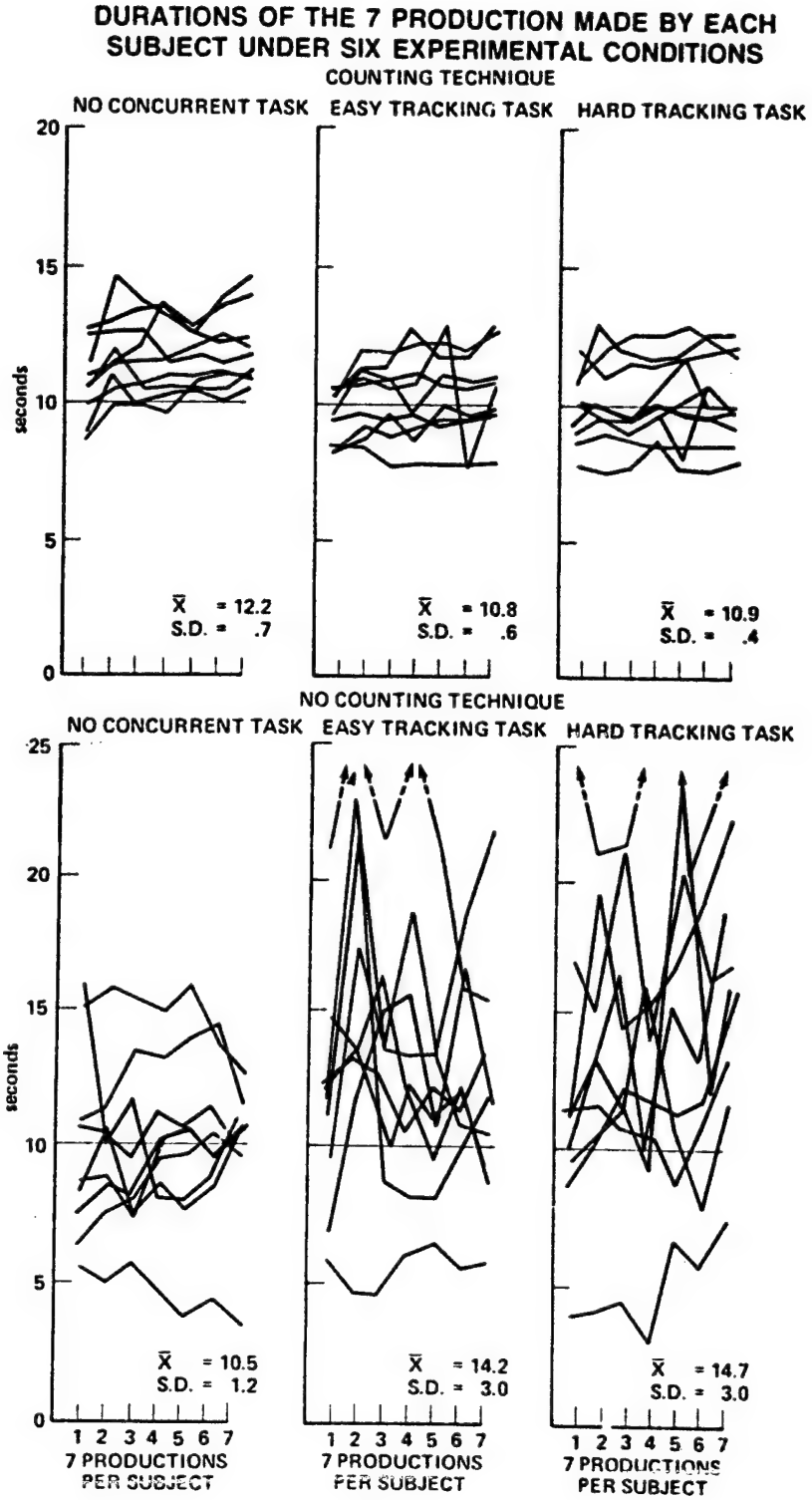
DURATIONS OF THE 7 PRODUCTION MADE BY EACH SUBJECT UNDER SIX EXPERIMENTAL CONDITIONS
COUNTING TECHNIQUE
NO CONCURRENT TASK
EASY TRACKING TASK
HARD TRACKING TASK
seconds
20
15
10
5
0
X̄ = 12.2
S.D. = .7
X̄ = 10.8
S.D. = .6
X̄ = 10.9
S.D. = .4
NO COUNTING TECHNIQUE
NO CONCURRENT TASK
EASY TRACKING TASK
HARD TRACKING TASK
25
20
15
10
5
0
X̄ = 10.5
S.D. = 1.2
X̄ = 14.2
S.D. = 3.0
X̄ = 14.7
S.D. = 3.0
1 2 3 4 5 6 7
7 PRODUCTIONS PER SUBJECT

It is likely that more demanding concurrent activity, such as simulated flight, would also impact the consistency of durations produced with a counting technique. However, no such effects were found with the moderately demanding tracking tasks that were used.

Interaction of Estimation Technique and Feedback

If the ability to estimate and produce intervals of time is learned, then it is likely that knowledge of results (feedback) should enhance timekeeping accuracy and consistency. In addition, the use of estimation techniques that provide rhythmic division of an interval into standard, repeatable units should focus attention on timekeeping and make the temporal dimension of the interval more concrete, thereby enhancing an individual's ability to take advantage of feedback.

In a recent study, Hart, Loomis and Wempe (ref. 8) found that individuals, using estimation techniques that did not involve some sort of overt counting, made less efficient initial use of feedback and did not experience any long term benefits from feedback. Overall accuracy of 10-sec productions, but not variability, was improved significantly by the presentation of feedback, with a rapid return to prefeedback performance levels when feedback was removed. (fig. 8 and fig. 9). During feedback, subjects repeatedly overcorrected. If told that one production was too long, the next production was typically too short and vice versa. Even after 30 trials with feedback following every production, subjects were unable to estimate accurately from trial to trial even though their estimate durations appeared to be accurate overall. If the subjects were instructed to rhythmically tap a button at 1-sec intervals in order to produce a series of 10-sec durations, both accuracy and variability were improved significantly by the addition of feedback. This improvement persisted for at least as long as 30 additional trials after feedback was removed. With this production technique, subjects were able to maintain consistent and accurate estimates from trial to trial, and did not overcorrect as they had

Figure 8.

REPRESENTATIVE DISTRIBUTIONS OF 10-SEC PRODUCED DURATIONS: INFLUENCE OF KNOWLEDGE OF RESULTS (FEEDBACK)

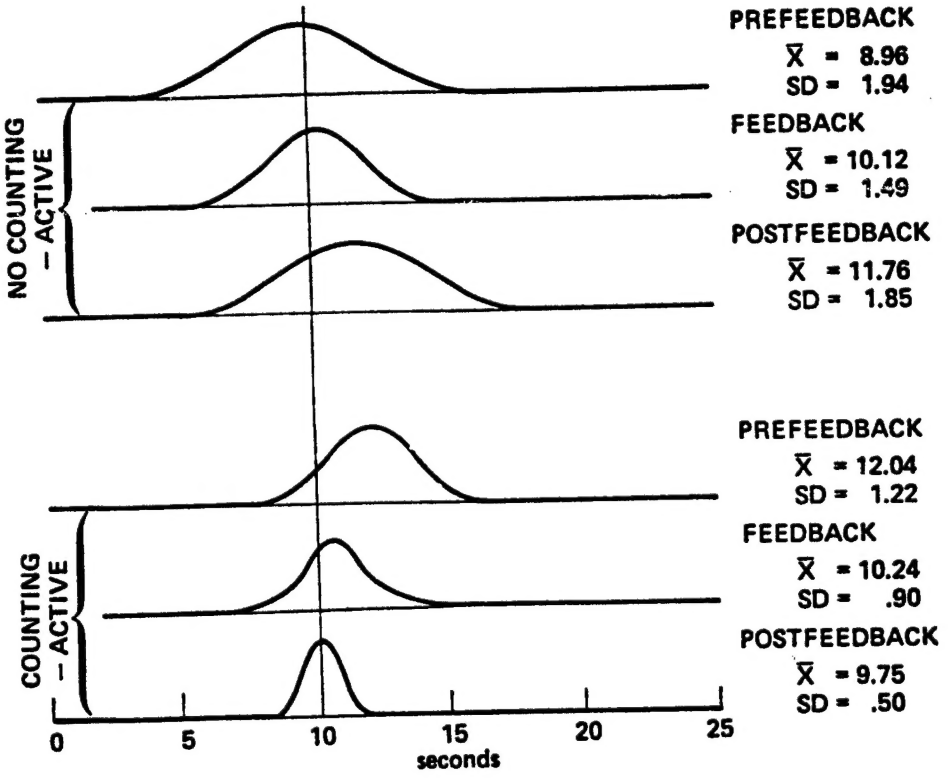

Figure 9.

COMPOSITE GRAPHS OF RAW SCORES OF 10 SUBJECTS

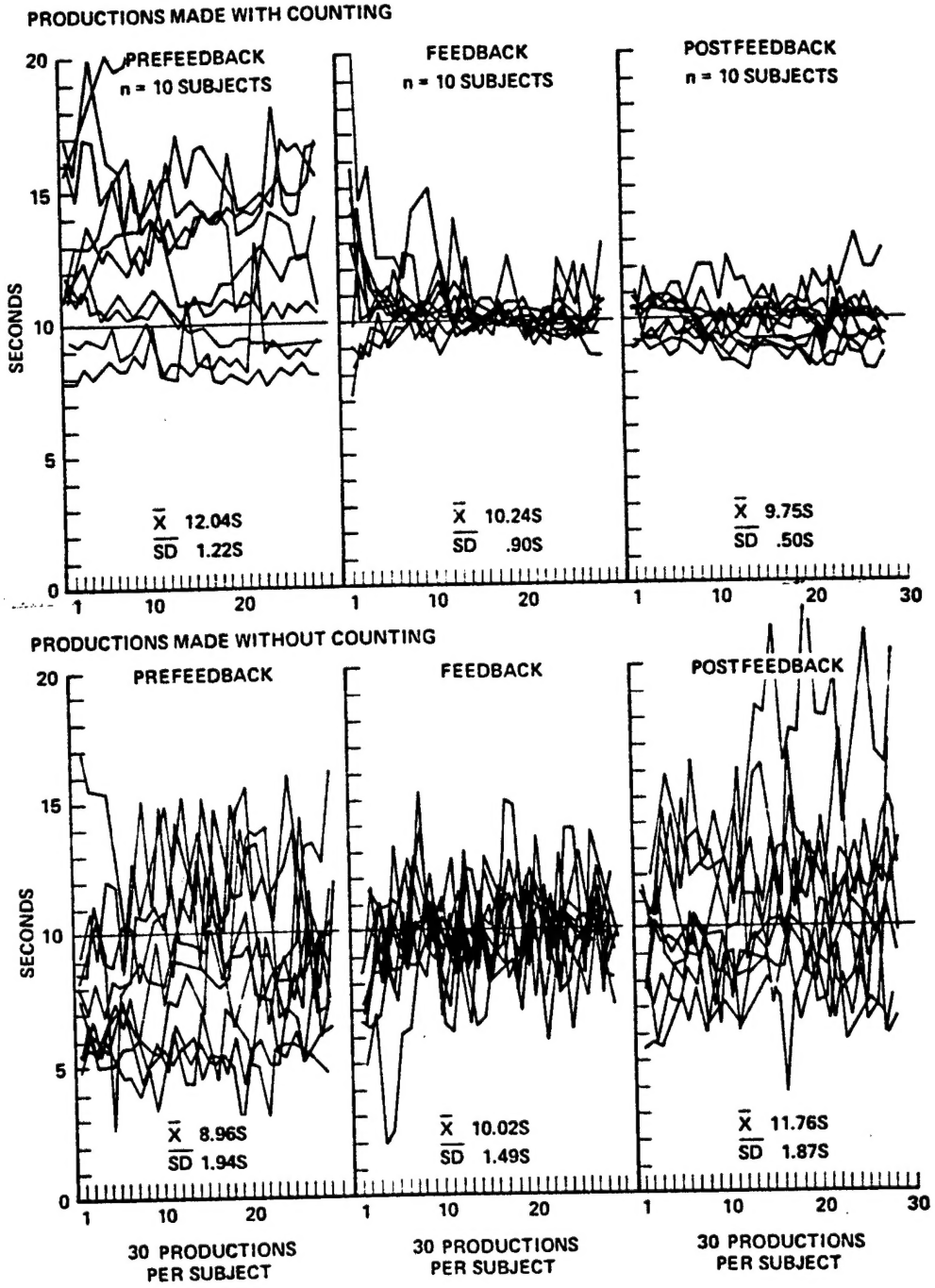

with the no-counting technique. The data suggest that tapping rhythmically not only provides a standardized repeatable temporal metric, but also fixes subject's attention on the time production task, which together combine to enable subjects to use feedback more effectively.

Conclusion

As a result of the foregoing research effort, several recommendations can be made concerning the use of time estimation as a secondary measure of the attention demands of a primary task.

Method

The production of brief intervals of time appears to be the most useful experimental method. The duration and variability of time productions in the range of 1 to 30 sec have been shown to reflect the attention demands of primary manual control, message recognition, and simulated flight tasks. Relatively brief intervals should be used so that the primary task load remains reasonably uniform and describable during the produced interval.

The verbal estimation method also shows some promise as a secondary measure of primary task workload. Its primary advantage over the production method is ease of implementation. Its primary disadvantage is that subjects tend to round off their estimates, thereby losing precision, and their responses tend to become stereotyped if a number of estimates are required. This method appears to have some value, but is less sensitive than the method of production.

Mode

Estimation mode (active or retrospective production or verbal estimation) must also be controlled or identified to obtain reliable and clear results with a time estimation task. Because retrospective productions decrease in length with increasing task load whereas active productions increase in length, care must be taken to identify the mode of production used. If retrospective and active productions are combined in an analysis, their direction of change with the addition of another

task would tend to cancel out masking detailed changes in the underlying processes.

Technique

Timekeeping techniques that are not externalized are most easily disrupted by concurrent task demands and thus provide the most useful measure of primary task demands. Thus, if time production is to be used as a measure of workload, subjects should not be allowed to use any overt time estimation technique such as tapping or counting. If estimation accuracy and consistency are required, however, an overt timekeeping technique should be used. Further research is required to determine at what level of concurrent task load the overt estimation technique would also be disrupted.

Feedback

If an overt timekeeping technique is used, feedback is effective in reducing both error and variability after only two or three repetitions, and the effects of feedback last long after it has been removed. With no overt timekeeping technique, however, estimation error is reduced only on the average, and variability remains high with a rapid return to pre-feedback error levels following removal of feedback.

Data Analysis

Time estimation performance is best evaluated relatively. That is, the amount and direction of change in estimation accuracy and consistency observed in the presence of additional primary tasks should be compared to estimates obtained from the same subject with no additional activity. Care should also be taken to select the appropriate measures of central tendency and variability as distributions of time productions are often positively skewed, particularly when obtained in the presence of competing concurrent activity.